Long-Range Chlorine, Bromine and Deuterium Isotope Shifts in the ^{19}F NMR Spectra of Some Fluorobenzenes and Fluoroanilines.

by

Guy M. Bernard

A Thesis

Submitted to the Faculty of Graduate Studies of the University

of Manitoba in Partial Fulfillment of the Requirements for

the Degree of

Master of Science

Winnipeg, Manitoba

ISBN 0-612-16094-7

Name _____

Dissertation Abstracts International and *Masters Abstracts International* are arranged by broad, general subject categories. Please select the one subject which most nearly describes the content of your dissertation or thesis. Enter the corresponding four-digit code in the spaces provided.

Physical Chemistry
SUBJECT TERM

0494
SUBJECT CODE

UMI

Subject Categories

THE HUMANITIES AND SOCIAL SCIENCES

COMMUNICATIONS AND THE ARTS
Architecture 0729
Art History 0377
Cinema 0900
Dance 0378
Fine Arts 0357
Information Science 0723
Journalism 0391
Library Science 0399
Mass Communications 0708
Music 0413
Speech Communication 0459
Theater 0465

EDUCATION
General 0515
Administration 0514
Adult and Continuing 0516
Agricultural 0517
Art 0273
Bilingual and Multicultural 0282
Business 0688
Community College 0275
Curriculum and Instruction 0727
Early Childhood 0518
Elementary 0524
Finance 0277
Guidance and Counseling 0519
Health 0680
Higher 0745
History of 0520
Home Economics 0278
Industrial 0521
Language and Literature 0279
Mathematics 0280
Music 0522
Philosophy of 0998
Physical 0523
Psychology 0525
Reading 0535
Religious 0527
Sciences 0714
Secondary 0533
Social Sciences 0534
Sociology of 0340
Special 0529
Teacher Training 0530
Technology 0710
Tests and Measurements 0288
Vocational 0747

LANGUAGE, LITERATURE AND LINGUISTICS
Language
- General 0679
- Ancient 0289
- Linguistics 0290
- Modern 0291

Literature
- General 0401
- Classical 0294
- Comparative 0295
- Medieval 0297
- Modern 0298
- African 0316
- American 0591
- Asian 0305
- Canadian (English) 0352
- Canadian (French) 0355
- English 0593
- Germanic 0311
- Latin American 0312
- Middle Eastern 0315
- Romance 0313
- Slavic and East European 0314

PHILOSOPHY, RELIGION AND THEOLOGY
Philosophy 0422
Religion
- General 0318
- Biblical Studies 0321
- Clergy 0319
- History of 0320
- Philosophy of 0322

Theology 0469

SOCIAL SCIENCES
American Studies 0323
Anthropology
- Archaeology 0324
- Cultural 0326
- Physical 0327

Business Administration
- General 0310
- Accounting 0272
- Banking 0770
- Management 0454
- Marketing 0338

Canadian Studies 0385
Economics
- General 0501
- Agricultural 0503
- Commerce-Business 0505
- Finance 0508
- History 0509
- Labor 0510
- Theory 0511

Folklore 0358
Geography 0366
Gerontology 0351
History
- General 0578
- Ancient 0579
- Medieval 0581
- Modern 0582
- Black 0328
- African 0331
- Asia, Australia and Oceania 0332
- Canadian 0334
- European 0335
- Latin American 0336
- Middle Eastern 0333
- United States 0337

History of Science 0585
Law 0398
Political Science
- General 0615
- International Law and Relations 0616
- Public Administration 0617

Recreation 0814
Social Work 0452
Sociology
- General 0626
- Criminology and Penology ... 0627
- Demography 0938
- Ethnic and Racial Studies 0631
- Individual and Family Studies 0628
- Industrial and Labor Relations 0629
- Public and Social Welfare 0630
- Social Structure and Development 0700
- Theory and Methods 0344

Transportation 0709
Urban and Regional Planning 0999
Women's Studies 0453

THE SCIENCES AND ENGINEERING

BIOLOGICAL SCIENCES
Agriculture
- General 0473
- Agronomy 0285
- Animal Culture and Nutrition 0475
- Animal Pathology 0476
- Food Science and Technology 0359
- Forestry and Wildlife 0478
- Plant Culture 0479
- Plant Pathology 0480
- Plant Physiology 0817
- Range Management 0777
- Wood Technology 0746

Biology
- General 0306
- Anatomy 0287
- Biostatistics 0308
- Botany 0309
- Cell 0379
- Ecology 0329
- Entomology 0353
- Genetics 0369
- Limnology 0793
- Microbiology 0410
- Molecular 0307
- Neuroscience 0317
- Oceanography 0416
- Physiology 0433
- Radiation 0821
- Veterinary Science 0778
- Zoology 0472

Biophysics
- General 0786
- Medical 0760

EARTH SCIENCES
Biogeochemistry 0425
Geochemistry 0996
Geodesy 0370
Geology 0372
Geophysics 0373
Hydrology 0388
Mineralogy 0411
Paleobotany 0345
Paleoecology 0426
Paleontology 0418
Paleozoology 0985
Palynology 0427
Physical Geography 0368
Physical Oceanography 0415

HEALTH AND ENVIRONMENTAL SCIENCES
Environmental Sciences 0768
Health Sciences
- General 0566
- Audiology 0300
- Chemotherapy 0992
- Dentistry 0567
- Education 0350
- Hospital Management 0769
- Human Development 0758
- Immunology 0982
- Medicine and Surgery 0564
- Mental Health 0347
- Nursing 0569
- Nutrition 0570
- Obstetrics and Gynecology .. 0380
- Occupational Health and Therapy 0354
- Ophthalmology 0381
- Pathology 0571
- Pharmacology 0419
- Pharmacy 0572
- Physical Therapy 0382
- Public Health 0573
- Radiology 0574
- Recreation 0575
- Speech Pathology 0460
- Toxicology 0383

Home Economics 0386

PHYSICAL SCIENCES
Pure Sciences
Chemistry
- General 0485
- Agricultural 0749
- Analytical 0486
- Biochemistry 0487
- Inorganic 0488
- Nuclear 0738
- Organic 0490
- Pharmaceutical 0491
- Physical 0494
- Polymer 0495
- Radiation 0754

Mathematics 0405
Physics
- General 0605
- Acoustics 0986
- Astronomy and Astrophysics 0606
- Atmospheric Science 0608
- Atomic 0748
- Electronics and Electricity 0607
- Elementary Particles and High Energy 0798
- Fluid and Plasma 0759
- Molecular 0609
- Nuclear 0610
- Optics 0752
- Radiation 0756
- Solid State 0611

Statistics 0463

Applied Sciences
Applied Mechanics 0346
Computer Science 0984
Engineering
- General 0537
- Aerospace 0538
- Agricultural 0539
- Automotive 0540
- Biomedical 0541
- Chemical 0542
- Civil 0543
- Electronics and Electrical 0544
- Heat and Thermodynamics ... 0348
- Hydraulic 0545
- Industrial 0546
- Marine 0547
- Materials Science 0794
- Mechanical 0548
- Metallurgy 0743
- Mining 0551
- Nuclear 0552
- Packaging 0549
- Petroleum 0765
- Sanitary and Municipal 0554
- System Science 0790

Geotechnology 0428
Operations Research 0796
Plastics Technology 0795
Textile Technology 0994

PSYCHOLOGY
General 0621
Behavioral 0384
Clinical 0622
Developmental 0620
Experimental 0623
Industrial 0624
Personality 0625
Physiological 0989
Psychobiology 0349
Psychometrics 0632
Social 0451

THE UNIVERSITY OF MANITOBA

FACULTY OF GRADUATE STUDIES

COPYRIGHT PERMISSION

LONG-RANGE CHLORINE, BROMINE AND DEUTERIUM ISOTOPE SHIFTS IN THE ^{19}F NMR SPECTRA OF SOME FLUOROBENZENES AND FLUOROANILINES

BY

GUY M. BERNARD

A Thesis/Practicum submitted to the Faculty of Graduate Studies of the University of Manitoba in partial fulfillment of the requirements for the degree of

MASTER OF SCIENCE

To Alice, Doris and Al

Acknowledgments.

I would like to thank Dr. Ted Schaefer for his help and encouragement during the years that I worked in his laboratory, and particularly for his advice during the writing of this thesis.

I thank Dr. Frank Hruska for the many engaging conversations over the past few years. I also thank him, along with Dr. Jim Peeling, for reading this thesis.

I thank Dr. Kirk Marat and Mr. Tad Foniok for their assistance with the spectrometer, and for their help with the computer software and hardware used in this laboratory.

I am very grateful to Dr. Kathy Gough for her advice on vibrational spectroscopy, and also for providing some computer software used in this work.

During my years at the University of Manitoba, I made many new friends. I will always be grateful to Mark Soliven, Vinh Pham, Randy Babiuk, Allyson Kula, Kerri-Ann Lee, Jeremy Kunkel, Ayeda Ayed, Rob Schurko and Maria Orobia for their support and friendship. I especially want to thank my 'old' friends, Gérald and Sandra Dubé, Norbert and Linda Bellec, as well as Joan and Darell Diebert, for their understanding and continuing friendship.

It is impossible to express in a few words the gratitude I feel towards my family for their unfailing support during my university years. Their encouragement has been invaluable.

Finally, I would like to acknowledge the financial assistance of the Natural Sciences and Engineering Research Council of Canada and the University of Manitoba.

List of Publications.

1 T. Schaefer, J. P. Kunkel, R. W. Schurko, and G. M. Bernard. A precise analysis of the ^{1}H nuclear magnetic resonance spectrum of 2-phenyl-1,3-dithiane. Ring pucker, signs of long-range J(H,H), internal rotational barrier, and van der Waals shifts. *Can. J. Chem.* **72,** 1722, (1994).

2 T. Schaefer, R. W. Schurko, and G. M. Bernard. Does the Csp^2-Csp^3 barrier in ethylbenzene have a hyperconjugative component? An indirect experimental and theoretical approach. *Can. J. Chem.* **72,** 1780, (1994).

3 T. Schaefer, C. S. Takeuchi, G. M. Bernard, and F. E. Hruska. Theoretical and experimental barriers to internal rotation in 2,6-difluorobenzaldehyde and 2,4,6-trifluorobenzaldehyde. Relatively low barriers. *Can. J. Chem.* **73,** 106 (1995).

4 G. M. Bernard and R. W. Schurko. Long-Range $^{37}Cl/^{35}Cl$ and $^{81}Br/^{79}Br$ Isotope Shifts in the ^{19}F NMR Spectra of Some Substituted Fluorobenzenes. *Magn. Reson. Chem.* **33,** 879 (1995).

5 T. Schaefer, G. M. Bernard and F. E. Hruska. An estimate of the spin-spin coupling constant, $^{1}J(^{1}H,^{13}C)$, in gaseous benzene. *Can. J. Chem.* in press (1996).

6 T. Schaefer, G. M. Bernard and F. E. Hruska. Reflection in the ^{1}H nmr spectrum of $^{37}Cl/^{35}Cl$ isotope effects on the ^{19}F nmr chemical shifts of 1-chloro-2,4-difluorobenzene. An isotope effect over five bonds. *Can. J. Chem.* in press (1996).

7 T. Schaefer, G. M. Bernard, Y. Bekkali and D. W. McKinnon. Theoretical and experimental approaches to the effects of solvation on the small internal rotational potential of benzal fluoride. *Can. J. Chem.* in press (1996).

8 X. Ou, G. M. Bernard and F. A. Janzen. Oxidative addition and isomerization reactions: the synthesis of *cis*- and *trans*-$ArSF_4Cl$ and *cis*- and *trans*-$PhTeF_4Cl$. In preparation, to be submitted to *Can. J. Chem.* (1996).

Table of Contents

List of Tables

List of Figures.

Abstract.

Isotope shifts in the ^{19}F NMR spectra of some fluorobenzenes, arising from the natural abundance isotopes of chlorine and bromine, are reported. The heavier isotope of chlorine results in increased shielding of the ^{19}F nucleus, and its effects are observed over as many as six formal bonds. The almost equal natural abundances of the bromine isotopes make the determination of a sign for this isotope shift less certain, but slight differences in intensity suggest that the heavier isotope of bromine also increases the shielding. This isotope shift is observed over three and four bonds.

While the three-bond isotope shifts appear invariant to the substitution pattern on the ring, large variations occur for the remaining isotope shifts. These isotope shifts do not correlate with other molecular properties, such as spin-spin coupling constants or the chemical shift of the observed nucleus. This implies that the secondary shielding derivative, arising from the change in the C—Cl or C—Br bond length following isotopic substitution, is not the only significant factor in these isotope shifts. It is shown that the resonant and substituted nuclei are subject to vibrational coupling, possibly a significant factor in the magnitude of the isotope shifts.

Long-range deuterium isotope shifts on the ^{19}F NMR spectra of some fluoroanilines are also reported. These isotope shifts, arising from substitution of the amino protons with deuterium, usually result in deshielding of the ^{19}F nucleus, located at the *ortho*, *meta* or *para* positions. The deshielding is attributed to a slight perturbation of the conjugation of the electron pair of the amino group. A distinctive feature of most of these isotope shifts, their non-additivity, may also arise from a perturbation of conjugation.

1. Introduction

1. Introduction.

The mass effect of isotopic substitution on a molecule will manifest itself in various ways, such as altered equilibria or reaction rates. As another example, isotopic substitution will result in a change in the shielding of the molecule's nuclei. Such effects, when they are observed at other nuclei on the molecule, are known as secondary isotope effects. Here, we are concerned with the secondary effect of isotopic substitution on the NMR chemical shift of the resonant nuclei of the molecule, which, for the sake of brevity, will be referred to as an isotope shift.

Secondary isotope shifts may be subdivided into two categories. Intrinsic, or direct, isotope shifts are ones which may be directly attributed to the isotopic substitution. Rigid molecules exhibit primarily intrinsic isotope shifts. Equilibrium isotope shifts are ones in which isotopic substitution leads to changed molecular properties, such as conformer populations, which are also reflected in the chemical shift of the observed nucleus. Such an effect is most often observed when the substituted isotope is subject to hydrogen-bonding or to internal rotation. If the observed nucleus is not too distant, both intrinsic and equilibrium isotope shifts can occur simultaneously.

We will follow the notation introduced by Gombler[1] where ${}^{n}\Delta A({}^{m'/m}X)$ represents the change in the nuclear shielding of nucleus A resulting from the isotopic substitution of ${}^{m}X$ by ${}^{m'}X$ ($m' > m$), X being n bonds distant from A. This isotope shift is defined by

$$ {}^{n}\Delta A({}^{m'/m}X) = \delta A({}^{m'}X) - \delta A({}^{m}X). \qquad (1.1) $$

In (1.1), $\delta A({}^{m'}X)$ and $\delta A({}^{m}X)$ represent the chemical shifts, in ppm with respect to a reference, of A in the presence of ${}^{m'}X$ and ${}^{m}X$, respectively. ${}^{n}\Delta A({}^{m'/m}X)$ is usually reported in

ppb or, for larger isotope shifts, in ppm. From (1.1), we see that a negative isotope shift implies increased shielding. This sign convention is far from universal in the literature. To avoid confusion, reported isotope shifts using the opposite sign convention will be converted to fit the above definition.

When one or both of the substituted and resonant nuclei are on a cyclic system, there are two paths between the nuclei and hence two possible contributions to the observed isotope shift. For example, a ^{19}F atom *ortho* to a proton on a benzene ring experiences both $^{3}\Delta^{19}F(^{2/1}H)$ and $^{7}\Delta^{19}F(^{2/1}H)$ following substitution of the proton by deuterium. Unless otherwise stated, isotope shifts will be reported on the assumption that the major contribution to the observed isotope shift is the one arising from the shortest path along the ring between the substituted and resonant nuclei - the smallest value of n - it being understood that there may in fact be two significant contributions to the observed isotope shift.

The primary isotope shift is defined as[2]

$$^{P}\Delta = \delta(^{m'}X) - \delta(^{m}X). \qquad (1.2)$$

This, the change in the chemical shift of the substituted nucleus, is usually reported in ppm. Primary isotope shifts have rarely been observed and will not be considered further here.

1.1 An overview

In 1952, Ramsey[3] predicted that the effect of isotopic substitution on the vibrational and rotational (rovibrational) properties of the molecule would result in an isotope shift. The first observed isotope shift was reported by Winett[4] in 1953. He observed a one-bond deuterium isotope shift on the ^{1}H NMR spectrum of molecular hydrogen. The first observation of an isotope shift on a ^{19}F NMR spectrum was reported by Tiers[5] in 1957. In his investigation of the CF_2D group of n-heptafluoropropane, he determined that $^{2}\Delta^{19}F(^{2/1}H)$ was -0.60 ppm. The negative isotope shift was attributed to the greater electron-donating power of the deuteron compared to the proton. A similar, but much smaller effect on the ^{1}H spectrum of toluene was also reported by Tiers in 1958.[6]

In 1969, the first chlorine isotope shift on a ^{19}F NMR spectrum was observed by Carey *et al*, who showed that trichlorofluoromethane was not a suitable internal reference for ^{19}F NMR spectroscopy because of the asymmetry resulting from $^{2}\Delta^{19}F(^{37/35}Cl)$.[7] In 1995, long-range chlorine isotope shifts (n>3) on ^{19}F NMR spectra were reported by Bernard and Schurko,[8] who observed isotope shifts over three and four bonds in the ^{19}F NMR spectra of substituted fluorobenzenes. In the same paper, the first observation of a three-bond bromine isotope shift was reported. A few months earlier, the first bromine isotope shift on ^{19}F NMR spectroscopy had been reported by Tordeux *et al*, who observed a $^{2}\Delta^{19}F(^{81/79}Br)$ of 0.7 - 1.0 ppb on various substituted methanes and ethanes.[9] No sign for this isotope shift was given.

Initially, isotope shifts were observed primarily for ^{19}F and ^{13}C NMR, usually resulting from substitution of a proton by a deuteron. These effects were relatively easy to observe

because of the large shift range of the ^{13}C and ^{19}F nuclei and because of the large mass effect resulting from the substitution. Because of the ease of incorporation of deuterium into most molecules, deuterium isotope effects remain the most commonly measured isotope shift. However, the advent of high field Fourier Transform NMR spectrometers has facilitated the observation of less common nuclei and greatly improved the resolution of their spectra. This has permitted the measurement of isotope shifts on most resonant nuclei.[10] Recently reported isotope shifts include $^{1}\Delta^{51}V(^{13/12}C)$,[11] $^{1}\Delta^{29}Si(^{18/16}O)$,[12] $^{1}\Delta^{19}F(^{86/84/82}Kr)$[13] and $^{1}\Delta^{19}F(^{136/134/132/130/128}Xe)$.[14]

The improved spectrometer resolution also permits the measurement of long-range isotope shifts. For the reasons cited above, most of these are deuterium isotope shifts.[15] Isotope shifts over as many as twelve bonds have been reported. In their investigation of bridged biphenyl compounds, Berger and Künzer observed a $^{12}\Delta^{13}C(^{2/1}H)$ of -2 ppb for a derivative of 1,4-diphenylbutadiene.[16] Excluding deuterium isotope shifts, long-range shifts have also been reported for $^{3,4}\Delta^{1}H(^{13/12}C)$[17] and $^{3,4}\Delta^{19}F(^{13/12}C)$,[18] as well as the $^{3,4}\Delta^{19}F(^{37/35}Cl)$ and $^{3}\Delta^{19}F(^{81/79}Br)$ mentioned above.

1.2 Trends in isotope shifts.

Several general trends in isotope shifts have been observed:[19]

i. Substitution with the heavier isotope usually increases the shielding. Hence, based on equation (1.1), isotope shifts are usually negative.

ii. The magnitude of the shift usually decreases as the number of bonds between the observed and substituted nuclei increases.

iii. The magnitude of the shift is a function of the shift range of the observed nucleus. Hence, nuclei such as ^{13}C or ^{19}F, as well as heavier nuclei, are well suited for the observation of isotope shifts.

iv. The magnitude of the shift is related to $(m'-m)/m'$, the fractional change in mass upon isotopic substitution. Hence, the largest possible isotope shift will result from substitution of tritium for a proton, although deuterium substitution is much more common.

v. Isotope shifts are usually additive, provided the atoms being substituted are in chemically equivalent positions relative to the resonant nucleus.

Other trends are known:[20]

a. One-bond isotope shifts usually increase with increasing bond order and decrease with increasing bond length.

b. The isotope shifts in molecules with similar bonds often correlate with the spin-spin coupling between the observed nucleus and the substituted atom.

c. Magnitudes of one-bond isotope shifts correlate with the chemical shift of the observed nucleus.

d. Lone-pair electrons in the molecule have an effect on isotope shifts.

e. Isotope shifts tend to increase when electronegative substituents are introduced at the substitution site.

These less general trends are discussed in greater detail in section 1.4.

1.3 Theoretical considerations.

When isotopic substitution occurs, the mass change affects the electronic properties of the molecule. In particular, all resonant nuclei linked to the substitution site by an efficient electronic pathway will be affected.[21] The magnitude and signs of isotope shifts are affected by a dynamic factor and an electronic factor. The dynamic factor is the slight change in the rovibrationally averaged geometry resulting from isotopic substitution. The electronic factor depends on the chemical shift range of the resonant nucleus and on the electronic pathway(s) between the substitution site and the resonant nucleus.

The proton/electron mass ratio ($\approx$ 1836) results in much greater electron speeds, relative to the nucleus. This permits us to consider the nucleus as stationary, with the electron moving in the electrostatic potential energy field generated by the nucleus.[22] This approximation, known as the Born-Oppenheimer approximation, means that the potential energy surface for a molecule depends on nuclear charges rather than nuclear masses. Hence, within this approximation, isotopomers have the same potential energy surface. If we consider the harmonic approximation to this potential surface, then the energy levels within this potential surface are described by:

$$E = \hbar\left(\upsilon + \frac{1}{2}\right)\left(\frac{k}{\mu}\right)^{1/2} \qquad (1.3)$$

where υ is the vibrational quantum number, k is the force constant for the bond, and μ is the effective mass. Hence, substitution of a heavier isotope will result in a lower potential energy. Because the potential energy is in fact anharmonic, this lower energy translates into a shorter equilibrium bond-length (see figure 1.1, inset).

The Born-Oppenheimer approximation also permits us to consider a shielding surface, $\sigma(r)$, which gives values of nuclear shielding at fixed nuclear configurations. There is a characteristic nuclear shielding based on the geometry of the molecule. Since this geometry is based on the rovibrational state of the molecule, the nuclear shielding is intimately connected to the molecular vibrational state. Small changes in the equilibrium geometry of the bond will be reflected in the nuclear shielding of the observed nucleus, giving rise to the isotope shift. The shielding surface for the H_2^+ ion was calculated by Hegstrom.[23] It was found that nuclear shielding decreased as the bond was extended beyond the equilibrium configuration. A similar conclusion was reached by Chesnut, who calculated the shielding derivatives for first row hydrides.[24] He found negative shift derivatives resulting from extension of the X—H bond for elements on the right-hand portion of the periodic table. Hence, as for H_2^+, the shielding is expected to decrease as the bond is extended beyond the equilibrium geometry. In Figure 1.1, a hypothetical shielding surface has been superimposed on a potential surface, showing that a shorter bond length will result in increased shielding, consistent with observed one-bond isotope shifts, which are usually negative.

The dependence of one-bond isotope shifts on the rovibrational surface of the molecule was verified by Nakashima and Takahashi, who found a linear correlation between $^1\Delta^{13}C(^{2/1}H)$ and the C—H stretching frequency of some monosubstituted methane derivatives, as determined by IR spectroscopy.[25] The authors obtained a good correlation ($r = 0.945$) if one point, due to nitromethane, was ignored. No explanation for this anomalous datum is given.

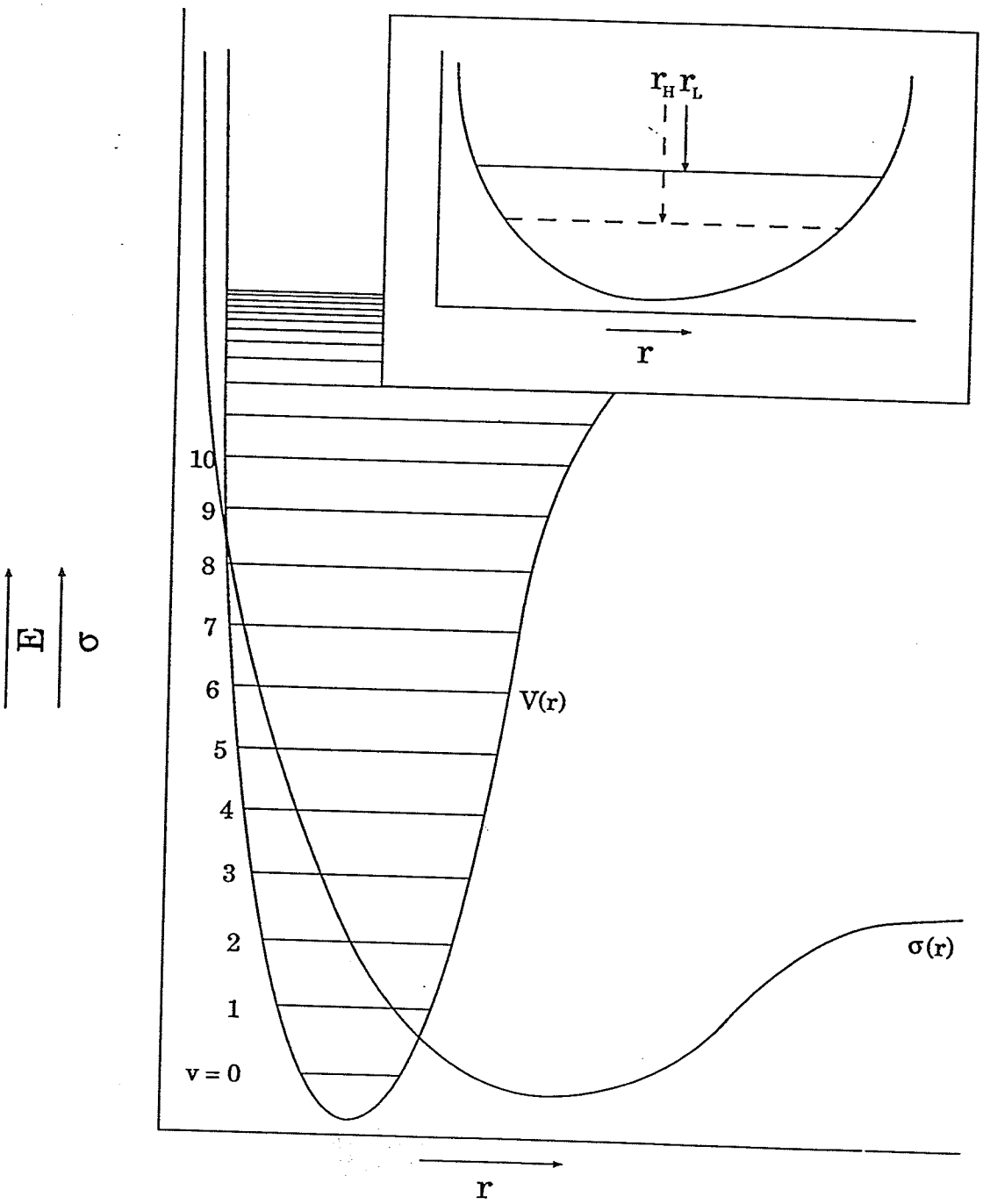
E
σ
r_H r_L
r
10
9
8
7
6
5
4
3
2
1
v = 0
V(r)
σ(r)
r

Figure 1.1

A hypothetical shielding surface, $\sigma(r)$, superimposed on a hypothetical potential energy surface, $V(r)$, both plotted as a function of internuclear separation, r (from reference 20). Inset: The zero-point energies of two isotopomers. The dashed line represents the isotopomer with the heavier nucleus, r_H, indicating its equilibrium bond length, while the solid line and r_L indicate the zero-point energy and equilibrium bond length of the lighter isotopomer. The relative energy differences and anharmonicity of the potential surface have been exaggerated to emphasize the reduced bond length anticipated upon isotopic substitution.

A good theoretical description of one-bond isotope shifts in diatomic molecules is possible.[20] This shift involves a primary dynamic factor, the change in the bond length of the molecule, as well as a primary electronic factor, the change in the shielding resulting from this changed bond length. Using *ab initio* methods, Ditchfield accurately predicted the deuterium isotope shift of HD and D_2 relative to H_2, as well as the deuterium isotope shift on the ^{19}F spectrum of HF.[26]

When considering isotope shifts over more than one bond, secondary factors must be considered. The secondary dynamic factor is the change in the length of the bond to the resonant nucleus resulting from the change in bond length at the substitution site. The change in the nuclear shielding of the resonant nucleus arising from the change in the bond length at the substitution site is known as the secondary electronic factor. If we consider a molecule containing the fragments X—Y and A—Z (A—Y if we are considering a two-bond isotope shift), then the isotope shift at A following substitution of X is

$$^{n}\Delta A(^{m'/m}X) = \frac{\partial \sigma^{A}}{\partial \Delta r_{XY}}\Delta + \frac{\partial \sigma^{A}}{\partial \Delta r_{AZ}}\delta + \cdots \qquad (1.4)$$

The first derivative in (1.4) is the secondary shielding derivative resulting from a change in the X—Y bond length; $\Delta = \langle \Delta r_{XY} \rangle - \langle \Delta r_{XY} \rangle'$, the primary change in the X—Y bond length following isotopic substitution. The derivative in the second term of (1.4) is the primary shielding derivative resulting from a change in the A—Z bond length and $\delta = \langle \Delta r_{AZ} \rangle - \langle \Delta r_{AZ} \rangle'$, the secondary change in the A—Z bond length due to substitution of X by X'. There are also higher order terms in equation (1.4) which are not thought to be significant.[20]

The sign of the secondary shielding derivative is not always the same since secondary effects are more dependent than primary effects on the electronic distribution of the molecule, as well as on its potential surface. Since δ is usually much less important than Δ, the term in equation (1.4) involving δ can often be ignored. The remaining term, which includes the secondary shielding derivative, $\partial\sigma^{A}/\partial\Delta r_{XY}$, is stereospecific and is dependent on the electronic transmission path, as are other observable molecular properties, such as spin-spin coupling constants and substituent effects on chemical shielding. This results in linear correlations with these parameters (see Section 1.4).

Using *ab initio* methods, Raynes *et al* accurately predicted $^{2}\Delta^{1}H(^{37/35}Cl)$ in chloromethane.[27] They found that a change of 4.1×10^{-5} Å in the C—Cl bond length and a change of 6.3×10^{-4} degrees in the Cl—C—H bond angle, as well as a change of 1.0×10^{-6} Å in the C—H bond length, yielded theoretical values for $^{2}\Delta^{1}H(^{37/35}Cl)$ which were in quantitative agreement with experimental results.[28,29]

Intrinsic isotope shifts are usually proportional to the number of substituted atoms in chemically equivalent positions.[20] Osten and Jameson calculated the mean bond displacements in the series of isotopomers $CH_{4-n}T_n$ and $CD_{4-n}T_n$.[30] A linear dependence of the shielding on n was found. Although a rigorous mathematical treatment is possible, a qualitative explanation can be seen from Figure 1.1. Since isotopic substitution results in very small bond displacements, the portion of the shielding surface within the range of the equilibrium bond lengths is effectively linear, resulting in the observed linear relationship between the number of substituents and the isotope shift.

Deviations from additivity can usually be attributed to equilibrium isotope effects. However, Jameson has shown that non-additivity may result from secondary isotope effects on the mean bond displacement.[30(b)] This is the small change in bond length at a given bond resulting from isotopic substitution at another bond. One of the few observed non-additive intrinsic isotope shifts was reported by Wasylishen and Friedrich in their investigation of deuterated ammonium ion isotopomers.[31] They found that the increase in $^{1}\Delta^{14}N(^{2/1}H)$ decreased slightly as the fractional change in mass increased. The degree of non-additivity is in good agreement with the values calculated by Jameson. However, in their study of deuterated halomethanes, Sergeyev *et al* found that Jameson's approach underestimated the degree of non-additivity found in $^{1}\Delta^{13}C(^{2/1}H)$.[32] While agreeing that the non-additivity may be attributed to secondary isotope effects on the bond lengths, the authors suggest that a correction to the term defining the dependence of bond lengths on substitution at other sites may be needed.

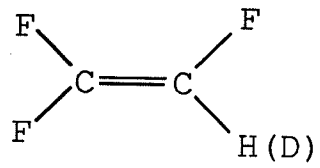

a

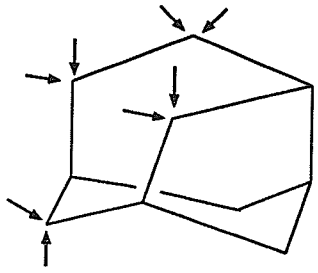

b

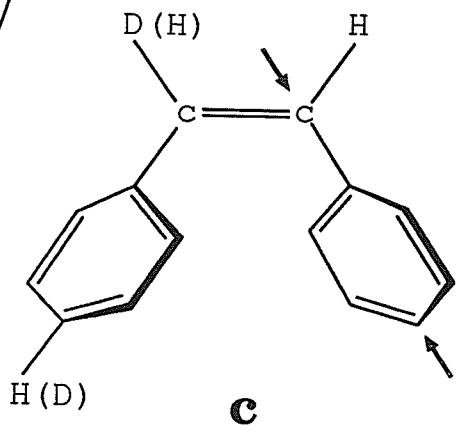

c

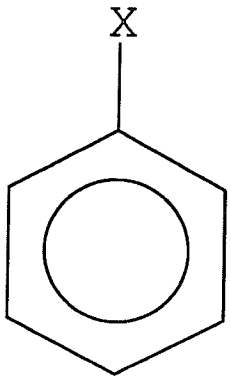

d X = CH_3

e X = CH_2CH_3

f X = $CH(CH_3)_2$

g X = $C(CH_3)_3$

h X = CHO

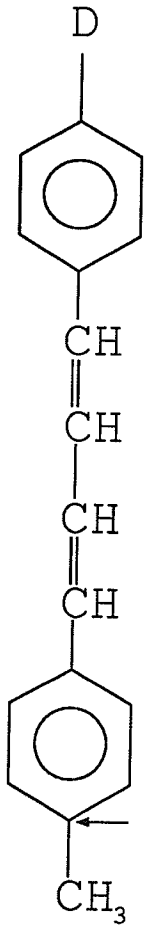

i

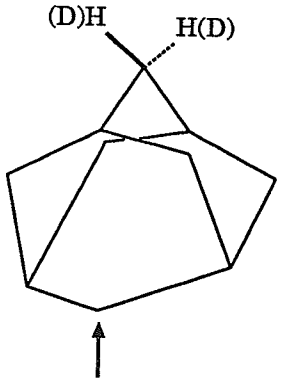

j

Scheme 1 Molecular structures as discussed in Section 1.4.

a. Trifluoroethene. Various mono-, di- and trifluoroethenes, as well as some chlorofluoroethenes were investigated (from reference 35).

b. Protoadamantane. The arrows indicate the deuteration sites for the various monodeuteration experiments. Some di-deuterated isotopomers were also investigated (from reference 36).

c. *Cis*-stilbene. The arrows indicate the two nuclei to which $^{6}\Delta^{13}C(^{2/1}H)$ was observed (from reference 42).

d. Toluene.

e. Ethylbenzene.

f. Isopropylbenzene.

g. *t*-butylbenzene

h. Benzaldehyde.

i. 1-(4-deuterophenyl)-4-(4-methylphenyl)-butadiene. The arrow indicates the nucleus to which $^{6}\Delta^{13}C(^{2/1}H)$ was observed. The authors do not specify which isomer of **i** was investigated (from reference 16).

j. Adamantane. Experiments with mono-deuterated and di-deuterated isotopomers were performed. The arrow indicates the site at which $^{5}\Delta^{13}C(^{2/1}H)$ was observed (from reference 38).

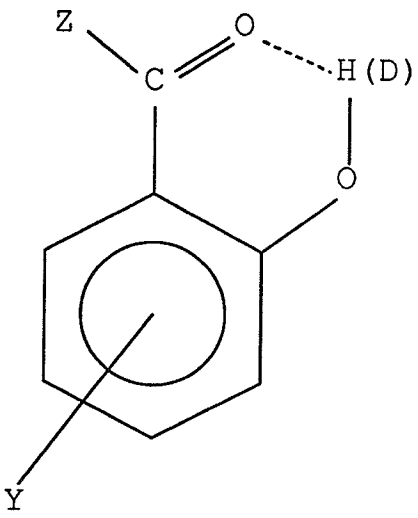
Z
O
C
H(D)
O
Y

k

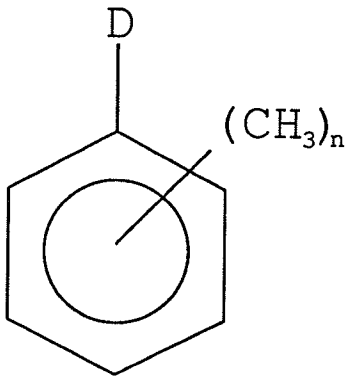
D
(CH3)n

l


H2 C
CHD

n


H3 C
CH2 D

m


HC
CD

o

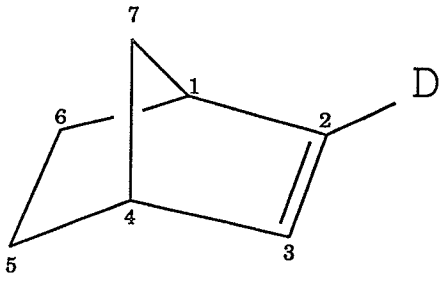
7
1
D
6
2
4
5
3

p

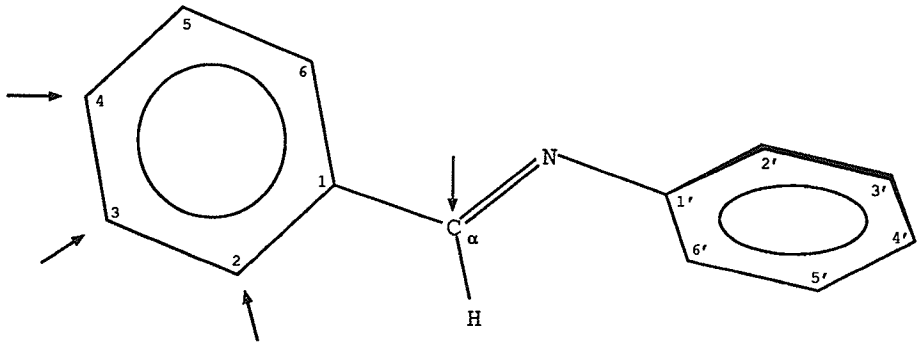
5
6
4
1
3
2
C
α
H
N
2′
1′
3′
6′
4′
5′

q

Scheme 1 (continued).

k. The hydroxyacyl compounds investigated by Hansen *et al.* Z = OR, H or C; R = CH_3 or C_2H_5 and Y = F, CH_3, OH, OCH_3, Cl or Br (from reference 45).

l. Mono-deuterated methylated benzene. All 20 possible molecules with 0 - 5 methyl groups were investigated (from reference 46).

m. Ethane.

n. Ethylene.

o. Acetylene.

p. Norbornene. Derivatives considered had cyclic substituents which included C-5 and C-6, and also, in one case, C-7. Correlations were found between $^{3}\Delta^{13}C(^{2/1}H)$ and $^{1}J(^{13}C\text{-}5,H)$, as well as between $^{4}\Delta^{13}C(^{2/1}H)$ and $^{1}J(^{13}C\text{-}6,H)$ (from reference 49).

q. Trans-N-benzylideaniline. The arrows indicate the sites of mono-deuteration for the various experiments performed (from reference 53).

1.4 Empirical relationships.

While approximate methods of calculating isotope shifts for larger molecules exist,[20] theoretical calculations must await the refinement of the theory, as well as the advent of more powerful computers. Thus, in order to better understand long-range isotope shifts, correlations have been attempted with other molecular properties which are themselves related to small changes in molecular geometry.

1.4.1 Effect of geometry; correlation with coupling constants.

Due to the abundance of data and the strong theoretical background for spin-spin coupling constants,[33] linear correlations between these values and $^{n}\Delta A(^{m'/m}X)$ would elucidate long-range isotope shifts. Such a correlation was first reported in 1963 by Frankiss,[34] who found a linear relationship between $^{1}\Delta^{19}F(^{13/12}C)$ and $^{1}J_{CF}$ in substituted methanes. A separate linear relationship was also observed for the above in unsaturated systems.

Several studies have found correlations between isotope shifts and stereospecific coupling constants. In a detailed study of fluoroethenes (**a**), Osten *et al* reported a stereochemical dependence of the measured isotope shifts.[35] They found a linear relationship between the geminal and three-bond *trans* isotope shifts and the corresponding coupling constants. The small range of the *cis* coupling constants precluded such a comparison for the *cis* isotope shifts, but the same general trend was observed. It was also noted that $^{3}\Delta(trans) > {}^{3}\Delta(cis)$, consistent with the trends observed for coupling constants. The

authors suggest that, since the spin-spin coupling constant is a purely electronic property, the observed isotope shifts are indicative of the electronic distribution in the molecule.

Several investigators have reported a stereochemical dependence of $^{3}\Delta^{13}C(^{2/1}H)$.[36] In their investigation of protoadamantane isotopomers (**b**), Majerski *et al* found that $^{3}\Delta^{13}C(^{2/1}H)$ depended on the dihedral angle between the C_β—C_γ bond and the C_α—H(D) bond.[36] This dihedral angle dependence is analogous to the Karplus relationship, although a direct comparison cannot be made, since $^{3}\Delta$(0 degrees) > $^{3}\Delta$(180 degrees). The authors argue that at least a component of the isotope shift must be transmitted by the same mechanism as the vicinal coupling. In their investigation of isotope shifts in *cis*-stilbene (**c**), whose phenyl rings are 40 - 50° out of plane, Meić *et al* obtained values of -8.6 and -1.4 ppb for $^{6}\Delta^{13}C(^{2/1}H)$ resulting from mono-deuteration at C-α and C-4' respectively.[42] Comparing these values to the -10.2 ppb observed for $^{6}\Delta^{13}C(^{2/1}H)$ resulting from *para*-deuteration of *trans*-stilbene, for which the comparable dihedral angle is 10 - 20°, as well as with the -15.0 ppb obtained for planar diphenylacetylene, the authors conclude that deviation from planarity reduces long-range isotope shifts.

Schaefer *et al* found a very good linear relationship between $^{6}J(H_\alpha,H_p)$ and $^{5}\Delta^{13}C(^{2/1}H)$ in toluene (**d**), ethylbenzene (**e**) and isopropylbenzene (**f**).[37] $^{6}J(H_\alpha,H_p)$ has a $\langle\sin^2\Theta\rangle$ dependence, where Θ is the angle formed by the C_α—H(D) bond with the π plane of the ring and $\langle\sin^2\Theta\rangle$ is the expectation value of Θ. Since the hyperconjugative interaction will be maximal when the C—H(D) bond is perpendicular to the phenyl plane, it is also expected to have a $\langle\sin^2\Theta\rangle$ dependence. Hence, the authors argue that the hyperconjugative model

for deuterium isotope shifts proposed by Wesener and Günther is valid (see the following section, ref. 39).

Just as for coupling constants, π electrons are believed to be an important electronic factor in the transmission of isotope shifts. A deuterium isotope shift on ^{13}C over twelve bonds, a record, was transmitted entirely over the π system of 1-(4-deuterophenyl)-4-(4-methylphenyl)-butadiene (**i**).[16] In contrast, the only known five-bond intrinsic isotope shift in a saturated system was reported by Mlinaric-Majerski *et al* who observed $^{5}\Delta^{13}C(^{2/1}H)$ in some adamantane isotopomers (**j**).[38] Other long-range isotope shifts in saturated molecules have been reported, but these have been attributed to equilibrium isotope effects.

1.4.2 Deuterium as a substituent.

Long-range deuterium isotope shifts on ^{13}C NMR have been explained in terms of substituent effects, the deuterium atom simply being treated as a substituent. This explanation suggests different electronic properties for the deuteron compared to the proton, which implies a breakdown of the Born-Oppenheimer approximation. Nevertheless, such a model has been used successfully by several authors to explain observed deuterium isotope shifts. In their investigation of **d**, **e**, and **f**, Wesener and Günther explained the magnitudes of $^{3}\Delta^{13}C(^{2/1}H)$ in terms of the lower electron donating ability of the C—D bond relative to the C—H bond, resulting in reduced hyperconjugation of the C_i—C_α bond.[39] A similar model has been used by several authors.[40] However, it has been argued that these shifts can be explained equally well without violating the Born-Oppenheimer approximation.[20] Vikić-Topić *et al* investigated the charge/shift relationships of some deuterated aromatic

molecules using *ab initio* methods.[41] This was done by simulating the effect of deuteration on the stretching and bending modes by varying the bond lengths and angles. They found that the observed isotope shifts could be explained in terms of small changes in molecular geometry, consistent with the Born-Oppenheimer approximation. Yet, Meić *et al* argue that a small, vibrationally induced dipole moment resulting from deuterium substitution may induce a C—C π-bond polarization.[42] This is not a violation of the Born-Oppenheimer approximation since the π polarization arises from the slight changes in C—H(D) bond lengths upon isotopic substitution. They also argue that such a mechanism is consistent with the observed alternation of sign for the long-range isotope shifts observed in *cis*-stilbene.

1.4.3 The effect of other substituents; correlations with the chemical shift.

While treating deuterium as a substituent remains controversial, other substituents in the molecule are known to affect the isotope shift. This is not a violation of the Born-Oppenheimer approximation, since substituents in a molecule are known to affect the rovibrational state of the remaining atoms.[43] In their study of chlorinated methanes, Sergeyev *et al* found that $^{1}\Delta^{13}C(^{37/35}Cl)$ decreased with successive chlorine substitutions, from -6.0 ppb for chloromethane to -3.0 ppb per chlorine atom for carbon tetrachloride.[44] In his investigation of substituted ortho-hydroxyacyl compounds (**k**), Hansen found correlations between $^{n}\Delta^{13}C(^{2/1}H)$ on the one hand and δ(OH) and $\delta(^{13}C)$ on the other.[45] Observed isotope shifts following substitution at positions *ortho* or *para* to the hydroxyl group corre-

lated with δ(OH), as did *meta* substitution, albeit with a different slope. These correlations are discussed in terms of hydrogen bonding and of substituent effects on chemical shifts.

In a more systematic study, all possible mono-deuterated methylated benzenes (**l**) were investigated by Berger and Diehl.[46] They determined that, for those methylated benzenes which did not have adjacent methyl groups, $^{n}\Delta^{13}C(^{2/1}H)$ could be calculated accurately from the observed isotope shifts of *ortho, meta* and *para* deuterated toluene using an incremental system analogous to that used to calculate ^{13}C chemical shifts. For the molecules which did have adjacent methyl groups, the isotope shift could still be predicted accurately by including a correction term to allow for the steric factor between adjacent methyl groups. In their investigation of deuterated *t*-butyl groups on *t*-butylbenzene derivatives (**g**),[47] Balzer and Berger found that $^{3}\Delta^{13}C(^{2/1}H)$ correlated with $\delta(^{13}C_i)$. Since this chemical shift is affected by substituents, the substituent effects on isotope shifts are discussed.

1.4.4 Hybridization.

In their investigation of ethane (**m**), ethylene (**n**) and acetylene (**o**), Wesener *et al* found a linear relationship between the degree of hybridization, or s-character, of the carbon atoms and $^{1}\Delta^{13}C(^{2/1}H)$.[48] The relationship held only for molecules which were closely related in structure. Hence, a linear relationship with a different slope was found for the 1-phenyl derivatives of the above molecules, suggesting that substituent effects are also a major factor in these isotope shifts. Wondering if this relationship could be applied to long-range isotope shifts, Künzer *et al* investigated some norbornene derivatives (**p**).[49]

They found a linear relationship between $^{3,4}\Delta^{13}C(^{2/1}H)$ and the one-bond coupling at these positions, which is itself related to the hybridization of the carbon atom.

The s-character of an orbital affects the bond length as well as the bond order of the bond(s) to the nucleus being considered.[50] Hence, we also expect to find correlations between these parameters and isotope shifts. Such correlations were in fact found by Sardella and El-Din in their study of several neutral π systems.[51] The authors found that - $^{2}\Delta^{13}C(^{2/1}H)$ correlates with Hückel π-bond orders and with atom-atom polarizabilities, giving correlation coefficients of 0.914 and 0.924 respectively. Correlations were also found between the C—C bond length of the atoms adjacent to the substituted proton and $^{2}\Delta^{13}C(^{2/1}H)$, although with a correlation coefficient of only 0.889. The poor correlation in this case is attributed to limited data on C—C bond lengths, as well as to the small range of these bond lengths. A much better correlation coefficient (0.930) was obtained when calculated bond lengths were used.

1.4.5 The effect of lone-pair electrons on isotope shifts.

Lone-pair electron interactions may have a significant effect on isotope shifts. In their study of deuterated benzaldehydes (**h**), Vujanić *et al* investigated all the mono-deuterated benzaldehydes, as well as the two possible benzaldehydes with per-deuterated phenyl rings. They found that the mean value of $^{2}\Delta^{13}C(^{2/1}H)$ for the C-2, C-3 and C-4 sites was -109.5 ppb, while that for C-1, resulting from deuteration at C-α and C-*ortho*, was -72.6 and -69.6 ppb respectively.[52] Noting that similar decreases have been reported for other molecules containing a non-rigid group which includes an atom with lone-pair electrons,

the authors conclude that steric interactions of the lone-pair electrons with their surroundings is responsible for the decrease. Similarily, Smrečki *et al* found that deuteration of the C-α or C-2 positions of *trans*-N-benzylideanilines (**q**) both yielded $^{2}\Delta^{13}C(^{2/1}H)$ values of -73 ppb at C-1.[53] Since the lone-pair electrons are nearly coplanar with the C-phenyl moiety, the C-phenyl *ortho* protons are much closer to the electron pair than are the *ortho* protons of the other phenyl ring. Hence, the lower value is attributed to a steric interaction between the C-phenyl protons and the lone-pair electrons. The authors also attribute the unusual positive sign of $^{3}\Delta^{13}C(^{2/1}H)$ observed at C-1', resulting from deuteration at C-α, to an interaction between the lone-pair electrons and C-1'.

1.5 Applications

Isotope shifts have been used to study other molecular properties. Structural information has been obtained using the empirical relationships discussed above.[54] The magnitude of observed chlorine isotope shifts has been used to elucidate the substitution pattern on a phenyl ring.[55] In the course of this work, $^{3,4}\Delta^{19}F(^{37/35}Cl)$ were used to identify 1,2-dichloro-3-fluorobenzene as an impurity in a benzal chloride sample. The inclusion of chlorine in phenyl sulfur tetrafluoride monochloride derivatives was verified in this laboratory using $^{2}\Delta^{19}F(^{37/35}Cl)$.[56] Tordeux *et al* used $^{2}\Delta^{19}F(^{37/35}Cl)$ to determine the number of chlorine atoms geminal to a fluorine atom in ethane derivatives.[9] They also showed that the approach could be extended to bromine substitution.

Equilibrium isotope shifts have been used to monitor dynamic molecular properties, such as tautomeric processes, conformational interconversion and intermolecular interactions.[54] Hansen has also shown that intramolecular hydrogen bonding could be characterized through the observation of deuterium isotope shifts.[45]

1.6 Introduction to the problem.

Long-range $^{37}Cl/^{35}Cl$ and $^{81}Br/^{79}Br$ isotope shifts on the ^{19}F NMR spectra of substituted fluorobenzenes have been reported by this laboratory.[8] While $^{3}\Delta^{19}F(^{37/35}Cl)$ and $^{3}\Delta^{19}F(^{81/79}Br)$ appear to be invariant to the substitution pattern on the phenyl ring, a large range of values for $^{4}\Delta^{19}F(^{37/35}Cl)$ has been found. Several examples of $^{5}\Delta^{19}F(^{37/35}Cl)$, reported here for the first time, also show a large range of values. Examples of $^{4}\Delta^{19}F(^{81/79}Br)$ have also been found.

The intent of this study is to rationalize the observed values of $^{4,5}\Delta^{19}F(^{37/35}Cl)$ through empirical relationships. In order to do this, the ^{19}F spectra of a series of 2-chloro-6-fluorobenzene derivatives, with various substituents at the C-1 position, are investigated, as well as 10 of the 19 possible mono-chlorofluorobenzenes. Numerous bromofluorobenzene derivatives are also investigated in an attempt to elucidate $^{4}\Delta^{19}F(^{81/79}Br)$.

While investigating the above phenomena, previously unreported deuterium isotope shifts on the ^{19}F NMR spectra of some fluoroanilines, arising from the isotopic substitution of the amino protons with deuterium, were discovered. Hence, a further goal of this study is to investigate these isotope shifts, particularly their anomalous signs and their non-additivity.

2. Experimental Methods

2 Experimental Methods.

2.1 Sample Preparation.

Compounds **1-44** were acquired commercially and used without further purification (see Scheme 2 for the names and formulae of **1-44**). These samples were dissolved in a solution of acetone-d_6 containing 0.25 mol% C_6F_6 as the fluorine reference and 0.25 mol% TMS as the proton reference, except for **8** and **20** which were dissolved in CS_2 containing also 0.25 mol% C_6F_6, 0.25 mol% TMS and 10 mol% C_6D_{12}, (used as an internal lock reference). **19** was prepared in both acetone-d_6 and CS_2 as described above. The above were 5 mol% solutions, except **9,** which was a very dilute impurity in **4**. These samples were filtered into 5mm od NMR tubes which were then degassed by at least 5 cycles of the freeze-pump-thaw procedure and flame-sealed to give reasonably symmetric tops.

Compounds **45 - 47** (Scheme 2) were synthesized[56] from diphenyl disulfide, xenon disulfide and Cl^- and prepared as dilute solutions in a CD_2Cl_2/CH_2Cl_2 mixture, containing also a drop of C_6F_6. Because HF, which will react with glass, is a by-product of the synthesis procedure, these samples were filtered into teflon tubes which were then inserted into 5mm od NMR tubes. These samples were not degassed, since teflon leads to line-broadening, regardless of how the solution is prepared.

Another sample of **31,** as well as compounds **48-52** (Scheme 2), also acquired commercially, were prepared as 5 mol% solutions in acetone-d_6 and in a solution of CCl_4 containing also 0.25 mol% C_6F_6, 0.25 mol% TMS and 10 mol% C_6D_{12}. These samples were filtered into 5 mm od NMR tubes and analyzed without degassing. To promote exchange of the amino protons with deuterium, D_2O was added incrementally to **31.** Since D_2O

alone would not promote exchange for **48-52**, a 3.8 M solution of NaOH, dissolved in D_2O, was prepared. This solution was added in aliquots (3.0 to 20.0 μL) directly to the NMR tube containing the sample. Because D_2O is not miscible in CCl_4, these samples were shaken vigorously for about five minutes prior to acquisition of spectra to permit exchange with the amino protons.

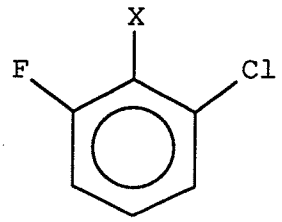

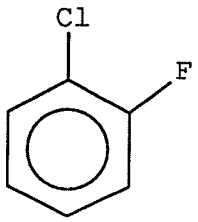

10

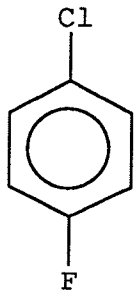

11

1 X = H

2 X = CH_3

3 X = CH_2Cl

4 X = $CHCl_2$

5 X = CCl_3

6 X = CN

7 X = COCl

8 X = CHO

9 X = Cl

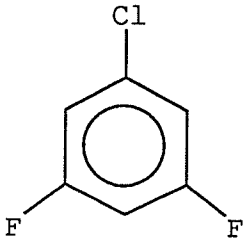

12

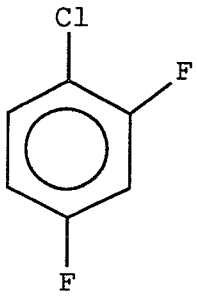

13

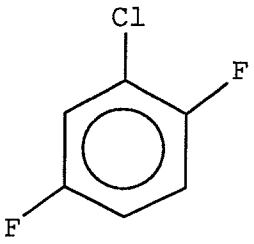

14

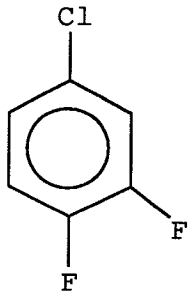

15

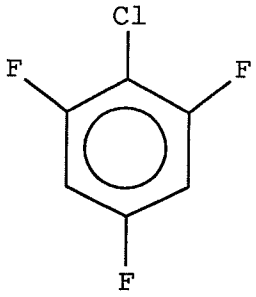

16

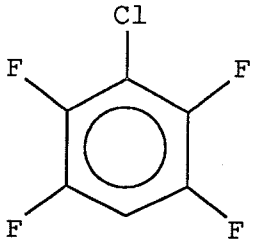

17

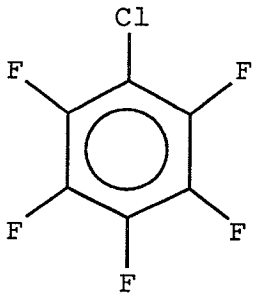

18

Scheme 2. Compounds **1-52**.

1. 1-chloro-3-fluorobenzene.

2. 2-chloro-6-fluorotoluene.

3. 2-chloro-6-fluorobenzyl chloride.

4. 2-chloro-6-fluorobenzal chloride.

5. 2-chloro-6-fluorotrichloromethylbenzene.

6. 2-chloro-6-fluorobenzonitrile.

7. 2-chloro-6-fluorobenzoyl chloride.

8. 2-chloro-6-fluorobenzaldehyde.

9. 1,2-dichloro-3-fluorobenzene.

10. 1-chloro-2-fluorobenzene.

11. 1-chloro-4-fluorobenzene.

12. 1-chloro-3,5-difluorobenzene.

13. 1-chloro-2,4-difluorobenzene.

14. 1-chloro-2,5-difluorobenzene.

15. 1-chloro-3,4-difluorobenzene.

16. 1-chloro-2,4,6-trifluorobenzene.

17. 1-chloro-2,3,5,6-tetrafluorobenzene.

18. chloropentafluorobenzene.

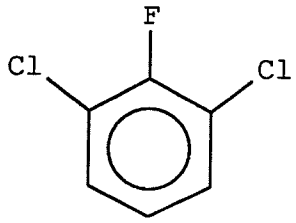

19

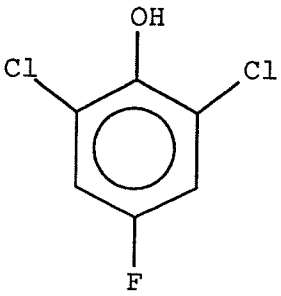

20

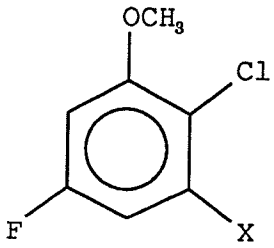

21 X = H

22 X = F

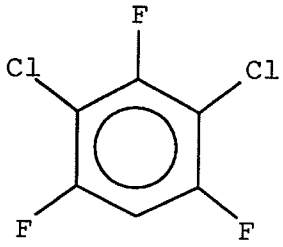

23

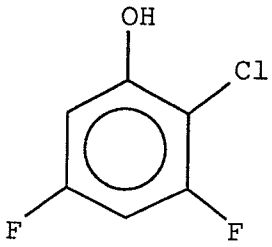

24

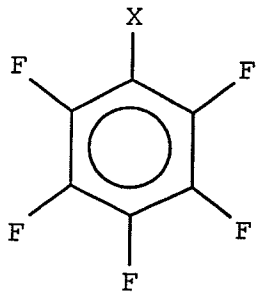

27 X = COCl

28 X = SO_2Cl

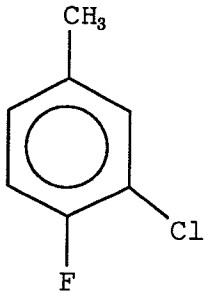

25

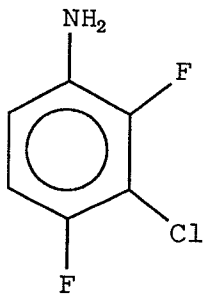

26

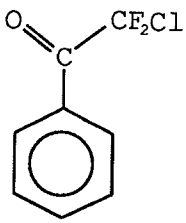

29

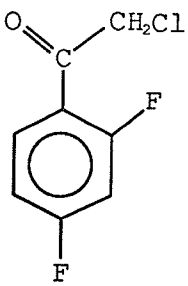

30

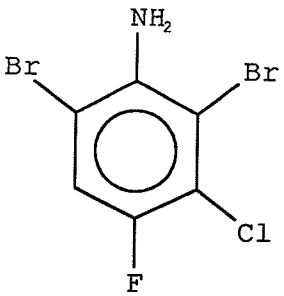

31

Scheme 2 (continued).

19. 1,3-dichloro-2-fluorobenzene.

20. 2,6-dichloro-4-fluorophenol.

21. 2-chloro-5-fluoroanisole.

22. 2-chloro-3,5-difluoroanisole.

23. 1,3-dichloro-2,4,6-trifluorobenzene.

24. 2-chloro-3,5-difluorophenol.

25. 3-chloro-4-fluorotoluene.

26. 3-chloro-2,4-difluoroaniline.

27. pentafluorobenzoyl chloride.

28. pentafluorophenylsulfonyl chloride.

29. 2-chloro-2,2-difluoroacetophenone.

30. 2',4'-difluoro-2-chloroacetophenone.

31. 2,6-dibromo-3-chloro-4-fluoroaniline.

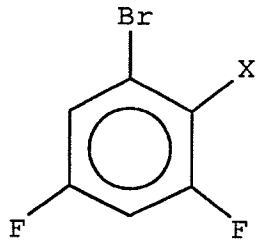

32 X = H

33 X = F

34 X = Br

35 X = I

36 OCH_2CH_2Cl

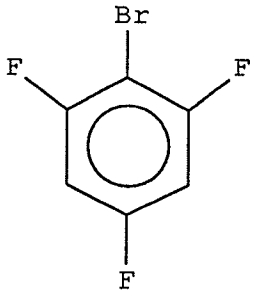

37

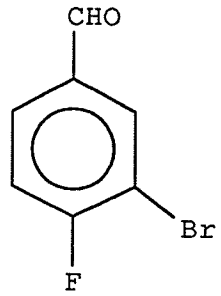

38

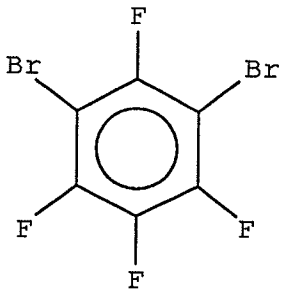

39

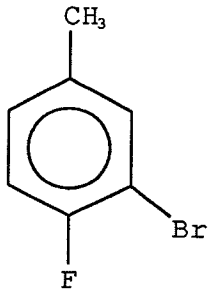

40

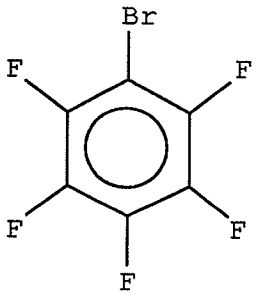

41

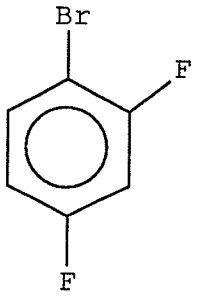

42

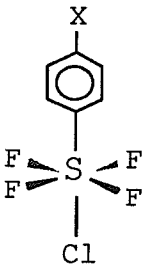

45 X = H

46 X = NO_2

47 X = CH_3

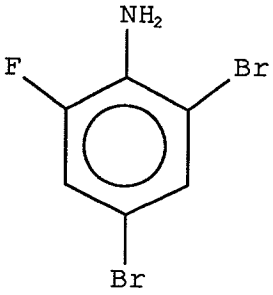

43

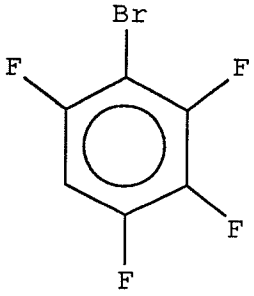

44

Scheme 2 (continued).

32. 1-bromo-3,5-difluorobenzene.

33. 1-bromo-2,3,5-trifluorobenzene.

34. 1,2-dibromo-3,5-difluorobenzene.

35. 1-bromo-3,5-difluoro-2-iodobenzene.

36. α-(2-bromo-4,6-difluorophenoxy)-β-chloroethane.

37. 1-bromo-2,4,6-trifluorobenzene.

38. 3-bromo-4-fluorobenzaldehyde.

39. 1,3-dibromo-2,4,5,6-tetrafluorobenzene.

40. 3-bromo-4-fluorotoluene.

41. bromopentafluorobenzene.

42. 1-bromo-2,4-difluorobenzene.

43. 2,4-dibromo-6-fluoroaniline.

44. 1-bromo-2,3,4,6-tetrafluorobenzene.

45. phenylsulfur(VI) tetrafluoride monochloride.

46. *p*-nitrophenylsulfur(VI) tetrafluoride monochloride.

47. *p*-methylphenylsulfur(VI) tetrafluoride monochloride.

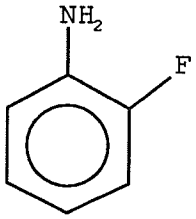

48

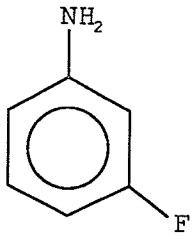

49

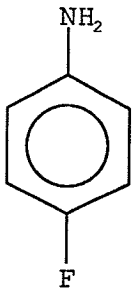

50

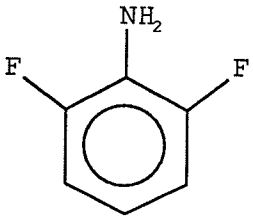

51

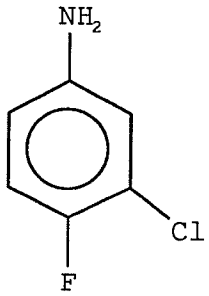

52

Scheme 2 (continued).

48. 2-fluoroaniline.

49. 3-fluoroaniline.

50. 4-fluoroaniline.

51. 2,6-difluoroaniline.

52. 3-chloro-4-fluoroaniline.

2.2 Spectroscopic Methods.

NMR spectra of **1-52** were acquired at 300 K on a Bruker AM 300 spectrometer. In addition, spectra for **4** were acquired on this spectrometer at temperatures ranging from 200 - 300 K. Extensive shimming was required to ensure a homogeneous field. This was done by shimming, first on the lock signal, then on the free induction decays (FIDs) of the C_6F_6 or TMS reference peaks. Once symmetric reference peaks with narrow line widths were obtained (usually less than 0.1 Hz at half-height for the degassed samples), the exact positions of these peaks were determined in order to reference properly the spectra which were subsequently acquired.

^{19}F NMR spectra of **1-44** were acquired at 282.363 MHz. Spectral widths of 100 - 200 Hz, acquisition times of approximately 40 seconds and 16 - 32 K data points gave a digital resolution of 0.013 Hz/pt; 32 - 64 transients of each region were usually acquired. As well, ^{1}H spectra of **3, 4, 6, 12, 13, 15, 19, 20, 22-26, 32-37, 43** and **44** were acquired at 300.135 MHz as for the ^{19}F spectra. Zero-filling to four times the original data set and resolution enhancement (LB = -0.1 - -0.15 Hz, GB = 0.6 Hz) gave line widths at half-height of as little as 0.03 Hz.

Proton-decoupled ^{19}F spectra of **45-47** were acquired with acquisition times of 25 - 30 seconds and spectral widths of 200 - 300 Hz giving an FID resolution before zero-filling of 0.017 Hz/pt. Line widths at half-height were approximately 1 Hz.

8 - 16 transients of the proton decoupled ^{19}F spectra of **48-52,** as well as the coupled spectrum of **31**, were acquired with acquisition times of 10-20 seconds, a relaxation delay

of 5 seconds and spectral widths of 100 Hz, giving an FID resolution of 0.05 Hz/pt. Line widths at half-height were approximately 1 Hz.

^{13}C spectra of **1-8** and **23** were acquired at 75.48 MHz. Spectral widths of 6000 - 12000 Hz, acquisition times of 3 - 5 seconds with 64K data points gave an FID resolution of 0.1 - 0.2 Hz/pt. The FIDs were zero-filled to twice the original data set prior to Fourier transformation, which, with GB and LB equal to zero, gave line widths at half-height of approximately 0.2 Hz.

2.3 Spectral analysis.

Spectra of **6, 13, 15 18-20, 22-24, 28, 29, 33-37** and **44** were analyzed using a highly modified (R. Sebastian and K. Marat) Numarit program.[57] Where possible, separate fits were performed for each series of peaks in the fluorine region attributed to a particular isotopomer. After that, the peak intensities were adjusted to reflect the expected intensity based on the natural abundance of the isotope being considered and the peak files were merged to give the complete computer generated spectrum. Isotope shifts were determined by substituting the optimized chemical shifts from the separate fits into equation (1.1). A complete spectral analysis was not performed for the remaining compounds, precluding the above procedure. For these, the isotope shifts were measured directly from the experimental spectra, as were the ^{13}C parameters, ($\nu(^{13}C)$ and $^{n}J_{C,F}$), of **1 - 8** and **23.**

2.4 Molecular orbital calculations.

Molecular orbital calculations were performed on **1, 2, 6, 7, 9, 11, 13, 15, 16, 18, 21, 22** and **24** using the program Gaussian 94[58]. Hartree-Fock Self Consistent Field (SCF) calculations were performed at the STO-3G and 6-31G* levels. A preliminary semi-empirical calculation (AM1) was also performed. Second-order Møller-Plesset perturbation theory calculations (MP2) were performed on **1,2** and **9** using the 6-31g* basis. The SCF calculations on **7** were performed with conformers in which the sidegroup was rotated in increments of 15° in order to determine the most stable conformer, based on the calculated SCF energy. All other molecular geometries were optimized, with the exception of the phenyl ring, which was constrained to a planar conformation.

3. Experimental Results

3. Experimental results.

3.1 ^{19}F and ^{1}H NMR spectral parameters.

^{19}F and, if required, ^{1}H NMR spectra of compounds **6, 13, 18-20, 22-24, 28, 29, 33-37** and **44** were analyzed using the NUMARIT program.[57] The results of these analyses are reported in Tables 3.1.1 - 3.1.19. Also reported are parameter correlations whose absolute values were greater than 0.2. The chemical shifts of the ^{1}H NMR spectra, acquired at 300.135 MHz, and those of the ^{19}F NMR spectra, acquired at 282.363 MHz, are reported in Hz and ppm to high frequency of internal TMS and C_6F_6, respectively. The numbers in brackets are the standard deviations of the last digit, as determined by the NUMARIT analysis.

3.1.1 2-chloro-6-fluorobenzonitrile, 6.

Spectra of **6**, prepared as a 5 mol% solution in acetone-d_6, were analyzed as an ABCX system. Peaks in the ^{19}F region, resulting from coupling to the protons, were split into doublets with a 3:1 intensity ratio (see Figure 3.1.1), which corresponds to the ratio of the natural abundances of ^{35}Cl and ^{37}Cl (75.53% and 24.47% respectively). The results of the analysis are reported in Table 3.1.1. There were no parameter correlations greater than 0.0055.

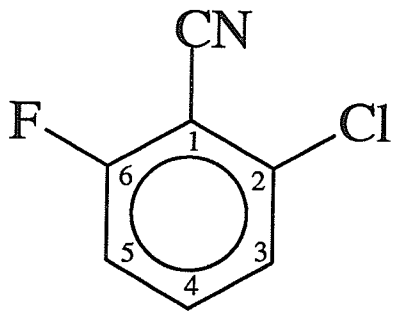

6

Table 3.1.1 Final ^{19}F and ^{1}H NMR spectral parameters for a 5 mol% solution of 2-chloro-6-fluorobenzonitrile, **6**, in acetone-d_6/C_6F_6/TMS.

	Chemical Shift (Hz)		Chemical Shift (ppm)	
	^{35}Cl peaks	^{37}Cl peaks	^{35}Cl peaks	^{37}Cl peaks
H-3	2269.715(2)	2269.713(2)	7.562	7.562
H-4	2347.572(2)	2347.577(2)	7.822	7.822
H-5	2234.887(2)	2234.887(2)	7.446	7.446
F	16630.086(2)	16629.930(2)	58.896	58.895

Coupling Constants (Hz)			Convergence Data		
	^{35}Cl peaks	^{37}Cl peaks		^{35}Cl peaks	^{37}Cl peaks
$^{3}J_{34}$	8.259(2)	8.258(2)	Calc. Transitions	32	32
$^{3}J_{45}$	8.634(2)	8.640(2)	Assigned Transitions	32	32
$^{3}J_{56}$	8.884(2)	8.883(2)	Peaks Observed	32	32
$^{4}J_{35}$	0.872(2)	0.874(2)	Largest Difference	0.009	0.009
$^{4}J_{46}$	6.170(2)	6.170(2)	RMS Deviation	0.005	0.004
$^{5}J_{36}$	-0.830(2)	-0.834(2)	$^{4}\Delta^{19}F(^{37/35}Cl)$	-0.552(1) ppb	

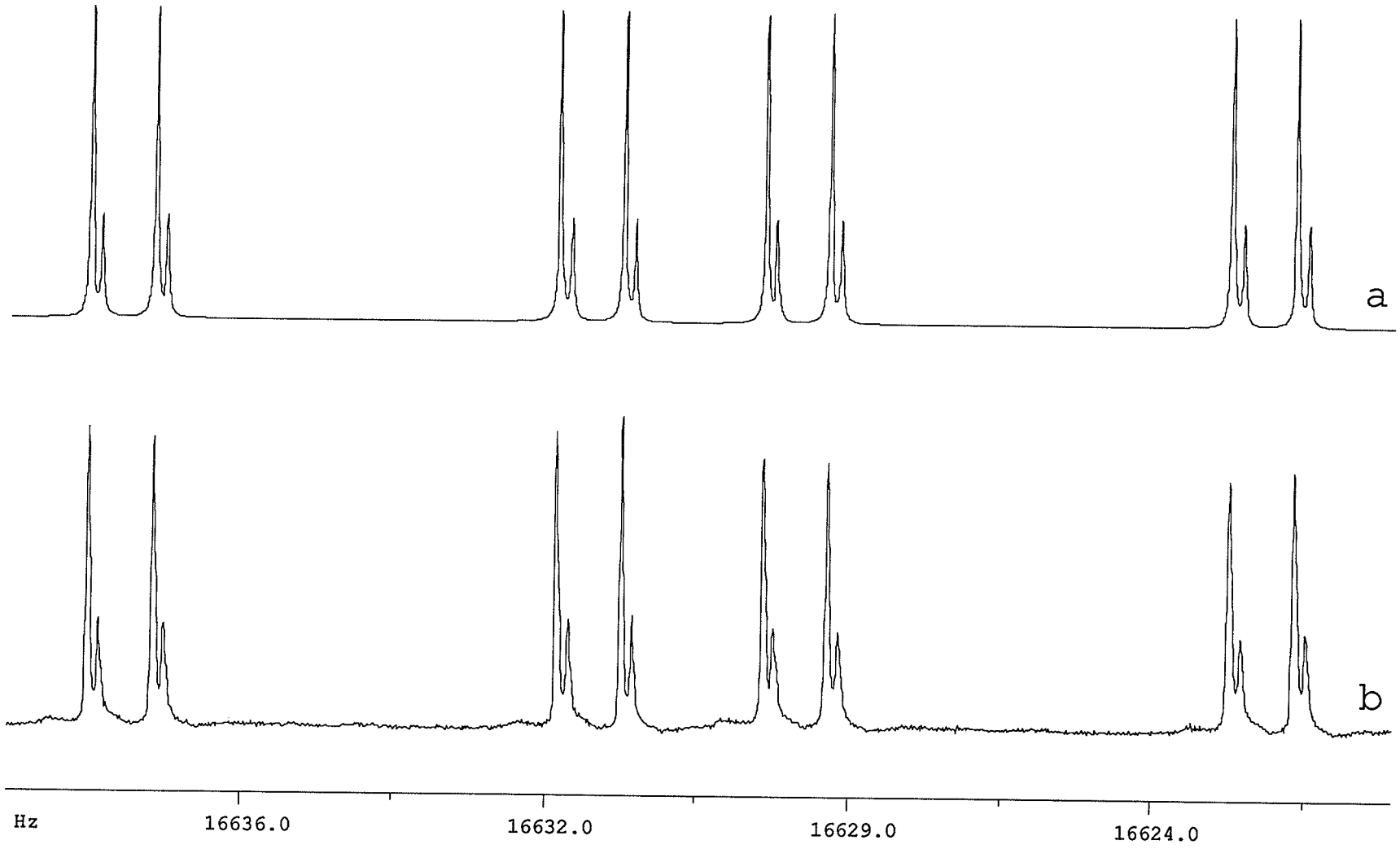
a
b
Hz
16636.0
16632.0
16629.0
16624.0

Figure 3.1.1

The calculated (a) and experimental (b) ^{19}F NMR spectrum of 2-chloro-6-fluorobenzonitrile, **6**, acquired at 282.363 MHz, showing the 3:1 peak intensity ratio resulting from $^{4}\Delta^{19}F(^{37/35}Cl)$. The calculated spectrum was generated using the parameters listed in Table 3.1.1. The scale is in Hz to high frequency of internal C_6F_6.

3.1.2 1-chloro-2,4-difluorobenzene, 13.

13 was prepared as a 5 mol% solution in acetone-d_6 and analyzed as an ABXYZ system. The proximity of the chemical shifts in the ^{19}F region resulted in combination lines in the H-5 region of the ^{1}H NMR spectrum which were split into doublets with a 3:1 peak intensity ratio resulting from the different relative chemical shifts of the ^{19}F nuclei of the two isotopomers (see section 6.4 for a further discussion of this effect). The ^{19}F region consisted of eight AB quartets whose peaks were split into doublets with a 3:1 ratio as for **6**. The greater magnitude of $^{3}\Delta^{19}F(^{37/35}Cl)$ compared to $^{5}\Delta^{19}F(^{37/35}Cl)$ aided in assigning the chemical shifts of these fluorine nuclei. During the analysis, small inconsistencies were noted between the ^{1}H and ^{19}F NMR spectra. These are attributed to small changes in the relative chemical shifts of the ^{19}F nuclei which occurred during the acquisition (all spectra were acquired in less than one hour). The results of this analysis are reported in Table 3.1.2.

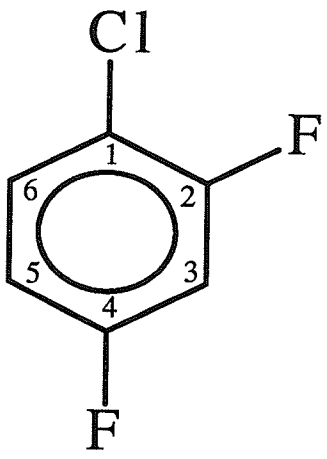

13

Table 3.1.2 Final ^{19}F and ^{1}H NMR spectral parameters for a 5 mol% solution of 1-chloro-2,4-difluorobenzene, **13**, in acetone-d_6/C_6F_6/TMS.

	Chemical Shift (Hz)		Chemical Shift (ppm)	
	^{35}Cl peaks	^{37}Cl peaks	^{35}Cl peaks	^{37}Cl peaks
F-2	14712.629(4)	14712.167(5)	52.105	52.104
H-3	2166.819(1)	2166.817(2)	7.219	7.219
F-4	14719.985(3)	14719.834(6)	52.131	52.131
H-5	2121.979(1)	2121.978(2)	7.070	7.070
H-6	2271.078(1)	2271.076(2)	7.567	7.567

Coupling Constants (Hz)		
	^{35}Cl peaks	^{37}Cl peaks
$^{3}J_{23}$	9.579(2)	9.576(3)
$^{3}J_{34}$	8.763(2)	8.765(3)
$^{3}J_{45}$	8.081(3)	8.081(4)
$^{3}J_{56}$	8.988(1)	8.990(2)
$^{4}J_{24}$	6.830(5)	6.830(5)
$^{4}J_{26}$	8.523(2)	8.517(3)
$^{4}J_{35}$	2.897(2)	2.899(2)
$^{4}J_{46}$	5.762(2)	5.767(3)
$^{5}J_{25}$	-1.558(4)	-1.559(5)
$^{5}J_{36}$	0.320(2)	0.319(2)

Convergence Data		
	^{35}Cl peaks	^{37}Cl peaks
Calc. Transitions	84	84
Assigned Transitions	82	70
Peaks Observed	88	88
Largest Difference	0.009	0.017
RMS Deviation	0.005	0.006
$^{3}\Delta^{19}F(^{37/35}Cl)$	-1.64(3) ppb	
$^{5}\Delta^{19}F(^{37/35}Cl)$	-0.54(3) ppb	

Table 3.1.2 (continued)

Significant Parameter Correlations

Parameter	^{35}Cl peaks	^{37}Cl peaks	Parameter	^{35}Cl peaks	^{37}Cl peaks
J_{23}:J_{34}	-0.251	-0.251	υ_2:J_{26}	0.189	0.283
J_{26}:J_{56}	-0.285	-0.263	υ_4:J_{23}	0.468	0.430
J_{25}:J_{45}	-0.542	-0.574	υ_2:J_{45}	0.469	0.417
υ_2:J_{25}	-0.528	-0.472	υ_4:J_{45}	-0.528	-0.499

3.1.3 1-chloro-3,4-difluorobenzene, 15.

15, prepared as a 5 mol% solution in acetone-d_6, was analyzed as an ABCXY system. Peak widths at half-height of 0.06 and 0.05 Hz, respectively, for F-3 and F-4, permitted the measurement of $^4\Delta^{19}F(^{37/35}Cl)$ and $^5\Delta^{19}F(^{37/35}Cl)$. The results of this analysis, for which there were no significant parameter correlations, are reported in Table 3.1.3.

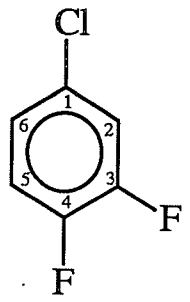

15

Table 3.1.3 Final ^{19}F and ^{1}H NMR spectral parameters for a 5 mol% solution of 1-chloro-3,4-difluorobenzene, **15**, in acetone-d_6/C_6F_6/TMS.

	Chemical Shift (Hz)		Chemical Shift (ppm)	
	^{35}Cl peaks	^{37}Cl peaks	^{35}Cl peaks	^{37}Cl peaks
H-2	2234.0773(7)	2234.0772(9)	7.444	7.444
F-3	7864.4771(7)	7864.3185(9)	27.852	27.852
F-4	6444.3532(7)	6444.2243(9)	22.823	22.822
H-5	2212.9054(7)	2212.906(1)	7.373	7.373
H-6	2180.0595(7)	2180.0596(9)	7.264	7.264

Coupling Constants (Hz)		
	^{35}Cl peaks	^{37}Cl peaks
$^{3}J_{23}$	10.439(1)	10.439(1)
$^{3}J_{34}$	-20.531(1)	-20.534(1)
$^{3}J_{45}$	10.415(1)	10.415(1)
$^{3}J_{56}$	8.914(1)	8.914(1)
$^{4}J_{24}$	6.990(1)	6.991(1)
$^{4}J_{26}$	2.580(1)	2.580(1)
$^{4}J_{35}$	8.657(1)	8.659(1)
$^{4}J_{46}$	3.841(1)	3.839(1)
$^{5}J_{25}$	0.289(1)	0.288(1)
$^{5}J_{36}$	-1.825(1)	-1.826(1)

Convergence Data		
	^{35}Cl peaks	^{37}Cl peaks
Calc. Transitions	80	80
Assigned Transitions	76	78
Peaks Observed	79	79
Largest Difference	0.006	0.008
RMS Deviation	0.003	0.004
$^{4}\Delta^{19}F(^{37/35}Cl)$	-0.562(4) ppb	
$^{5}\Delta^{19}F(^{37/35}Cl)$	-0.457(4) ppb	

3.1.4 Chloropentafluorobenzene, 18.

18 was prepared as a 5 mol% solution in acetone-d_6 and analyzed as an AA'BB'C system. All transitions were split into doublets with a 3:1 peak intensity ratio. The results of the analysis are reported in Table 3.1.4. There were no parameter correlations greater than 0.19.

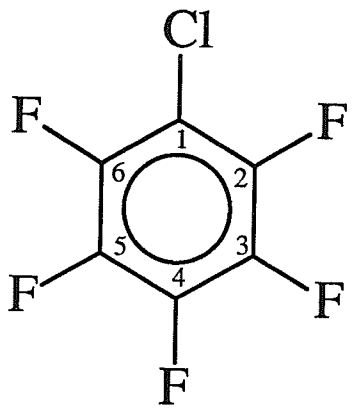

18

Table 3.1.4 Final ^{19}F NMR spectral parameters for a 5 mol% solution of chloropentafluorobenzene, **18**, in acetone-d_6/C_6F_6/TMS.

	Chemical Shift (Hz)		Chemical Shift (ppm)	
	^{35}Cl peaks	^{37}Cl peaks	^{35}Cl peaks	^{37}Cl peaks
F-2,6	6147.401(1)	6146.963(2)	21.771	21.770
F-3,5	392.485(1)	392.363(2)	1.390	1.390
F-4	1855.744(2)	1855.552(2)	6.572	6.572

Coupling Constants (Hz)		
	^{35}Cl peaks	^{37}Cl peaks
$^3J_{23} = {}^3J_{56}$	-21.541(3)	-21.540(3)
$^3J_{34} = {}^3J_{45}$	-20.676(2)	-20.673(2)
$^4J_{24} = {}^4J_{46}$	0.563(2)	0.564(3)
$^4J_{26}$	-5.196(2)	-5.194(3)
$^4J_{35}$	-1.812(2)	-1.810(3)
$^5J_{25} = {}^5J_{36}$	5.6250(4)	5.6277(7)

Convergence Data		
	^{35}Cl peaks	^{37}Cl peaks
Calc. Transitions	64	64
Assigned Transitions	62	56
Peaks Observed	56	52
Largest Difference	0.019	0.025
RMS Deviation	0.007	0.008
$^3\Delta^{19}F(^{37/35}Cl)$	-1.553(4) ppb	
$^4\Delta^{19}F(^{37/35}Cl)$	-0.431(1) ppb	
$^5\Delta^{19}F(^{37/35}Cl)$	-0.680(2) ppb	

3.1.5 1,3-Dichloro-2-fluorobenzene, 19.

19 was prepared as 5 mol% solutions in acetone-d_6 and CS_2. The spectra were analyzed as A_2BX systems. The ^{19}F region consisted of a series of multiplets with a 1.0:0.65:0.10 peak intensity ratio, expected for a spectrum of a ^{19}F nucleus with two chemically equivalent chlorine atoms (see Figure 3.1.2). The acetone-d_6 sample gave sharp, symmetric peaks, with line widths at half-height of 0.06 Hz. Although not as well resolved because of difficulties with shimming, the CS_2 sample was nevertheless sufficiently resolved to observe $^3\Delta^{19}F(^{37/35}Cl)$. The results of these analyses, for which there were no significant parameter correlations, are reported in Tables 3.1.5 and 3.1.6.

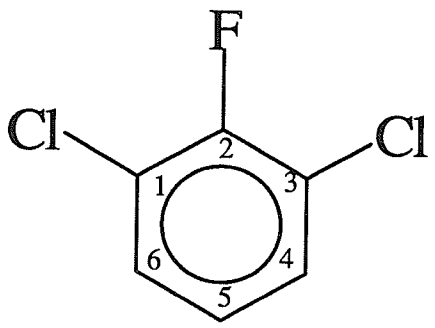

19

Table 3.1.5 Final ^{19}F and ^{1}H NMR spectral parameters for a 5 mol% solution of 1,3-dichloro-2-fluorobenzene, **19**, in acetone-d_6/C_6F_6/TMS.

	Chemical Shift (Hz)			Chemical Shift (ppm)[a]
	$^{35}Cl_2$ peaks	$^{35}Cl^{37}Cl$ peaks	$^{37}Cl_2$ peaks	
F-2	13064.5236(9)	13064.076(1)	13063.6277(7)	46.266
H-4,6	2250.0809(9)	2250.078(1)	2250.0803(7)	7.497
H-5	2173.8378(9)	2173.838(1)	2173.8336(8)	7.243

	Coupling Constants (Hz)		
	$^{35}Cl_2$ peaks	$^{35}Cl^{37}Cl$ peaks	$^{37}Cl_2$ peaks
$^{3}J_{45} = {}^{3}J_{56}$	8.197(1)	8.1991(8)	8.1991(8)
$^{4}J_{24} = {}^{4}J_{26}$	6.693(1)	6.6933(8)	6.6933(8)
$^{5}J_{25}$	-1.654(1)	-1.657(1)	-1.657(1)

Table 3.1.5 (continued).

Convergence Data

	$^{35}Cl_2$ peaks	$^{35}Cl^{37}Cl$ peaks	$^{37}Cl_2$ peaks
Calc. Transitions	24	24	24
Assigned Transitions	24	24	24
Peaks Observed	24	24	24
Largest Difference	0.004	0.006	0.004
RMS Deviation	0.003	0.003	0.002
$^{3}\Delta^{19}F(^{37/35}Cl)$	-1.585(10) ppb[b]; -1.588(10) ppb[c]		

a. The chemical shifts reported in ppm are for the shifts obtained from the fit performed on the taller peaks of the multiplets in the ^{19}F region, attributed to the isotopomer containing two ^{35}Cl atoms.

b. The calculated shifts from the tallest peaks to the central peaks, attributed to the isotopomer containing both a ^{35}Cl and a ^{37}Cl atom.

c. The calculated shifts from the central peaks to the smaller peaks, attributed to the $^{37}Cl_2$ isotopomer.

Table 3.1.6 Final ^{19}F and ^{1}H NMR spectral parameters for a 5 mol% solution of 1,3-dichloro-2-fluorobenzene, **19**, in $CS_2/C_6D_{12}/C_6F_6$/TMS.

	Chemical Shift (Hz)			Chemical Shift (ppm)[a]
	$^{35}Cl_2$ peaks	$^{35}Cl^{37}Cl$ peaks	$^{37}Cl_2$ peaks	
F-2	13287.216(2)	13286.766(1)	13286.311(2)	47.057
H-4,6	2170.499(2)	2170.499(1)	2170.499(2)	7.232
H-5	2093.308(2)	2093.308(1)	2093.3084(2)	6.975

Coupling Constants (Hz)

	$^{35}Cl_2$ peaks	$^{35}Cl^{37}Cl$ peaks	$^{37}Cl_2$ peaks
$^3J_{45} = {}^3J_{56}$	8.131(2)	8.131(1)	8.131(2)
$^4J_{24} = {}^4J_{26}$	6.405(2)	6.404(1)	6.410(3)
$^5J_{25}$	-1.644(3)	-1.645(2)	-1.641(3)

Table 3.1.6 (continued).

Convergence Data			
	$^{35}Cl_2$ peaks	$^{35}Cl^{37}Cl$ peaks	$^{37}Cl_2$ peaks
Calc. Transitions	24	24	24
Assigned Transitions	22	23	23
Peaks Observed	24	24	24
Largest Difference	0.013	0.006	0.013
RMS Deviation	0.005	0.003	0.006
$^{3}\Delta^{19}F(^{37/35}Cl)$	-1.594(10) ppb[b] ; -1.611(10) ppb[c]		

a. The chemical shifts reported in ppm are for the shifts obtained from the fit performed on the taller peaks of the multiplets in the ^{19}F region, attributed to the isotopomer containing two ^{35}Cl atoms.

b. The calculated shifts from the tallest peaks to the central peaks, attributed to the isotopomer containing both a ^{35}Cl and a ^{37}Cl atom.

c. The calculated shifts from the central peaks to the smaller peaks, attributed to the $^{37}Cl_2$ isotopomer.

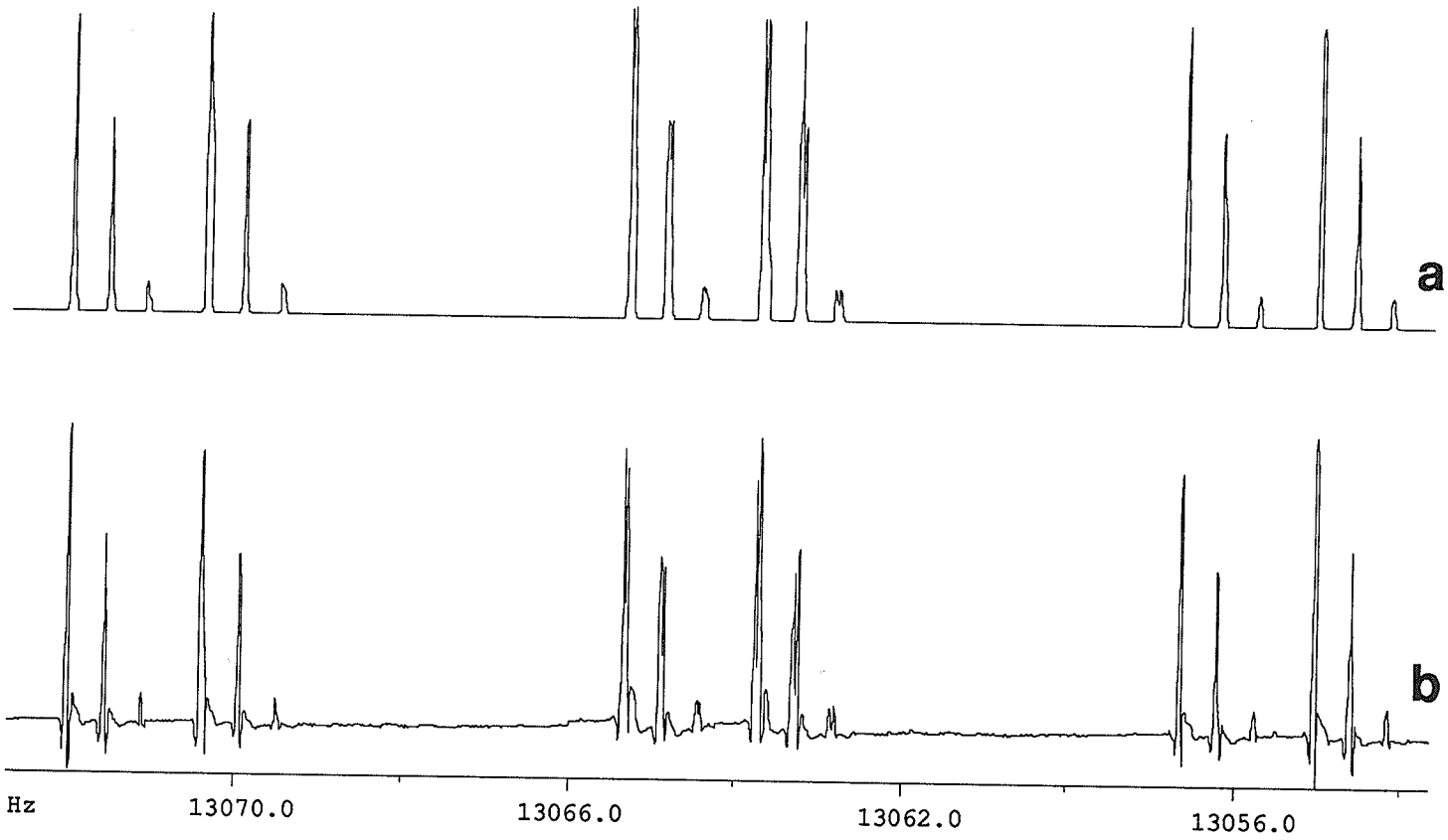
a
b
Hz
13070.0
13066.0
13062.0
13056.0

Figure 3.1.2

The calculated (a) and experimental (b) ^{19}F NMR spectrum of 1,3-dichloro-2-fluorobenzene, **19**, prepared in acetone-d_6. The spectrum, acquired at 282.363 MHz, has multiplets with a 1.0:0.65:0.1 peak intensity ratio, characteristic of a fluorine nucleus with 2 chemically equivalent chlorine atoms. Trace (a) was calculated from the parameters listed in Table 3.1.5. The scale is in Hz to high frequency of internal C_6F_6.

3.1.6 2,6-dichloro-4-fluorophenol, 20.

20 was prepared as a 5 mol% solution in CS_2 and analyzed as an A_2X system - the hydroxyl region, broadened because of exchange, did not couple to the other nuclei. Line widths at half-height of approximately 0.04 Hz in the ^{19}F region permitted the measurement of $^4\Delta^{19}F(^{37/35}Cl)$ despite its relatively small value. As for **19**, the two chemically equivalent chlorine atoms, relative to the ^{19}F site, resulted in a characteristic 1.0:0.65:0.10 splitting of all the transitions in this region. The results of the analysis, for which there were no significant parameter correlations, are tabulated in Table 3.1.7

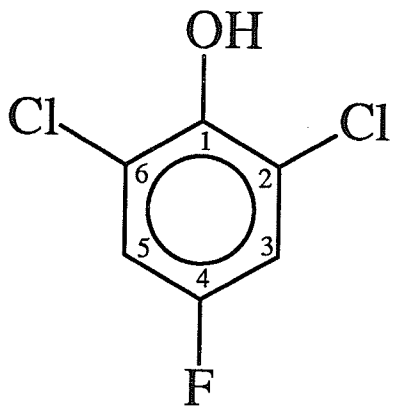

29

Table 3.1.7 Final ^{19}F and ^{1}H NMR spectral parameters for a 5 mol% solution of 2,6-dichloro-4-fluorophenol, **29**, in $CS_2/C_6D_{12}/C_6F_6$/TMS.

	Chemical Shift (Hz)			Chemical Shift (ppm)[a]
	$^{35}Cl_2$ peaks	$^{35}Cl^{37}Cl$ peaks	$^{37}Cl_2$ peaks	
H-3,5	2084.1739(4)	2084.1739(3)	2084.1739(3)	6.944
OH	1663.3(1)[b]	1663.3(1)[b]	1663.3(1)[b]	5.542
F-4	11912.1590(4)	11912.1145(3)	11912.0686(3)	42.185

	Coupling Constants (Hz)		
	$^{35}Cl_2$ peaks	$^{35}Cl^{37}Cl$ peaks	$^{37}Cl_2$ peaks
$^{3}J_{34} = {}^{3}J_{45}$	7.6661(4)	7.6657(3)	7.6661(4)
$^{5}J_{OH,3} = {}^{5}J_{OH,5}$	0.0[c]	0.0[c]	0.0[c]
$^{6}J_{OH,4}$	0.0[c]	0.0[c]	0.0[c]

Table 3.1.7 (continued).

Convergence Data			
	$^{35}Cl_2$ peaks	$^{35}Cl^{37}Cl$ peaks	$^{37}Cl_2$ peaks
Calc. Transitions	80	80	80
Assigned Transitions	48	48	48
Peaks Observed	12	12	12
Largest Difference	0.003	0.002	0.003
RMS Deviation	0.001	0.001	0.001
$^4\Delta^{19}F(^{37/35}Cl)$	-0.158(1) ppb[d]; -0.163(1) ppb[e]		

a. The chemical shifts reported in ppm are the shifts obtained from the fits performed on the taller peaks of the multiplets in the ^{19}F region, attributed to the isotopomer containing two ^{35}Cl atoms.

b. Measured directly from the experimental spectrum.

c. Neither observed nor optimized.

d. The calculated shifts from the tallest peaks to the central peaks, attributed to the isotopomer containing both a ^{35}Cl and a ^{37}Cl atom.

e. The calculated shifts from the central peaks to the smaller peaks, attributed to the $^{37}Cl_2$ isotopomer.

3.1.7 2-chloro-3,5-difluoroanisole, 22.

22 was prepared as a 5 mol% solution in acetone-d_6. A sample was also prepared in CS_2, but a crowded spectrum with poor resolution precluded analysis in this case. The spectrum from the acetone-d_6 sample was analyzed as an ABM_3XY system. The sign of $^5J_{6\beta}$ was determined by a partial decoupling experiment. The results of this analysis, which showed no significant parameter correlations, are reported in Table 3.1.8.

The F-3 region consisted of eight doublets with a 3:1 peak intensity ratio resulting from the isotopes of chlorine. In the F-5 region, eight asymmetric quartets were observed. Examination of these quartets show that what initially appears to be the βββ transition of a quartet is actually the αββ transition of the ^{37}Cl isotopomer overlapping with the βββ transition of the ^{35}Cl isotopomer; either of these would have approximately 1/3 the intensity of the αββ transition of the ^{35}Cl isotopomer. The shift of this peak from the αββ peak is less than the calculated coupling (see Figure 3.1.3). For these reasons, $^5\Delta^{19}F(^{37/35}Cl)$, reported below, is the shift from the third to the fourth peaks of these multiplets. For the other peaks of the quartet, the effect is less apparent since the overlap occurs in the tall peaks of the ^{35}Cl component of the multiplet.

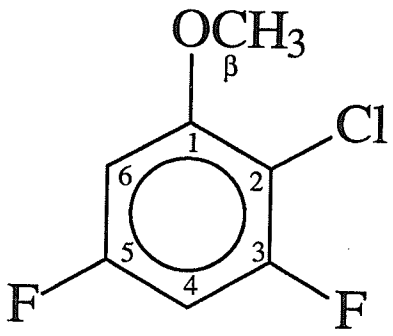

22

Table 3.1.8 Final ^{19}F and ^{1}H NMR spectral parameters for a 5 mol% solution of 2-chloro-3,5-difluoroanisole, **22**, in acetone-d_6/C_6F_6/TMS.

	Chemical Shift (Hz)		Chemical Shift (ppm)	
	^{35}Cl peaks	^{37}Cl peaks	^{35}Cl peaks	^{37}Cl peaks
H-β	1191.5171(2)	1191.5186(3)	3.970	3.970
F-3	14458.8253(3)	14458.3789(3)	51.207	51.205
H-4	2035.6081(3)	2035.6097(3)	6.782	6.782
F-5	14878.9131(3)	14878.9131(4)[a]	52.692	52.692
H-6	2056.0440(3)	2056.0431(3)	6.850	6.850

Table 3.1.8 (continued).

Coupling Constants (Hz)			Convergence Data		
	^{35}Cl peaks	^{37}Cl peaks		^{35}Cl peaks	^{37}Cl peaks
$^{3}J_{34}$	9.3858(4)	9.3836(4)	**Calc. Transitions**	256	256
$^{3}J_{45}$	8.8358(4)	8.8351(5)	**Assigned Transitions**	226	230
$^{3}J_{56}$	10.7248(4)	10.7217(5)	**Peaks Observed**	92	92
$^{4}J_{35}$	6.0526(4)	6.0546(5)	**Largest Difference**	0.005	0.006
$^{4}J_{46}$	2.7584(4)	2.7604(4)	**RMS Deviation**	0.002	0.002
$^{5}J_{36}$	-1.9693(4)	-1.9661(4)	$^{3}\Delta^{19}F(^{37/35}Cl)$	-1.580(1) ppb	
$^{5}J_{6\beta}$	-0.3101(3)	-0.3115(3)	$^{5}\Delta^{19}F(^{37/35}Cl)$	-0.39(3)[b]	
$^{6}J_{5\beta}$	0.1194(3)	0.1206(4)			
$^{6}J_{3\beta}$	not observed	not observed			
$^{7}J_{4\beta}$	not observed	not observed			

a. Because of the almost equal magnitudes of $^{6}J_{5\beta}$ and $^{5}\Delta^{19}F(^{37/35}Cl)$, it was not possible to iterate on the transitions of this region attributed to the ^{37}Cl isotopomer. Instead, on the assumption that there is no significant isotope effect on $^{6}J_{5\beta}$, analysis was done on the taller peaks, attributed to the ^{35}Cl isotopomers.

b. Measured directly from the experimental spectrum.

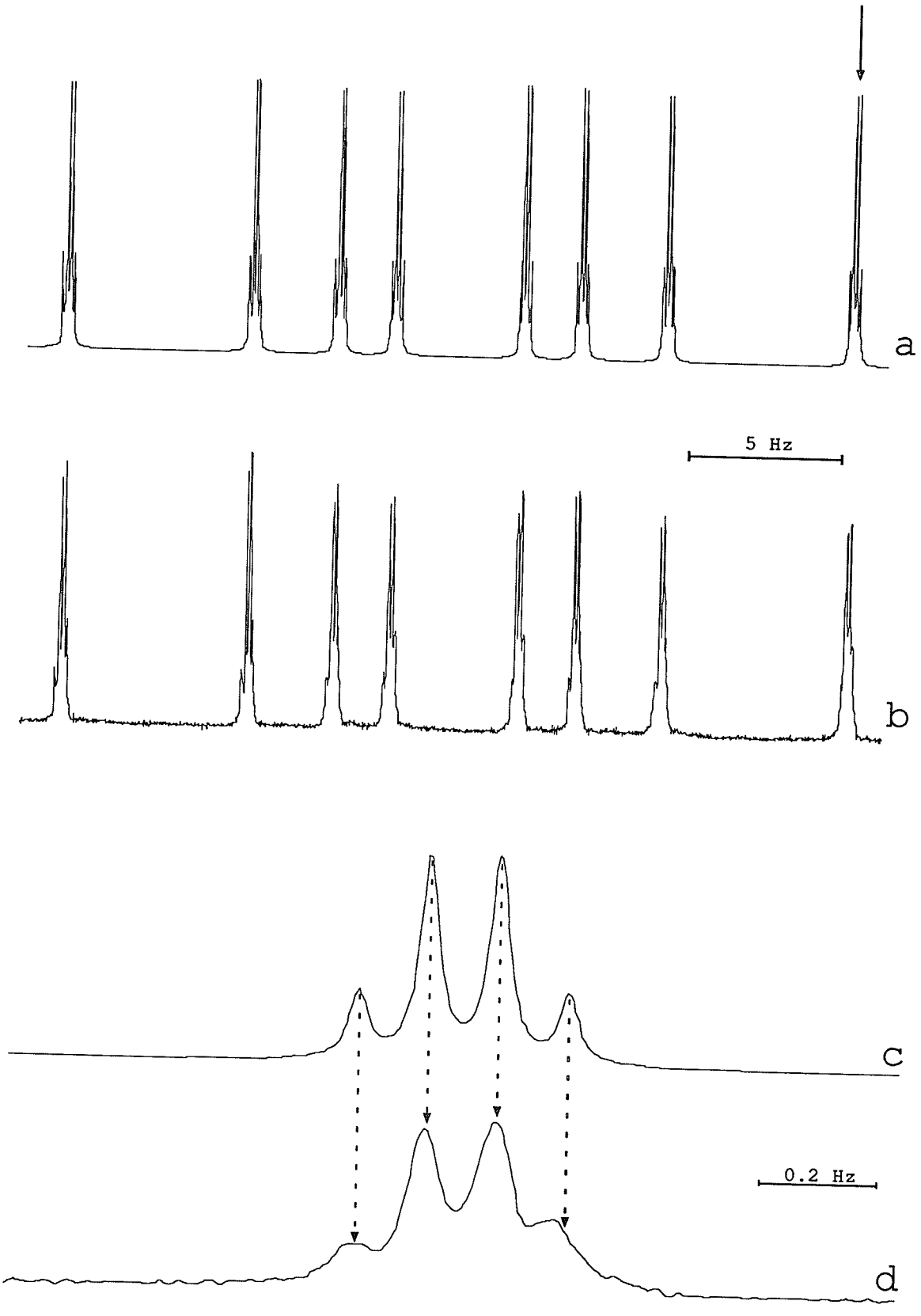
a
5 Hz
b
c
0.2 Hz
d

Figure 3.1.3

The calculated (a) and experimental (b) ^{19}F NMR spectrum of the F-5 region of 2-chloro-3,5-difluoroanisole, **22**, acquired at 282.363 MHz. The calculated spectrum was obtained from the parameters listed in Table 3.1.8. The asymmetric multiplets in the experimental spectrum are attributed to an overlap of $^{5}\Delta^{19}F(^{37/35}Cl)$ with $^{6}J_{5\beta}$. Traces (c) and (d) show respectively an expansion of the calculated and experimental multiplet indicated with an arrow in (a). The dotted arrows show that the low frequency peak is displaced slightly as a result of $^{5}\Delta^{19}F(^{37/35}Cl)$.

3.1.8 1,3-dichloro-2,4,6-trifluorobenzene, 23.

23 was prepared as a 5 mol% solution in acetone-d_6 and analyzed as an A_2BX system. The peaks of the F-2 region of the spectrum showed the splitting with a 1.0:0.65:0.10 peak intensity ratio expected for a fluorine atom with two equivalent chlorine atoms. A similar pattern was observed for F-4,6. Because these nuclei, which are chemically equivalent, experience both $^3\Delta^{19}F(^{37/35}Cl)$ and $^5\Delta^{19}F(^{37/35}Cl)$, the average value $((^3\Delta + {}^5\Delta)/2)$ of these is observed. The results of this analysis, for which there were no significant parameter correlations, are tabulated in Table 3.1.9.

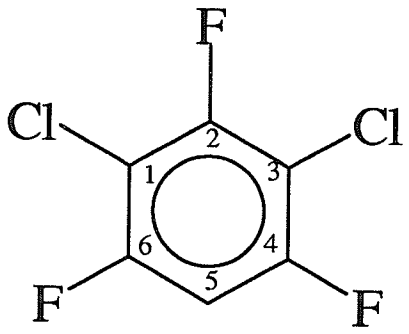

23

Table 3.1.9 Final ^{19}F and ^{1}H NMR spectral parameters for a 5 mol% solution of 1,3-dichloro-2,4,6-trifluorobenzene, **23**, in acetone-d_6/C_6F_6/TMS.

	Chemical Shift (Hz)			Chemical Shift (ppm)[a]
	$^{35}Cl_2$ peaks	$^{35}Cl^{37}Cl$ peaks	$^{37}Cl_2$ peaks	
F-2	14536.906(3)	14536.444(3)	14535.982(3)	51.483
F-4,6	14470.422(3)	14470.129(3)	14469.838(3)	51.247
H-5	2226.315(3)	2226.315(3)	2226.316(3)	7.418

Coupling Constants (Hz)			
	$^{35}Cl_2$ peaks	$^{35}Cl^{37}Cl$ peaks	$^{37}Cl_2$ peaks
$^3J_{45} = {}^3J_{56}$	9.233(3)	9.234(4)	9.234(3)
$^4J_{24} = {}^4J_{26}$	1.618(3)	1.618(3)	1.616(3)
$^5J_{25}$	2.367(4)	2.367(4)	2.366(4)

Table 3.1.9 (continued).

Convergence Data			
	$^{35}Cl_2$ peaks	$^{35}Cl^{37}Cl$ peaks	$^{37}Cl_2$ peaks
Calc. Transitions	24	24	24
Assigned Transitions	22	21	24
Peaks Observed	16	16	16
Largest Difference	0.01	0.01	0.01
RMS Deviation	0.007	0.007	0.007
$^3\Delta^{19}F(^{37/35}Cl)$	-1.64(2) ppb[b]; -1.64(2) ppb[c]		
$(^3\Delta + {}^5\Delta)/2$	-1.04(2) ppb[b]; -1.03 (2) ppb[c]		

a. The chemical shifts reported in ppm are the shifts obtained from the fits performed on the taller peaks of the multiplets in the ^{19}F region, attributed to the isotopomer containing two ^{35}Cl atoms.

b. The calculated shifts from the tallest peaks to the central peaks, attributed to the isotopomer containing both a ^{35}Cl and a ^{37}Cl atom.

c. The calculated shifts from the central peaks to the smaller peaks, attributed to the $^{37}Cl_2$ isotopomer.

3.1.9 2-chloro-3,5-difluorophenol, 24.

24, prepared as a 5 mol% solution in acetone-d_6, was analyzed as an ABXY system - the peak of the hydroxyl proton was broadened, precluding the detection of any coupling to this nucleus. The proximity of the chemical shifts of the H-4 and H-6 protons resulted in combination lines in the F-3 region (see section 6.3 for a discussion of this effect). Line widths at half-height of 0.04 Hz in the ^{19}F region permitted the measurement of $^{3}\Delta^{19}F(^{37/35}Cl)$ as well as $^{5}\Delta^{19}F(^{37/35}Cl)$. The results of the analysis, for which there were no significant parameter correlations, are tabulated in Table 3.1.10.

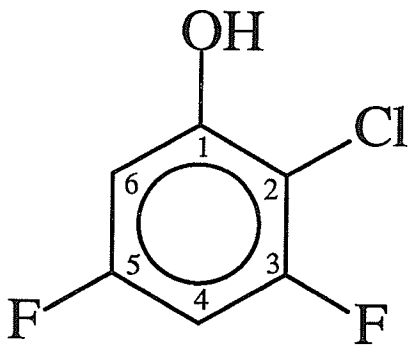

24

Table 3.1.10 Final ^{19}F and ^{1}H NMR spectral parameters for a 5 mol% solution of 2-chloro-3,5-difluorophenol, **24**, in acetone-d_6/C_6F_6/TMS.

	Chemical Shift (Hz)		**Chemical Shift (ppm)**	
	^{35}Cl peaks	**^{37}Cl peaks**	**^{35}Cl peaks**	**^{37}Cl peaks**
OH	2909.8(1)[a]		9.695	
F-3	14546.93(1)	14546.51(1)	51.519	51.517
H-4	2006.19(1)	2006.20(1)	6.668	6.668
F-5	14513.41(1)	14513.33(1)	51.400	51.400
H-6	2001.98(1)	2001.98(1)	6.670	6.670

Table 3.1.10 (continued).

Coupling Constants (Hz)			Convergence Data		
	^{35}Cl peaks	**^{37}Cl peaks**		**^{35}Cl peaks**	**^{37}Cl peaks**
$^{3}J_{34}$	9.52(2)	9.52(2)	**Calc. Transitions**	80	80
$^{3}J_{45}$	8.95(2)	8.94(2)	**Assigned Transitions**	70	70
$^{3}J_{56}$	10.08(2)	10.09(2)	**Peaks Observed**	35	35
$^{4}J_{35}$	5.94(2)	5.93(2)	**Largest Difference**	0.10	0.10
$^{4}J_{46}$	2.85(2)	2.85(2)	**RMS Deviation**	0.06	0.06
$^{4}J_{6,OH}$	not observed		$^{3}\Delta^{19}F(^{37/35}Cl)$	-1.49(4)	
$^{5}J_{36}$	-2.21(1)	-2.21(1)	$^{5}\Delta^{19}F(^{37/35}Cl)$	-0.28(5)	
$^{5}J_{5,OH}$	not observed				
$^{5}J_{3,OH}$	not observed				
$^{6}J_{4,OH}$	not observed				

a. This peak was broadened, probably because of proton exchange. The reported value was obtained directly from the experimental spectrum; a fit on these transitions was not performed.

3.1.10 Pentafluorophenylsulfonyl chloride, 28.

28 was prepared as a 5 mol% solution in acetone-d_6 and analyzed as an AA'BB'C system. The peaks of the *ortho* region were broadened, precluding the detection of isotope shifts to this nucleus. The peaks of the *meta* region were asymmetric, perhaps because of $^{5}\Delta^{19}F(^{37/35}Cl)$. However, because of the uncertainty, and because separate peaks were not resolved, an isotope shift to this nucleus is not reported. Line widths at the *para* position of approximately 0.15 Hz permitted the measurement of $^{6}\Delta^{19}F(^{37/35}Cl)$ at this site (Figure 3.1.4). The results of this analysis are reported in Table 3.1.11.

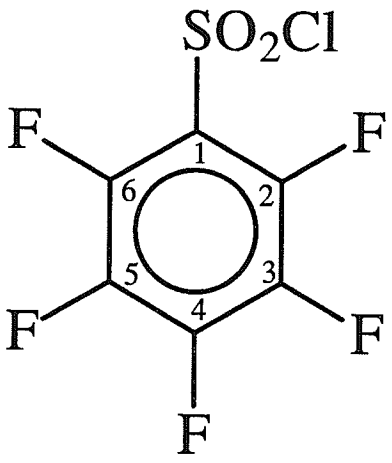

28

Table 3.1.11 Final ^{19}F NMR spectral parameters for a 5 mol% solution of pentafluorophenylsulfonyl chloride, **28**, in acetone-d_6/C_6F_6/TMS.

	Chemical Shift (Hz)		Chemical Shift (ppm)	
	^{35}Cl peaks	^{37}Cl peaks	^{35}Cl peaks	^{37}Cl peaks
F-2,6	7795.546(7)	7795.532(4)	27.608	27.608
F-3,5	1288.417(6)	1288.397(4)	4.563	4.563
F-4	6168.462(8)	6168.232(4)	21.846	21.845

Coupling Constants (Hz)			Convergence Data		
	^{35}Cl peaks	^{37}Cl peaks		^{35}Cl peaks	^{37}Cl peaks
$^3J_{23} = {}^3J_{56}$	-22.64(1)	-22.637(8)	**Calc. Transitions**	64	64
$^3J_{34} = {}^3J_{45}$	-20.764(8)	-20.769(4)	**Assigned Transitions**	59	39
$^4J_{24} = {}^4J_{46}$	9.629(9)	9.627(4)	**Peaks Observed**	47	47
$^4J_{26}$	-11.02(1)	-11.053(7)	**Largest Difference**	0.066	0.018
$^4J^a_{35}$	0.46(1)	0.423(6)	**RMS Deviation**	0.03	0.01
$^5J_{25} = {}^5J_{36}$	7.182(1)	7.1844(6)	$^4\Delta^{19}F(^{37/35}Cl)$	not observed	
			$^5\Delta^{19}F(^{37/35}Cl)$	not observed	
			$^6\Delta^{19}F(^{37/35}Cl)$	-0.81(3)	
Parameter Correlation:			ν_4:J_{35}	-0.246	-0.353

a. The sign of $^4J_{35}$ is that reported by Moniz *et al.* for a concentrated sample containing also 30% vol./vol. 1,4-bis (trifluoromethyl) benzene.[59]

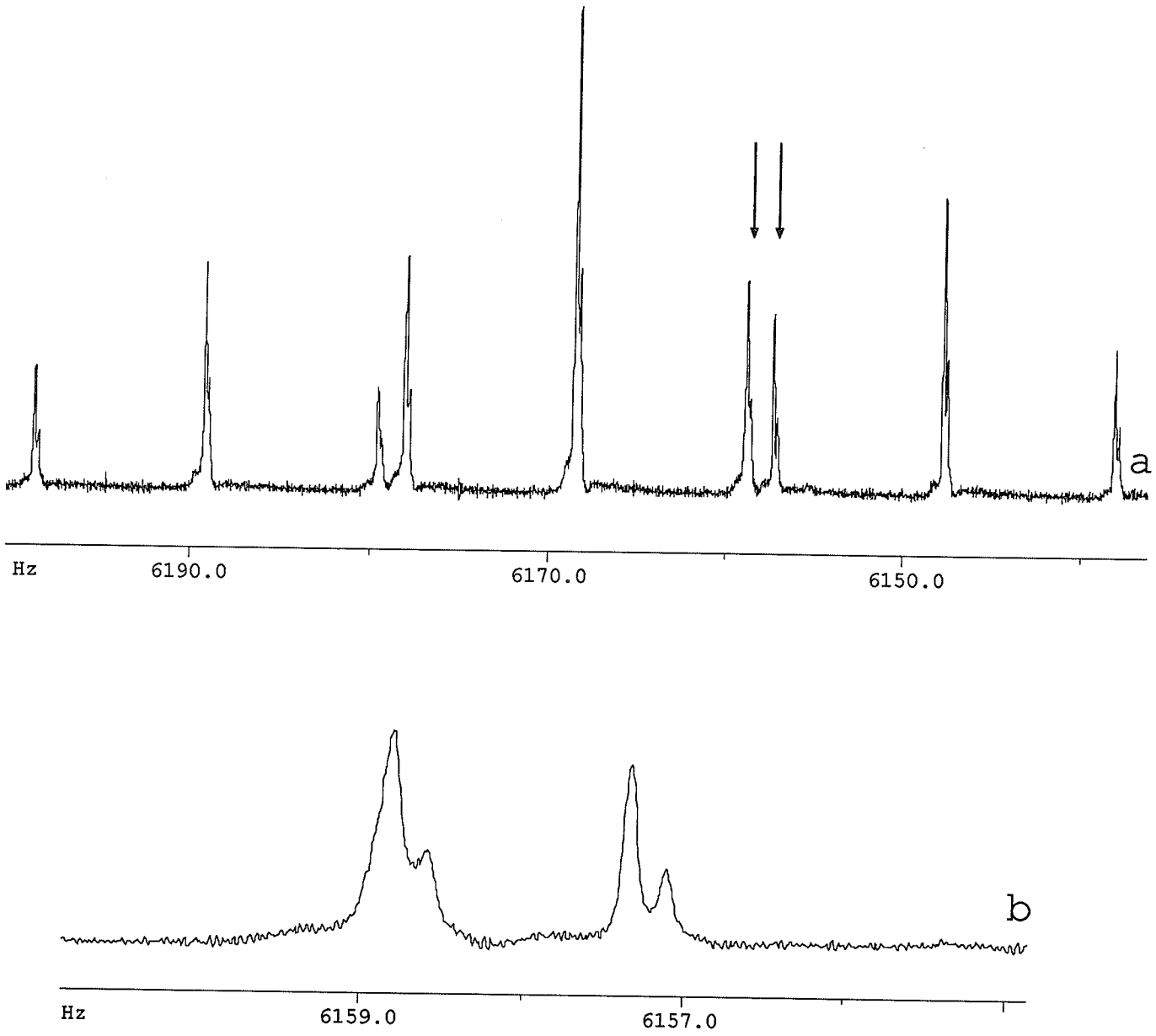
a
Hz
6190.0
6170.0
6150.0
b
Hz
6159.0
6157.0

Figure 3.1.4

The F-4 region of the ^{19}F NMR spectrum of pentafluorophenylsulfonyl chloride, **28**, acquired at 282.363 MHz (a). Trace (b) shows an expansion of the region indicated by arrows in (a). The 3:1 peak intensity ratio is attributed to $^{6}\Delta^{19}F(^{37/35}Cl)$. The scale is in Hz to high frequency of internal C_6F_6.

3.1.11 2-chloro-2,2-difluoroacetophenone, 29.

29, prepared as a 5 mol% solution in acetone-d_6, was analyzed as an AA'BB'CX_2 system. A complicated ^{19}F region precluded the measurement of $^{2}\Delta^{19}F(^{37/35}Cl)$ from the calculated spectrum. Instead, a proton decoupled ^{19}F NMR spectrum was acquired and $^{2}\Delta^{19}F(^{37/35}Cl)$ was measured directly. From the ^{13}C satellite peaks of this spectrum, $^{1,2}\Delta^{19}F(^{13/12}C)$ was determined, as well $^{1,2}J_{CF}$. These satellite peaks also were split into doublets from $^{2}\Delta^{19}F(^{37/35}Cl)$, permitting the measurement of a possible carbon isotope effect on $^{2}\Delta^{19}F(^{37/35}Cl)$. The results of this analysis, for which there were no significant parameter correlations, are tabulated in Table 3.1.12.

Table 3.1.12 Final ^{19}F and ^{1}H NMR spectral parameters for a 5 mol% solution of 2-chloro-2,2-difluoroacetophenone, **29**, in acetone-d_6/C_6F_6/TMS.

	Chemical Shift	
	Hz	**ppm**
H-2,6	2443.5121(7)	8.141
H-3,5	2299.6338(6)	7.662
H-4	2347.0180(8)	7.820
F	29009.6555(8)	102.739

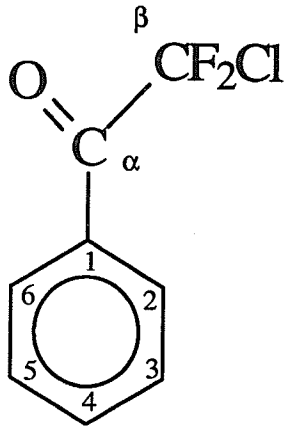

Coupling Constants (Hz)

$^{1}J_{CF}$	304.01(3)	$^{4}J_{24} = {}^{4}J_{46}$	1.2369(9)	$^{5}J_{F,2} = {}^{5}J_{F,6}$	1.0832(8)
$^{2}J_{CF}$	28.51(3)	$^{4}J_{26}$	2.013(1)	$^{6}J_{F,3} = {}^{6}J_{F,5}$	not observed
$^{3}J_{23} = {}^{3}J_{56}$	8.009(1)	$^{4}J_{35}$	1.328(1)	$^{7}J_{F,4}$	0.089(1)
$^{3}J_{34} = {}^{3}J_{45}$	7.5046(9)	$^{5}J_{25} = {}^{5}J_{36}$	0.6140(2)		

Convergence Data

Calc. Transitions	320	$^{2}\Delta^{19}F(^{37/35}Cl)^{a}$	-5.1(1) ppb
Assigned Transitions	286	$^{2}\Delta^{19}F(^{37/35}Cl)^{b}$	-5.0(1) ppb
Peaks Observed	119	$^{1}\Delta^{19}F(^{13/12}C)^{c}$	-143(1) ppb
Largest Difference	0.015	$^{2}\Delta^{19}F(^{13/12}C)^{c}$	-13.6(4) ppb
RMS Deviation	0.006		

a. Observed in the proton decoupled ^{19}F spectrum. The isotope shift was measured from the tall central peaks, attributed to the isotopomer containing ^{12}C isotopes at the α and carbonyl positions.

b. Observed in the proton decoupled ^{19}F spectrum. Here, the isotope shift was measured from the ^{13}C satellite peaks. The average of the 3 resolved multiplets is reported.

c. Measured from the proton decoupled ^{19}F spectrum. The carbon atom giving rise to the isotope shift was assigned on the basis of $^{1,2}J_{CF}$.

3.1.12 1-bromo-2,3,5-trifluorobenzene, 33.

Spectra of **33** were acquired from a 5 mol% solution in acetone-d_6 and analyzed as an ABCXY system. The sixteen transitions in the F-2 region were split into doublets of almost equal intensity (Figure 3.1.5), corresponding to the almost equal natural abundance of the ^{79}Br and ^{81}Br isotopes (50.69% and 49.31% respectively). Extreme resolution enhancement of the peaks in the F-3 and F-5 regions failed to give any indication of $^{4}\Delta^{19}F(^{81/79}Br)$ despite line widths of less than 0.04 Hz. The results of this analysis, for which there were no significant parameter correlations, are reported in Table 3.1.13.

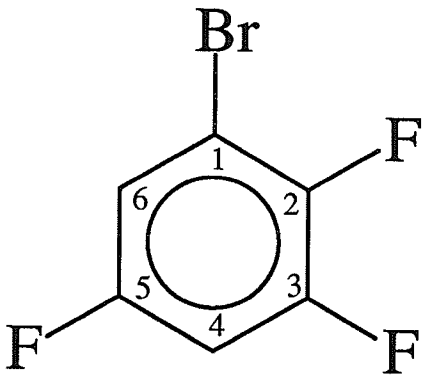

33

Table 3.1.13 Final ^{19}F and ^{1}H NMR spectral parameters for a 5 mol% solution of 1-bromo-2,3,5-trifluorobenzene, **33**, in acetone-d_6/C_6F_6/TMS.

	Chemical Shift (Hz)		Chemical Shift (ppm)	
	^{79}Br peaks	^{81}Br peaks	^{79}Br peaks	^{81}Br peaks
F-2	7525.350(3)	7525.270(3)	26.651	26.650
F-3	9032.096(3)	9032.092(3)	31.986	31.986
H-4	2202.019(3)	2202.021(3)	7.337	7.337
F-5	13849.959(3)	13849.962(3)	47.773	47.773
H-6	2217.208(3)	2217.209(3)	7.387	7.387

Coupling Constants (Hz)		
	^{79}Br peaks	^{81}Br peaks
$^{3}J_{23}$	-21.014(4)	-21.011(4)
$^{3}J_{34}$	10.399(4)	10.397(4)
$^{3}J_{45}$	8.486(4)	8.486(4)
$^{3}J_{56}$	7.890(4)	7.891(4)
$^{4}J_{24}$	5.980(4)	5.981(4)
$^{4}J_{26}$	4.704(4)	4.706(4)
$^{4}J_{35}$	3.044(4)	3.043(4)
$^{4}J_{46}$	3.062(4)	3.061(4)
$^{5}J_{25}$	12.469(4)	12.470(4)
$^{5}J_{36}$	2.102(4)	2.102(4)

Convergence Data		
	^{79}Br peaks	^{81}Br peaks
Calc. Transitions	80	80
Assigned Transitions	79	79
Peaks Observed	80	80
Largest Difference	0.021	0.022
RMS Deviation	0.011	0.010
$^{3}\Delta^{19}$F($^{81/79}$Br)	-0.283(1) ppb	
$^{4}\Delta^{19}$F-3($^{81/79}$Br)	not observed	
$^{4}\Delta^{19}$F-5($^{81/79}$Br)	not observed	

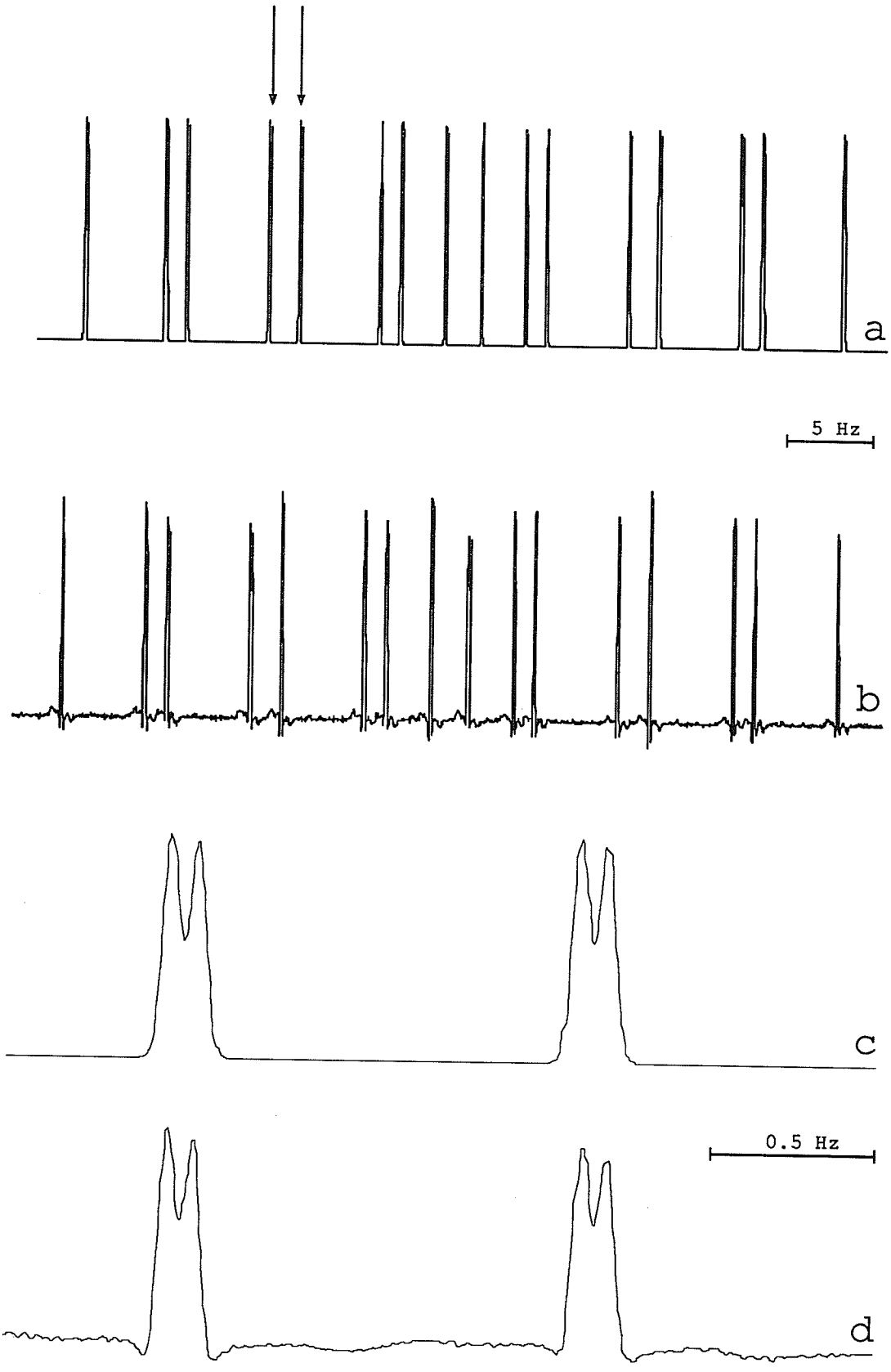
a
5 Hz
b
c
0.5 Hz
d

Figure 3.1.5

The calculated (a) and experimental (b) ^{19}F NMR spectrum of the F-2 region of 1-bromo-2,3,5-trifluorobenzene, **33**, acquired at 282.363 MHz. Traces (c) and (d) show, respectively, the calculated and experimental spectrum of the region indicated with arrows in (a), illustrating the 1:1 peak intensity ratio resulting from $^{3}\Delta^{19}F(^{81/79}Br)$. The slightly lower intensity of the low frequency peaks of the multiplets suggests that the sign of this isotope shift is negative. The calculated spectra were generated using the parameters listed in Table 3.1.13.

3.1.13 1,2-dibromo-3,5-difluorobenzene, 34.

34 was prepared as a 5 mol% solution in acetone-d_6; its NMR spectra were analyzed in terms of an ABXY system. The transitions of the F-3 region were split into four peaks of almost equal intensity, suggesting the presence of both $^{3}\Delta^{19}F(^{81/79}Br)$ and $^{4}\Delta^{19}F(^{81/79}Br)$ (Figure 3.1.6). There was no indication of $^{4}\Delta^{19}F(^{81/79}Br)$ for F-5, despite extreme resolution enhancement. To verify that the splitting observed in the F-3 region was due to isotope shifts rather than to a shimming error, this region of the spectrum was reacquired on another day, giving the same splitting pattern, although the spectrum was not as well resolved. The spectra acquired on the first day, which gave line widths of less than 0.04 Hz, were used for the analysis, which entailed doing separate fits for each of the four peaks of the multiplets observed in the F-3 region. From other observed $^{3}\Delta^{19}F(^{81/79}Br)$ values, the larger of the two isotope shifts was attributed to the isotopomer in which the bromine vicinal to the observed ^{19}F nucleus underwent isotopic substitution. Listed in Table 3.1.14 are the results of this analysis, for which there were no significant parameter correlations.

34

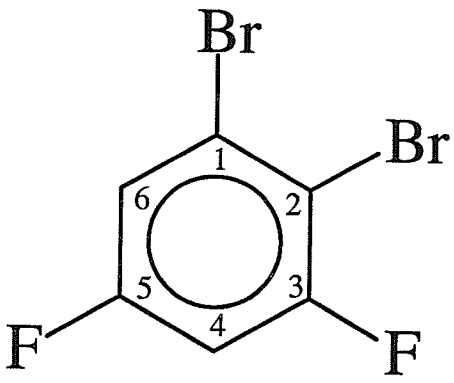

Table 3.1.14 Final ^{19}F and ^{1}H NMR spectral parameters for a 5 mol% solution of 1,2-dibromo-3,5-difluorobenzene, **34**, in acetone-d_6/C_6F_6/TMS.

Chemical Shifts

	Hz	Hz	Hz	Hz	ppm[a]
	^{79}Br-1;^{79}Br-2	^{81}Br-1;^{79}Br-2	^{79}Br-1;^{81}Br-2	^{81}Br-1;^{81}Br-2	
F-3	19158.0127(9)	19157.9843(7)	19157.9344(4)	19157.9033(7)	67.845
H-4	2187.1873(9)	2187.1870(7)	2187.1892(5)	2187.1870(7)	7.287
F-5	15119.0356(9)	15119.0340(7)	15119.0323(4)	15119.0357(7)	53.542
H-6	2255.1770(9)	2255.1755(7)	2255.1767(4)	2255.1775(7)	7.514

Coupling Constants (Hz)

	^{79}Br-1;^{79}Br-2	^{81}Br-1;^{79}Br-2	^{79}Br-1;^{81}Br-2	^{81}Br-1;^{81}Br-2
$^{3}J_{34}$	8.796(1)	8.796(1)	8.7952(7)	8.795(1)
$^{3}J_{45}$	8.662(1)	8.662(1)	8.6614(7)	8.661(1)
$^{3}J_{56}$	8.166(1)	8.169(1)	8.1677(6)	8.170(1)
$^{4}J_{35}$	7.330(1)	7.330(1)	7.3311(6)	7.332(1)
$^{4}J_{46}$	2.822(1)	2.823(1)	2.8244(7)	2.823(1)
$^{5}J_{36}$	-1.873(1)	-1.875(1)	-1.8740(6)	-1.875(1)

Table 3.1.14 (continued)

Convergence Data

	^{79}Br-1;^{79}Br-2	^{81}Br-1;^{79}Br-2	^{79}Br-1;^{81}Br-2	^{81}Br-1;^{81}Br-2
Calc. Transitions	32	32	32	32
Ass. Transitions	32	32	32	32
Peaks Observed	32	32	32	32
Largest Diff.	0.005	0.004	0.002	0.004
RMS Deviation	0.003	0.002	0.001	0.002
$^{3}\Delta^{19}$F($^{81/79}$Br)	-0.2773(3) ppb[b]		-0.2869(3) ppb[c]	
$^{4}\Delta^{19}$F-3($^{81/79}$Br)	-0.1006(1) ppb[d]		-0.1101(1) ppb[e]	

a. The chemical shift reported in ppm refers to the chemical shift obtained from iteration on the high frequency peaks of the multiplets in the F-3 region, attributed to isotopomers containing two ^{79}Br atoms.

b. The shift from the highest frequency peaks of the multiplet to the third highest frequency peaks, attributed to isotopomers with a ^{79}Br at the C-1 site, undergoing isotopic substitution at the C-2 site.

c. The shift from the second to the fourth highest frequency peaks of the multiplets. This shift is attributed to isotopomers with ^{81}Br at the C-1 position, undergoing isotopic substitution at the C-2 position.

d. The shift from the highest frequency peaks of the multiplets to the second highest frequency peaks. In this case, the C-2 position has a ^{79}Br atom while the C-1 site undergoes isotopic substitution.

e. The shift from the third to the fourth highest frequency peaks of the multiplets. Here, the C-2 site has an ^{81}Br atom while the C-1 position undergoes isotopic substitution.

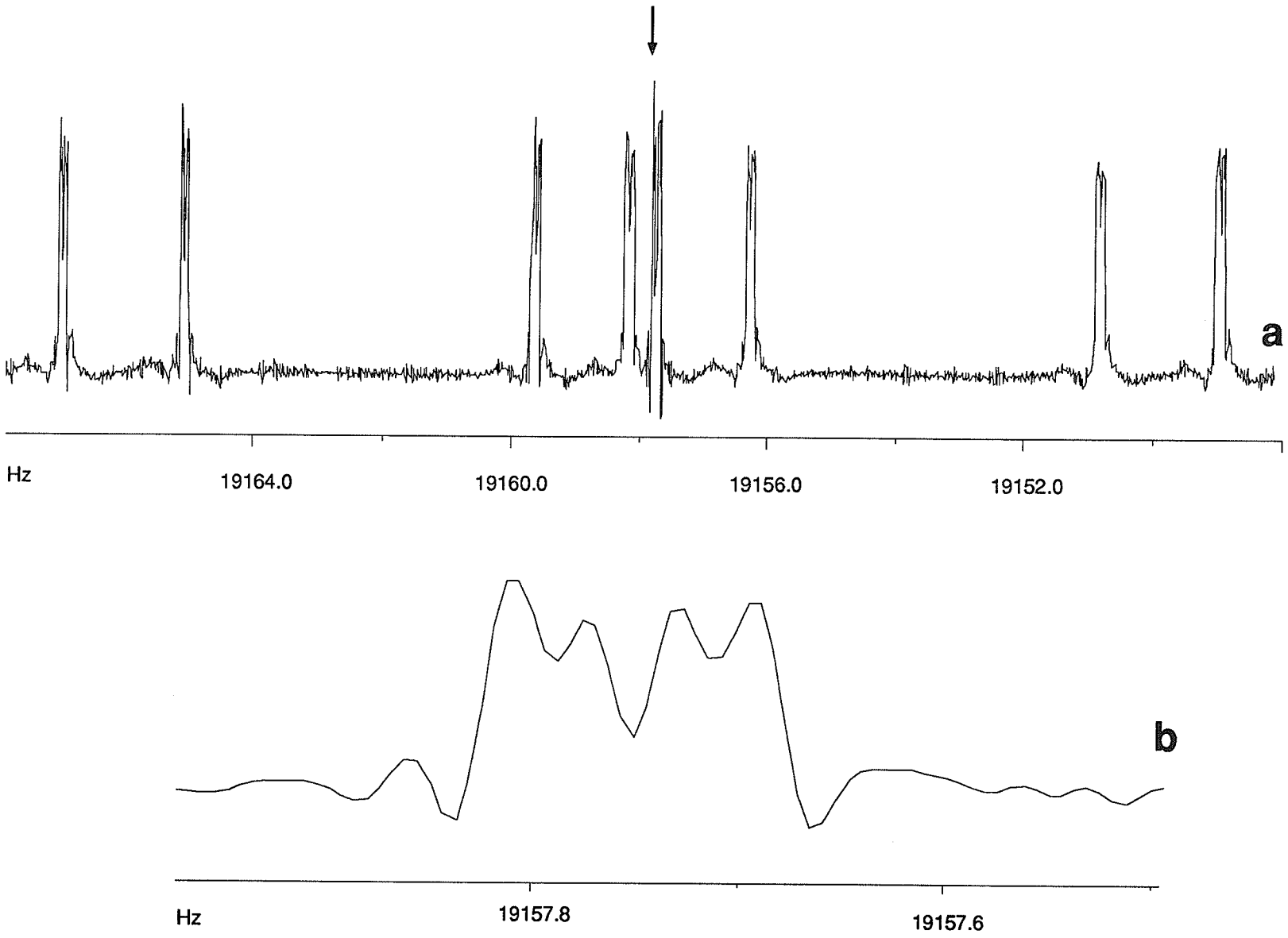
a
Hz
19164.0
19160.0
19156.0
19152.0
b
Hz
19157.8
19157.6

Figure 3.1.6

The ^{19}F NMR spectrum of the F-3 region of 1,2-dibromo-3,5-difluorobenzene, **34**, acquired at 282.363 MHz. Trace (b), which is an expansion of the multiplet indicated with an arrow in (a), shows the four peaks resulting from $^{3}\Delta^{19}F(^{81/79}Br)$ and $^{4}\Delta^{19}F(^{81/79}Br)$. The larger isotope shift, from the first to third peaks and from the second to fourth peaks, is attributed to $^{3}\Delta^{19}F(^{81/79}Br)$, while the shift from the first to second peaks and from the third to fourth peaks is attributed to $^{4}\Delta^{19}F(^{81/79}Br)$. The scale is in Hz to high frequency of internal C_6F_6.

3.1.14 1-bromo-3,5-difluoro-2-iodobenzene, 35.

35, prepared as a 5 mol% solution in acetone-d_6, was analyzed as an ABXY system. The F-3 region of the ^{19}F spectrum was split into asymmetric mutiplets, which were not reproduced by the spectral analysis. To determine whether these peaks were an artifact of the acquisition process, the spectrum of this region was reacquired on another day. Improved resolution (Figure 3.1.7) showed fine structure on the multiplets as well as a doubling of all the peaks. This doubling has been attributed to $^{4}\Delta^{19}F(^{81/79}Br)$. However, the additional peaks in this region precluded doing separate fits for the two isotopomers of this molecule. The results of the analysis on the ^{79}Br isotopomer are reported in Table 3.1.15.

Table 3.1.15 Final ^{19}F and ^{1}H NMR spectral parameters for a 5 mol% solution of 1-bromo-3,5-difluoro-2-iodobenzene, **35,** in acetone-d_6/C_6F_6/TMS.

Chemical Shift

	Hz	ppm
F-3	23508.380(2)	83.256
H-4	2148.687(1)	7.159
F-5	15179.246(1)	53.758
H-6	2249.621(1)	7.495

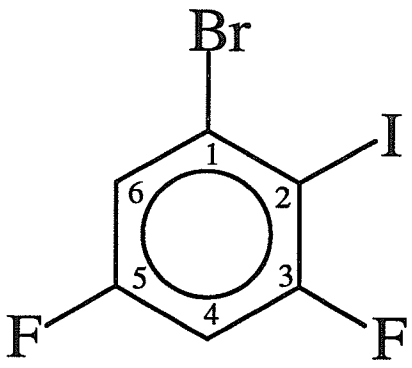

Coupling Constants (Hz)		**Convergence Data**	
$^{3}J_{34}$	8.207(2)	**Calculated Transitions**	32
$^{3}J_{45}$	8.802(2)	**Assigned Transitions**	28
$^{3}J_{56}$	8.291(2)	**Peaks Observed**	32
$^{4}J_{35}$	8.070(2)	**Largest Difference**	0.008
$^{4}J_{46}$	2.709(2)	**RMS Deviation**	0.004
$^{5}J_{36}$	1.656(2)	$^{4}\Delta^{19}$**F-3(**$^{81/79}$**Br)**	±0.15(1)[a]
		$^{4}\Delta^{19}$**F-5(**$^{81/79}$**Br)**	not observed
Parameter Correlation:		ν_6:J_{35} = -0.333	

a. Calculated from the repeated splitting pattern in the F-3 region. Because of varying peak intensities, the sign of this isotope shift is uncertain.

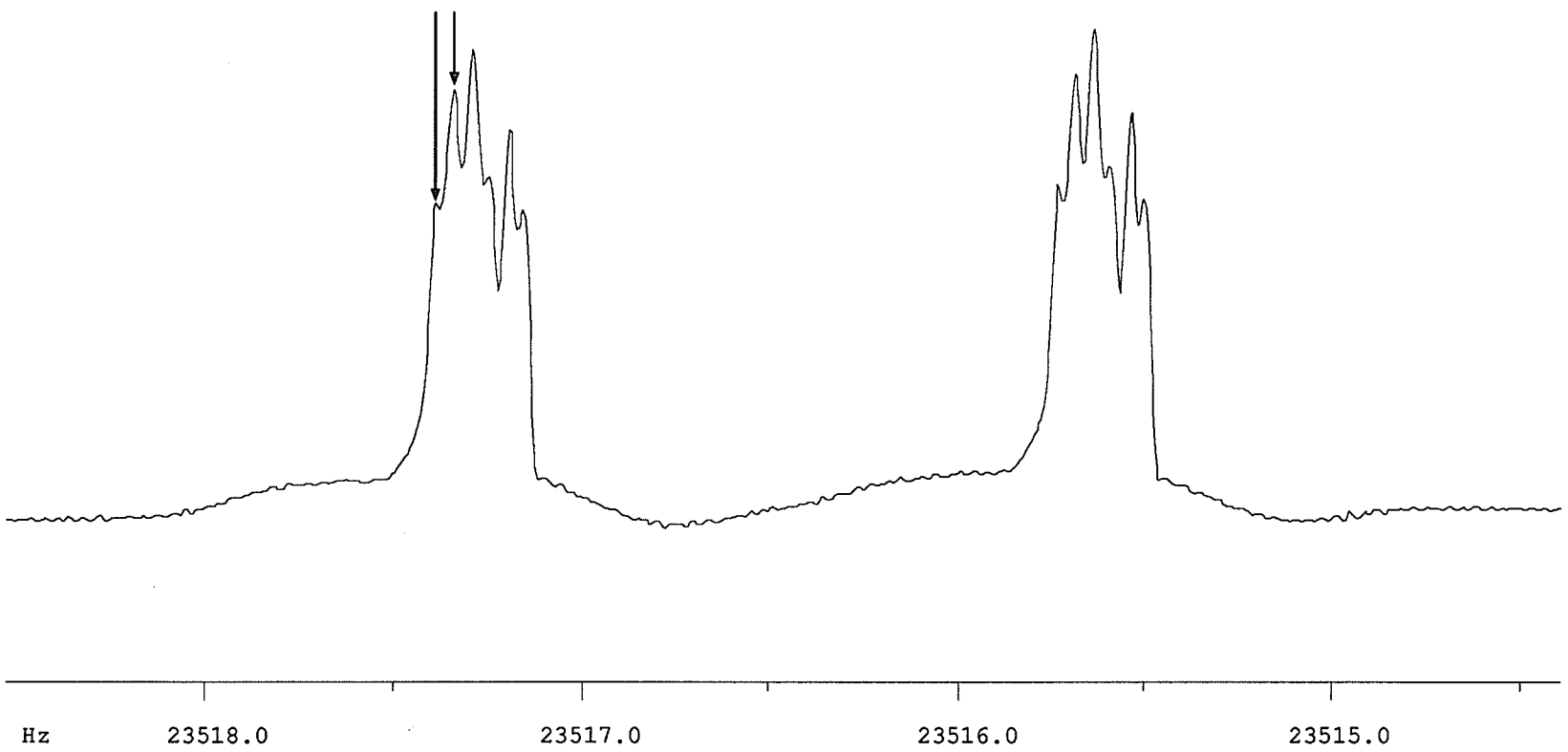
Hz
23518.0
23517.0
23516.0
23515.0

Figure 3.1.7

The ^{19}F NMR spectrum of part of the F-3 region of 1-bromo-3,5-difluoro-2-iodobenzene, **35**, acquired at 282.363 MHz. The small splitting indicated by the two arrows repeats throughout the region and has been attributed to $^{4}\Delta^{19}F(^{81/79}Br)$. The remaining transitions are unexplained. The scale is in Hz to high frequency of internal C_6F_6.

3.1.15 α-(2-bromo-4,6-difluorophenoxy)-β-chloroethane, 36.

36 was prepared as a 5 mol% solution in acetone-d_6; its spectrum was analyzed as an ABMM'NN'XY system. Partial decoupling experiments were performed to determine the signs of $^5J_{\alpha 6}$ and $^6J_{\beta 6}$ relative to $^3J_{\alpha\beta}$. Extreme resolution enhancement (LB = -0.4, GB = 0.4) gave line widths at half-height of 0.06 Hz, but there was no indication of $^4\Delta^{19}F(^{81/79}Br)$ for either fluorine nucleus. Apart from a parameter correlation of 1.0 between $^2J_{\alpha\alpha'}$ and $^2J_{\beta\beta'}$, resulting in a large standard deviation for these two parameters, there were no significant correlations. The results of this analysis are tabulated in Table 3.1.16.

Table 3.1.16 Final ^{19}F and ^{1}H NMR spectral parameters for a 5 mol% solution of α-(2-bromo-4,6-difluorophenoxy-β-chloroethane, **36**, in acetone-d_6/C_6F_6/TMS.

	Chemical Shift (Hz)	Chemical Shift (ppm)
H-α	1304.6899(8)	4.374
H-β	1177.5397(8)	3.923
H-3	2190.5267(9)	7.299
F-4	13737.3094(9)	45.770
H-5	2153.0553(9)	7.174
F-6	11457.5244(9)	38.175

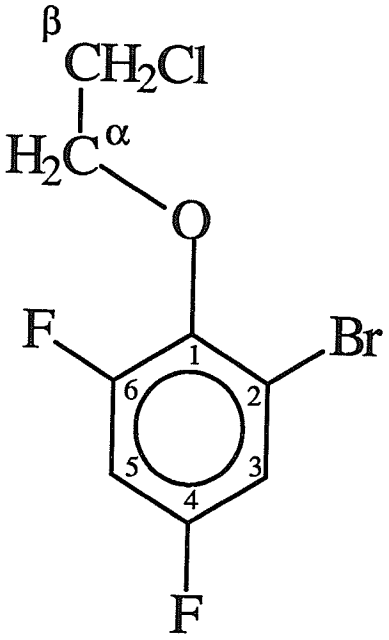

Coupling Constants (Hz)

$^{2}J_{\alpha\alpha'}$	-12.5(2)	$^{3}J_{56}$	10.953(1)	$^{6}J_{\alpha 3}$	not observed
$^{2}J_{\beta\beta'}$	-11.5(2)	$^{4}J_{35}$	3.019(1)	$^{6}J_{\alpha 5}$	not observed
$^{3}J_{\alpha\beta}$	6.3753(1)	$^{4}J_{46}$	3.853(1)	$^{7}J_{\alpha 4}$	not observed
$^{3}J_{\alpha\beta'}$	4.587(2)	$^{5}J_{\alpha 6}$	0.732(1)	$^{7}J_{\beta 3}$	not observed
$^{3}J_{34}$	7.992(1)	$^{5}J_{36}$	-2.149(1)	$^{7}J_{\beta 5}$	not observed
$^{3}J_{45}$	8.585(1)	$^{6}J_{\beta 6}$	0.500(1)	$^{8}J_{\beta 4}$	not observed

Table 3.1.16 (continued).

Convergence Data			
Calc. Transitions	832	**RMS Deviation**	0.011
Assigned Transitions	832	**$^{4}\Delta^{19}$F-4($^{81/79}$Br)**	not observed
Peaks Observed	145	**$^{4}\Delta^{19}$F-6($^{81/79}$Br)**	not observed
Largest Difference	0.033		

3.1.16 1-bromo-2,4,6-trifluorobenzene, 37.

37 was prepared as a 5 mol% solution in acetone-d_6 and analyzed as an AA'BXX' system. Line widths of less than 0.04 Hz after resolution enhancement (LB = -0.14, GB = 0.6) permitted the measurement of $^{3}\Delta^{19}$F($^{81/79}$Br). Although slightly broadened (0.07 Hz), the sharp peaks in the F-5 region suggested that $^{5}\Delta^{19}$F($^{81/79}$Br), if present, is too small to be detected at this resolution. The results of this analysis, for which there were no significant parameter correlations, are listed in Table 3.1.17.

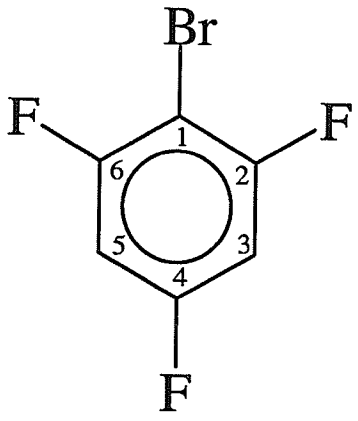

37

Table 3.1.17 Final ^{19}F and ^{1}H NMR spectral parameters for a 5 mol% solution of 1-bromo-2,4,6-trifluorobenzene, **37**, in acetone-d_6/C_6F_6/TMS.

	Chemical Shift (Hz)		Chemical Shift (ppm)	
	^{79}Br peaks	^{81}Br peaks	^{79}Br peaks	^{81}Br peaks
F-2,6	17063.720(1)	17063.6477(9)	60.429	60.428
H-3,5	2139.937(1)	2139.937(1)	7.130	7.130
F-4	15504.054(1)	15504.054(1)	54.905	54.905

Coupling Constants (Hz)			Convergence Data		
	^{79}Br peaks	^{81}Br peaks		^{79}Br peaks	^{81}Br peaks
$^3J_{23} = {}^3J_{56}$	8.9095(3)	8.9094(2)	**Calc. Transitions**	64	64
$^3J_{34} = {}^3J_{45}$	8.923(2)	8.922(1)	**Assigned Transitions**	59	59
$^4J_{24} = {}^4J_{46}$	6.179(1)	6.179(1)	**Peaks Observed**	49	49
$^4J_{26}$	2.807(2)	2.808(2)	**Largest Difference**	0.012	0.010
$^4J_{35}$	1.844(2)	1.845(2)	**RMS Deviation**	0.005	0.005
$^5J_{25} = {}^5J_{36}$	-2.105(2)	-2.106(2)	$^3\Delta^{19}F(^{81/79}Br)$	-0.256(3) ppb	
			$^5\Delta^{19}F(^{81/79}Br)$	not observed	

3.1.17 1,3-dibromo-2,4,5,6-tetrafluorobenzene, 39.

39 was prepared as a 5 mol% solution in acetone-d_6 and analyzed as an A_2BC system. The peaks of the F-2 region were split into 1:2:1 triplets, consistent with a fluorine site having two chemically equivalent bromine atoms. An analysis of the tall central peaks, the results of which are reported in Table 3.1.18, gave a good fit. However, fits on the other peaks of the multiplets gave much larger RMS values and a poor calculated spectrum. Thus, a simulated spectrum was generated using the coupling constants from the good fit and isotope shifts measured from the experimental spectrum (see Figure 3.1.8). There were no significant parameter correlations.

An interesting feature of this spectrum is the apparent non-additivity of the isotope shift. Although the difference in isotope shifts is just within the uncertainty, the spectrum could not be simulated accurately unless different isotope shifts were used. The peaks of F-4,6 were broadened considerably - line widths of 0.2 Hz, compared to 0.08 Hz for the C_6F_6 reference peak - but the anticipated doublet resulting from the average of $^3\Delta^{19}F(^{81/79}Br)$ and $^5\Delta^{19}F(^{81/79}Br)$ was not observed. The F-5 peaks were symmetrical with line widths of 0.1 Hz, with no indication of $^4\Delta^{19}F(^{81/79}Br)$.

Table 3.1.18 Final ^{19}F NMR spectral parameters[a] for a 5 mol% solution of 1,3-dibromo-2,4,5,6-tetrafluorobenzene, **39**, in acetone-d_6/C_6F_6/TMS.

Chemical Shift

	Hz	ppm
F-2	16910.557(3)	59.889
F-4,6	10436.071(3)	36.960
F-5	878.718(3)	3.112

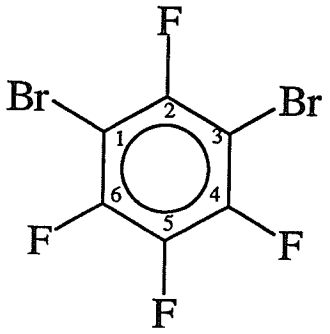

Coupling Constants (Hz)		**Convergence Data**	
$^3J_{45} = {}^3J_{56}$	-21.264(4)	**Calculated Transitions**	24
$^4J_{24} = {}^4J_{26}$	1.401(3)	**Assigned Transitions**	24
$^5J_{25}$	7.861(5)	**Peaks Observed**	16
		Largest Difference	0.014
		RMS Deviation	0.009
		$^3\Delta^{19}$**F-2(**$^{81/79}$**Br)**[b]	-0.26(2) ppb
		$^3\Delta^{19}$**F-2(**$^{81/79}$**Br)**[c]	-0.30(2) ppb
		$(^3\Delta + {}^5\Delta)/2$	not observed
		$^4\Delta^{19}$**F-5(**$^{81/79}$**Br)**	not observed

a. Optimized parameters following iteration on the tall central peaks of the multiplets appearing in the F-2 region are reported.

b. The shift from the high frequency peaks of the F-2 region, attributed to isotopomers containing two ^{79}Br atoms, to the central peaks, attributed to isotopomers containing both a ^{79}Br and an ^{81}Br atom.

c. The shift from the central peaks to the low frequency peaks, attributed to isotopomers containing two ^{81}Br atoms.

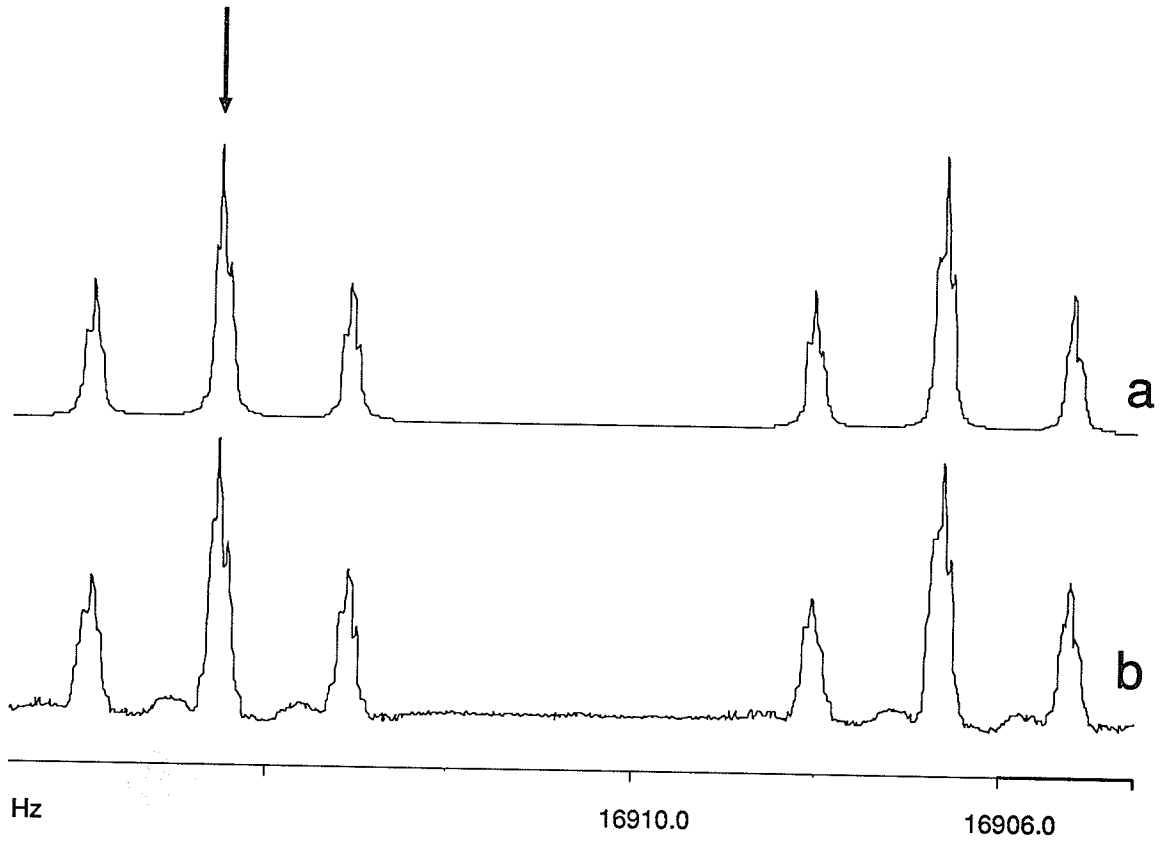
a
b
Hz
16910.0
16906.0

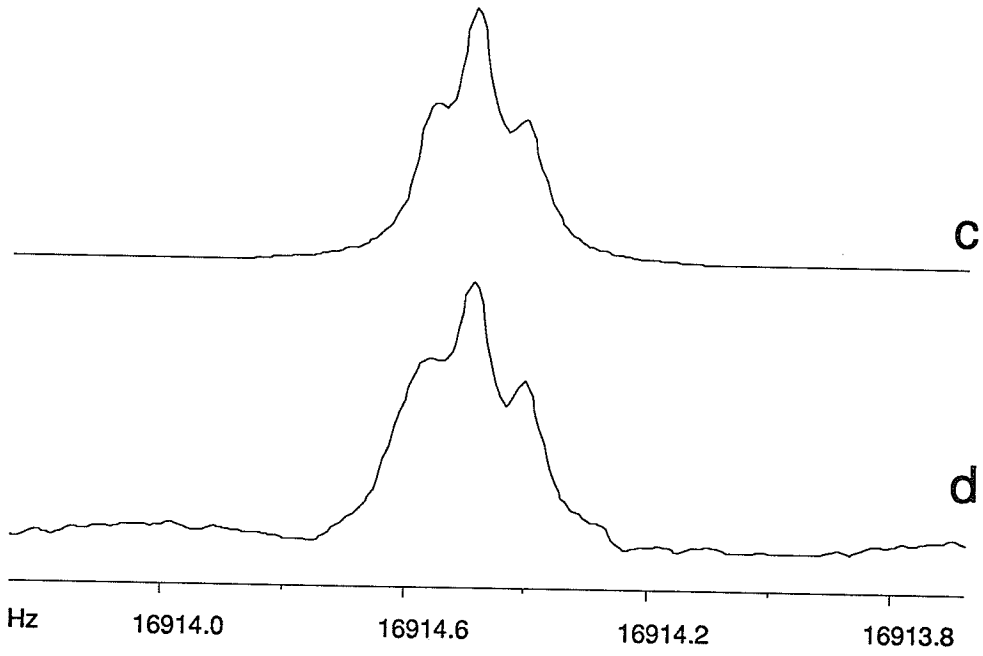
c
d
Hz
16914.0
16914.6
16914.2
16913.8

Figure 3.1.8

The calculated (a) and experimental (b) ^{19}F NMR spectrum of the F-2 region of 1,3-dibromo-2,4,5,6-tetrafluorobenzene, **39**, acquired at 282.363 MHz. The approximately 1:2:1 peak intensity ratio is attributed to the isotope shifts from the two bromine atoms, which are in chemically equivalent positions relative to the observed fluorine. Traces (c) and (d) are, respectively, the calculated and experimental spectra of an expansion of the multiplet indicated with an arrow in (a). The difference in peak heights seen for the outside peaks of each multiplet is greater than the 1.0:0.95 peak intensity ratio expected from the natural abundance of the bromine isotopes and may be due to a smaller shift from the high frequency peaks to the central peaks than from the central to the low frequency peaks.

3.1.18 1-bromo-2,3,4,6-tetrafluorobenzene, 44.

44, prepared as a 5 mol% solution in acetone-d_6, was analyzed as an ABCDX system. The F-2 and F-6 regions were well resolved; $^{3}\Delta^{19}F(^{81/79}Br)$ was observed in both cases. Despite line widths of less than 0.06 Hz at half-height, neither $^{4}\Delta^{19}F(^{81/79}Br)$ nor $^{5}\Delta^{19}F(^{81/79}Br)$ were detected at F-3 and F-4. The results of this analysis, for which there were no significant parameter correlations, are reported in Table 3.1.19.

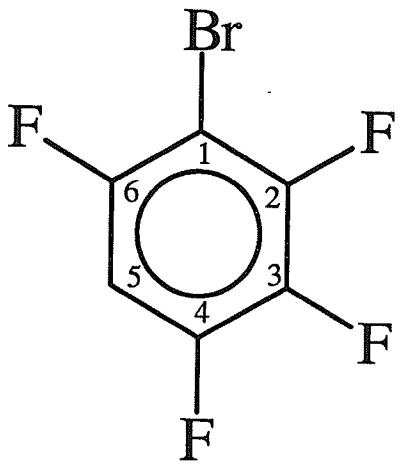

44

Table 3.1.19 Final ^{19}F and ^{1}H NMR spectral parameters for a 5 mol% solution of 1-bromo-2,3,4,6-tetrafluorobenzene, **44**, in acetone-d_6/C_6F_6/TMS.

	Chemical Shift (Hz)		Chemical Shift (ppm)	
	^{79}Br peaks	^{81}Br peaks	^{79}Br peaks	^{81}Br peaks
F-2	10532.680(2)	10532.616(2)	37.302	37.302
F-3	104.306(2)	104.306(2)	0.369	0.369
F-4	8525.146(2)	8525.146(2)	30.192	30.192
H-5	2225.243(2)	2225.243(2)	7.414	7.414
F-6	15201.873(2)	15201.810(2)	53.838	53.838

Coupling Constants (Hz)		
	^{79}Br peaks	^{81}Br peaks
$^{3}J_{23}$	-20.718(3)	-20.717(2)
$^{3}J_{34}$	-20.695(3)	20.695(2)
$^{3}J_{45}$	10.651(3)	10.651(2)
$^{3}J_{56}$	8.730(2)	8.729(2)
$^{4}J_{24}$	5.417(3)	5.419(2)
$^{4}J_{26}$	1.722(3)	1.724(2)
$^{4}J_{35}$	6.450(3)	6.449(2)
$^{4}J_{46}$	2.206(3)	2.209(2)
$^{5}J_{25}$	-2.533(3)	2.531(2)
$^{5}J_{36}$	9.519(3)	9.520(2)

Convergence Data		
	^{79}Br peaks	^{81}Br peaks
Calc. Transitions	80	80
Assigned Transitions	72	80
Peaks Observed	80	80
Largest Difference	0.016	0.012
RMS Deviation	0.007	0.006
$^{3}\Delta^{19}$F-2($^{81/79}$Br)	-0.227(2) ppb	
$^{3}\Delta^{19}$F-6($^{81/79}$Br)	-0.223(2) ppb	
$^{4}\Delta^{19}$F-3($^{81/79}$Br)	not observed	
$^{5}\Delta^{19}$F-4($^{81/79}$Br)	not observed	

3.2 Spectral parameters for ^{13}C NMR spectra.

Proton decoupled ^{13}C NMR spectra of **1-4, 6, 7** and **23** were acquired at 75.48 MHz. The ^{13}C chemical shifts, as well as $^{n}J_{CF}$, are reported in Tables 3.2.1 and 3.2.2. Most spectra were not sufficiently resolved to observe $^{n}\Delta^{13}C(^{37/35}Cl)$; however, by acquiring a narrower region with longer acquisition times (20 second acquisitions, with spectral widths of 150 Hz, giving an FID resolution of 0.025Hz/pt), $^{1}\Delta^{13}C(^{37/35}Cl)$ was measured for **3** and **6** (Table 3.7.1). All spectral parameters were measured directly from the experimental spectra.

3.2.1 1- substituted-2-chloro-6-fluorobenzenes.

^{13}C spectra of **1-4, 6** and **7** were acquired to investigate correlations between $^{4}\Delta^{19}F(^{37/35}Cl)$ and ^{13}C NMR parameters; ^{13}C spectra of **5** were not acquired since the ^{19}F spectrum was not sufficiently resolved to measure $^{4}\Delta^{19}F(^{37/35}Cl)$. These compounds were prepared as 5 mol% solutions in acetone-d_6. The results of these analyses are reported in Table 3.2.1. To simplify comparisons, the compounds in this table are listed with the chlorine at the C-2 position and the fluorine at the C-6 position, regardless of the compound's IUPAC name.

Table 3.2.1 The ^{13}C NMR spectral parameters of some 1-substituted-2-chloro-6-fluorobenzenes.

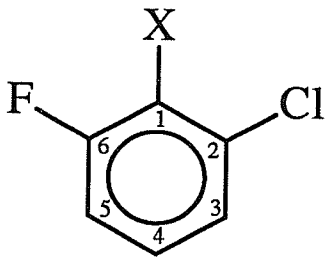

Chemical Shifts[a,b]

X	H	CH_3	CH_2Cl[c]	$CHCl_2$[d]	CN[c]	COCl
ν_1	8815.89(4)	9378.0(3)	9415.7(2)	not resolved	7804.6(3)	9580.2(2)
δ_1	116.798	124.245	124.744		103.400	126.924
ν_2	10230.80(4)	10242.5(3)	10268.11(2)	not resolved	10381.35(2)	9856.3(2)
δ_2	135.543	135.698	136.037		137.538	130.581
ν_3	9474.12(4)	9472.0(3)	9553.8(2)	9570.6(2)	9570.6(3)	9595.8(2)
δ_3	125.518	125.490	126.574	126.797	126.797	127.130
ν_4	9981.80(4)	9691.3(3)	9975.2(2)	10062.5(1)	10316.5(3)	10194.6(2)
δ_4	132.244	128.396	132.157	133.313	136.679	135.064
ν_5	8666.48(4)	8629.0(3)	8710.6(2)	8802.0(1)	8737.7(3)	8773.7(2)
δ_5	114.818	114.322	115.403	116.613	115.762	116.238
ν_6	12353.38(4)	12223.8(3)	12237.1(2)	not resolved	12407.7(1)	11991.6(2)
δ_6	163.664	161.948	162.124		164.384	158.871

Table 3.2.1 (continued).

Chemical Shifts[a,b]

X	H	CH_3	CH_2Cl[c]	$CHCl_2$[d]	CN[c]	COCl
ν_α	---	not acquired	2786.5(3)	not acquired	8423.2(3)	12370.8(2)
δ_α	---		36.917		111.595	163.895

Coupling Constants

$^1J_{6,F}$	-247.71(4)	-245.2(3)	-251.0(2)	not resolved	-259.1(1)	-254.0(2)
$^2J_{1,F}$	-25.00(4)	-19.6(3)	-17.4(2)	not resolved	-18.2(1)	-18.7(2)
$^2J_{5,F}$	-21.14(4)	-23.2(3)	-22.3(2)	-21.6(1)	-19.9(1)	-20.7(2)
$^3J_{2,F}$	10.28(4)	6.1(3)	4.66(2)	not resolved	2.23(2)	3.6(2)
$^3J_{4,F}$	9.01(4)	9.7(3)	9.9(2)	10.2(1)	9.8(1)	9.6(2)
$^3J_{\alpha,F}$	---	not acquired	5.4(2)	not acquired	not resolved	0.7(2)
$^4J_{4F}$	3.33(4)	3.5(3)	3.5(2)	3.3(1)	3.4(1)	3.4(2)

a. Chemical shifts are reported in Hz (ν_n) or ppm (δ_n) to high frequency of internal TMS.

b. Numbers in parentheses are the uncertainty in the last digit, as determined from the resolution of the experimental spectra.

c. A high resolution spectrum of the C-2 region was acquired.

d. There were extra peaks in this spectrum, probably due to conformational isomers. Only those peaks which could be unambiguously assigned are reported.

e. Signs of coupling constants are those obtained from double resonance experiments as reported in the literature. These signs have been found to be consistently as indicated in Table 3.2.1.[60]

3.2.2 ^{13}C NMR spectral parameters for 1,3-dichloro-2,4,6-trifluorobenzene, 23.

^{13}C NMR spectral parameters for **23** were acquired as for the compounds listed in Table 3.2.1. The spectral parameters, measured directly from this spectrum, are reported in Table 3.2.2. The spectra were not sufficiently resolved to observe $^{n}\Delta^{13}C(^{37/35}Cl)$.

Table 3.2.2 The ^{13}C NMR spectral parameters of 1,3-dichloro-2,4,6-trifluorobenzene, **23**, in acetone-d_6

Coupling Constants (Hz)

$^{1}J_{2,F-2}$	249.55(8)
$^{1}J_{4,F-4} = {}^{1}J_{6,F-6}$	250.05(8)
$^{2}J_{1,F-2} = {}^{2}J_{3,F-2}$	21.1(1) (24.0)[a]
$^{2}J_{1,F-6} = {}^{2}J_{3,F-4}$	24.0(2) (21.1)[a]
$^{2}J_{5,F-4} = {}^{2}J_{5,F-6}$	26.87(8)
$^{3}J_{2,F-4} = {}^{3}J_{2,F-6}$	5.45(8)
$^{3}J_{4,F-2} = {}^{3}J_{6,F-2}$	4.76(8)[b]
$^{3}J_{4,F-6} = {}^{3}J_{6,F-4}$	14.22(8)[b]
$^{4}J_{1,F-4} = {}^{4}J_{3,F-6}$	3.9(2)
$^{4}J_{5,F-2}$	3.87(8)

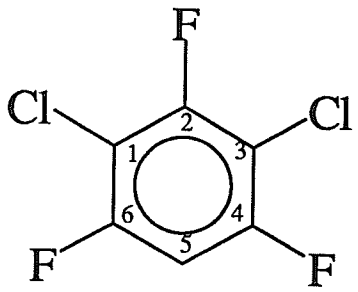

Chemical Shifts

	Hz	ppm
C-1,3	8115.9(2)	107.524
C-2	11771.60(8)	155.957
C-4,6	11904.9(8)	157.723
C-5	7741.03(8)	102.557

a. These assignments may be reversed.

b. $^{3}J_{4,F-6}$ (= $^{3}J_{6,F-4}$) and $^{3}J_{4,F-2}$ (= $^{3}J_{6,F-2}$) were assigned on the basis of the ^{13}C satellite peaks in the ^{19}F NMR spectrum.

3.3 Molecular orbital calculations.

SCF molecular orbital calculations at the STO-3G and 6-31G* level, using Gaussian 94, were performed on **1, 2, 6, 7** and **9** to investigate correlations between molecular properties and $^{4}\Delta^{19}F(^{37/35}Cl)$ in a series of 1-substituted-2-chloro-6-fluorobenzenes. MP2/6-31G* calculations on **1, 2** and **9** were also performed. Mulliken atomic charges at the site of isotopic substitution as well as at the observed nucleus are reported. Also investigated were the C—Cl and C—F bond lengths. Preliminary results indicated that there were no significant correlations; hence, it was decided not to proceed with calculations on the entire series. The results of these calculations are reported in Tables 3.3.1-3.3.3.

Because of rotation about the C-1—C-α bond in **7**, calculations were performed with the torsion angle between the C-α—Cl-α bond and the plane of the phenyl ring being constrained at 15° increments between 0° and 180°. The results from the minimum energy conformer are reported.

Gaussian 94 calculations at the SCF STO-3G and 6-31G* levels were done on the molecules experiencing $^{5}\Delta^{19}F(^{37/35}Cl)$, excluding 2-chloro-2',4'-difluoroacetophenone, **27**, for which the chlorine atom was not directly bonded to the phenyl ring. The calculated (6-31g* level) C—F and C—Cl bond lengths, as well as the Mulliken atomic charges of these nuclei are reported in Table 3.3.4.

Table 3.3.1 Mulliken atomic charges and internuclear bond lengths at the C-2 and C-6 positions of some 1-substituted-2-chloro-6-fluorobenzenes, as determined by Gaussian 94 calculations at the STO-3G level.

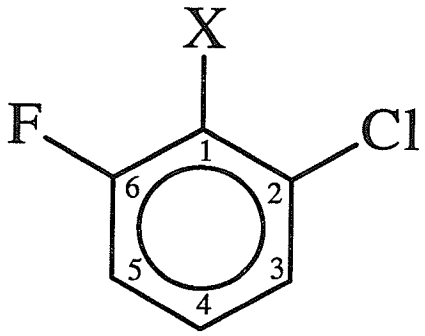

X	Bond Lengths (Å)		Atomic Charges				$^4\Delta^{19}F(^{37/35}Cl)$ (ppb)
	C—Cl	C—F	C-2	Cl-2	C-6	F	
H	1.783	1.354	0.056	-0.150	0.151	-0.125	-0.53(2)
CH_3	1.787	1.356	0.026	-0.125	0.140	-0.130	-0.76(1)
CN	1.777	1.350	0.068	-0.120	0.173	-0.111	-0.552(1)
COCl[a]	1.779	1.351	0.063	-0.126	0.168	-0.112	-0.37(1) (-0.31)[b]
Cl	1.776	1.351	0.056	-0.116	0.161	-0.109	-0.740(3)

a. The values reported are for a C-2—C-1—C-α—Cl-α torsion angle of 120°, which was found to be the lowest energy conformer.

b. Two isotope shifts were observed at this site, one from each of the two chlorine atoms in the molecule. It was not possible to definitely assign one of these to Cl-2, although it seems probable that the larger isotope shift is the one transmitted entirely through the phenyl ring.

Table 3.3.2 Mulliken atomic charges and internuclear bond lengths at the C-2 and C-6 positions of some 1-substituted-2-chloro-6-fluorobenzenes, as determined by Gaussian 94 calculations at the 6-31G* level.

X	Bond Lengths (Å)		Atomic Charges				$^4\Delta^{19}F(^{37/35}Cl)$ (ppb)
	C—Cl	C—F	C-2	Cl-2	C-6	F	
H	1.741	1.327	-0.122	0.009	0.483	-0.383	-0.53(2)
CH_3	1.747	1.332	-0.161	0.003	0.464	-0.386	-0.76(1)
CN	1.729	1.318	-0.113	0.078	0.521	-0.353	-0.552(1)
COCl[a]	1.735	1.324	-0.126	-0.024	0.511	-0.367	-0.37(1) (-0.31)[b]
Cl	1.725	1.320	-0.115	0.049	0.523	-0.363	-0.740(3)

a. The values reported are for a C-2—C-1—C-α—Cl-α torsion angle of 105°, which was found to be the lowest energy conformer.

b. See footnote (b) of Table 3.3.1.

Table 3.3.3 Mulliken atomic charges and internuclear bond lengths at the C-2 and C-6 positions of some 1-substituted-2-chloro-6-fluorobenzenes, as determined by Gaussian 94 calculations at the MP2/6-31G* level.

X	Bond Lengths (Å)		Atomic Charges				$^4\Delta^{19}F(^{37/35}Cl)$ (ppb)
	C—Cl	C—F	C-2	Cl-2	C-6	F	
H	1.740	1.356	-0.124	0.012	0.476	-0.398	-0.53(2)
CH_3	1.745	1.360	-0.160	0.007	0.457	-0.401	-0.76(1)
Cl	1.730	1.349	-0.116	0.051	0.513	-0.378	-0.740(3)

Table 3.3.4 Mulliken atomic charges and internuclear bond lengths, as determined by Gaussian 94 calculations at the 6-31G* level, for the substituted and observed nucleus of the molecules experiencing $^{5}\Delta^{19}F(^{37/35}Cl)$.

	Bond Lengths (Å)		Atomic Charges				$^{5}\Delta^{19}F(^{37/35}Cl)$ (ppb)
	C—Cl	C—F	C(Cl)	Cl	C(F)	F	
11[a]	1.744	1.328	-0.150	0.001	0.472	-0.384	-0.324(5)
13	1.733	1.324	-0.253	0.039	0.495	-0.378	-0.54(3)
15	1.740	1.323	-0.138	0.017	0.399	-0.369	-0.460(2)
16	1.723	1.321	-0.365	0.074	0.515	-0.372	-0.395(7)
18	1.718	1.312	-0.362	0.104	0.357	-0.344	-0.680(2)
21[b]	1.738	1.327	-0.226	0.025	0.502	-0.385	-0.23(1)
22[b]	1.728	1.324	-0.340	0.060	0.523	-0.379	-0.39(3)
24[c]	1.737	1.321	-0.361	0.031	0.520	-0.375	-0.29(1)

a. See Scheme 2.1 or Figure 3.3.1 for the names of the molecules analyzed.

b. Values reported are for the minimum energy conformer - the methyl group in the phenyl plane *trans* to the chlorine atom.

c. Values reported are for the minimum energy conformer, with the hydroxyl group in the phenyl plane proximate to the chlorine atom.

3.4 Chlorine isotope shifts on the ^{19}F NMR spectra of some aromatic compounds.

Chlorine isotope shifts are reported in Tables 3.4.1 to 3.4.4. Unless a full spectral analysis was performed (Tables 3.1.1 - 3.1.12), the isotope shifts were determined by direct measurement of the shift between peaks that could unambiguously be assigned to the specific isotope shift. For these, the uncertainty reported is the standard deviation of the observed isotope shifts based on the number of peaks, n, for which this measurement could be made. Unless otherwise specified, the samples were 5 mol% solutions in acetone-d_6. The chemical shift of the nucleus experiencing the isotope shift (ν(F)) for the lightest isotopomer is also reported.

If an isotope shift was not observed, an estimate was made of the threshold below which an isotope shift would not be detected for that particular spectrum. This was done by simulating one of the peaks in the region under consideration. Peaks, whose intensities were adjusted to that expected for the isotopes being considered, were simulated, initially with the same chemical shift and line width as the peak from the experimental spectrum. The relative chemical shift was then varied incrementally until an isotope shift became apparent on the simulated spectrum. This is reported as the maximum possible isotope shift for that site, although it should be noted that isotope shifts of this magnitude would still be poorly resolved and probably would not have been reported. Since no isotope shift was observed, a sign is not given for these, although they are probably negative, as are all chlorine and probably all the bromine isotope shifts observed thus far.

The ^{19}F NMR spectrum of 2-chloro-6-fluorobenzal chloride, **4**, was not resolved at 300 K, appearing as a very broad peak, suggesting conformational isomers which are near

the coalescence point. This was confirmed by low-temperature NMR. At 210 K, the more abundant conformer, as determined by the peak intensity, had multiplets with a peak intensity ratio of approximately 1.0:0.9:0.3. This compares with the peak intensity ratio of 1.0:0.98:0.32:0.035 expected for a ^{19}F nucleus with three chemically equivalent chlorine atoms. One of the multiplets of this region was simulated using this ratio (Figure 3.4.1), accurately reproducing the experimental spectrum; the smallest peaks are too small to be observed experimentally. This suggests that $^{4}\Delta^{19}F(^{37/35}Cl)$ from Cl-2 is of the same magnitude as $^{4}\Delta^{19}F(^{37/35}Cl)$ from the two Cl-α atoms. Measurement of $^{4}\Delta^{19}F(^{37/35}Cl)$ from the peaks of the less abundant isomer was not possible because they were still broadened at this temperature. Spectra of both regions were acquired at 200 K on another occasion, but the resolution was insufficient to measure $^{4}\Delta^{19}F(^{37/35}Cl)$ for either isomer.

The peaks of the fluorine region of 2-chloro-6-fluorotrichloromethylbenzene, **5,** were not sufficiently resolved to measure $^{4}\Delta^{19}F(^{37/35}Cl)$. This may be a because of the superposition of the isotope shift from the three chemically equivalent chlorine atoms at the α position upon the isotope shift from Cl-2.

Multiplets with a 9:3:3:1 peak intensity ratio were observed for the fluorine region of 2-chloro-6-fluorobenzoyl chloride, **7**. This is attributed to unequal isotope shifts from the two chlorine sites. However, it was not possible to assign the observed isotope shifts to a specific chlorine atom.

The 9:3:3:1 peak intensity ratio of the ^{19}F region of **9**, observed as an impurity in **4**, was used to identify it as 1,2-dichloro-3-fluorobenzene (Figure 3.4.2). Mass spectrometry was used to verify that the impurity was a dichlorofluorobenzene. The small range of the

observed $^{3}\Delta^{19}F(^{37/35}Cl)$ (Table 3.4.1) allowed the assignment of a 1-chloro-2-fluoro substitution pattern on the phenyl ring. Since $^{4}\Delta^{19}F(^{37/35}Cl)$ and $^{5}\Delta^{19}F(^{37/35}Cl)$ overlap (Tables 3.4.2 and 3.4.3), the remaining chlorine atom could not be assigned to the *meta* or *para* location, relative to the fluorine site, on the basis of isotope shifts. However, since this compound appears as an impurity in a 1,2,3-trisubstituted benzene, the impurity probably has the same substitution pattern. The magnitude of $^{3}\Delta^{19}F(^{37/35}Cl)$ was also used to distinguish the *ortho* fluorine region from the *meta* fluorine region(s) in **14** and **17.**

Spectra of pentafluorobenzoyl chloride, **27,** were acquired to investigate $^{6}\Delta^{19}F(^{37/35}Cl)$. Unfortunately, the *para* fluorine was poorly resolved, perhaps due to relaxation effects. However, $^{4}\Delta^{19}F(^{37/35}Cl)$ and $^{5}\Delta^{19}F(^{37/35}Cl)$ were observed in this case. A sample, prepared in CS_2, was poorly resolved.

2,6-Dibromo-3-chloro-4-fluoroaniline, **31**, initially prepared in acetone-d_6 as described in section 2.2, was not sufficiently resolved to observe $^{3}\Delta^{19}F(^{37/35}Cl)$. Another sample, prepared without degassing, was analyzed to investigate $^{6}\Delta^{19}F(^{2/1}H)$ (see section 3.6). D_2O was added to these samples to accelerate the exchange of the amino protons with deuterium. The peaks of the isotopomers containing deuterium were sharper, probably because of the smaller coupling to ND_2 and NDH ($^{n}J_{HF}$ is 6 times greater than the corresponding $^{n}J_{DF}$). This allowed the measurement of $^{3}\Delta^{19}F(^{37/35}Cl)$ from isotopomers containing one and two deuterium atoms and also showed that there was no deuterium isotope effect on $^{3}\Delta^{19}F(^{37/35}Cl)$. **31** was also prepared in CCl_4 as described for acetone-d_6 above. Here, only the peaks attributed to isotopomers containing two deuterium atoms were sufficiently resolved to observe $^{3}\Delta^{19}F(^{37/35}Cl)$.

Table 3.4.1 Three-bond chlorine isotope shifts on the ^{19}F NMR spectra of some substituted fluorobenzenes.

Compound	Nucleus	n[a]	ν(F) (Hz)	$^3\Delta^{19}F(^{37/35}Cl)$ (ppb)
9[b]	F-3	11	14897.205(5)	-1.559(8)
10	F-2	16	13290.977(6)	-1.43(2)
13	F-2	NA	14712.167(5)	-1.64(3)
14	F-2	16	11706.4580(4)	-1.412(1)
16	F-2,6	18	14857.79(1)	-1.49(4)
17	F-2,6	18	6048.46(1)	-1.47(3)
18	F-2,6	NA	6147.40(1)	-1.553(4)
19	F-2	NA	13064.5236(9)	-1.585(10)[c] 1.588(10)[d]
19[e]	F-2	NA	13287.216(2)	-1.594(10)[c] -1.611(10)[d]
22	F-3	NA	14458.8253(3)	-1.580(1)
23	F-2	NA	14536.906(3)	-1.64(2)[c] -1.64(2)[d]
23[f]	F-4,6	NA	14470.422(3)	-1.04(3)[c] -1.03(2)[d]
24	F-3	17	14547.076(4)	-1.52(5)
25	F-4	15	11812.303(8)	-1.44(3)
26	F-2	NA	7904.7(2)	≤ 2
	F-4	8	9007.641(8)	-1.25(3)
31	F-4	4	11349.47(1)	-1.45(1)[g]
	F-4	8	11167.51(7)	-1.42(3)[h]

a. For isotope shifts measured directly from the experimental spectra, the number of measurements, n, which could unambiguously be assigned to a particular isotope shift is reported. For these, the uncertainty in the isotope shift is the standard deviation of the n measurements. The isotope shifts of the remaining spectra, indicated with NA, were determined from a simulation.

b. Measured as a very dilute impurity in **4**.

c. The shift from the high frequency peaks, attributed to isotopomers containing two ^{35}Cl isotopes, to the central peak, attributed to isotopomers containing a ^{35}Cl and a ^{37}Cl isotope.

d. The shift from the central peaks to the low frequency peaks, attributed to isotopomers containing two ^{37}Cl isotopes.

e. Prepared as a 5 mol% solution in CS_2, containing also 0.25 mol% C_6F_6, 0.25 mol% TMS and 10 mol% C_6D_{12}.

f. The observed isotope shift reported here is $[^3\Delta^{19}F(^{37/35}Cl) + {}^5\Delta^{19}F(^{37/35}Cl)]/2$. See section 3.1.8 for a discussion of this effect.

g. Prepared as a 5 mol% solution in CCl_4 to which D_2O was added in increments of 7.5 μL. Within experimental error, these values did not deviate for the three samples measured.

h. Prepared as a 5 mol% solution in acetone-d_6, to which D_2O was added in increments of 20.0 μL. Within experimental error, these values did not deviate for the three samples measured.

Table 3.4.2 Four-bond chlorine isotope shifts on the ^{19}F NMR spectra of some substituted fluorobenzenes.

Compound	Nucleus	n	ν(F) (Hz)	$^4\Delta^{19}F(^{37/35}Cl)$ (ppb)
1	F-6	14	14742.309(5)	-0.53(2)
2	F-6	19	14161.709(5)	-0.76(1)
3	F-6	21 16[a]	14060.834(6)	-0.71(2)[b] -0.71(2)[c]
4[d]	F-6	16 13	16740.16(2)	-0.92(7)[e] -0.92(7)[f]
5	F-6	---	17592.4(3)	not resolved[g]
6	F-6	NA	16630.082(2)	-0.552(1)
7	F-6	8	14380.111(3)	-0.37(1)[h] -0.31(1)[h]
8[i]	F-6	12	13583.113(4)	-1.16(1)
9[j]	F-3	11	14897.205(3)	-0.740(3)
12	F-3,5	20	15551.217(3)	-0.32(1)
14	F-5	16	13116.3071(7)	-0.387(2)
15	F-3	15	7865.333(2)	-0.562(4)
17	F-3,5	23	7082.343(3)	-0.38(1)
18	F-3,5	NA	392.485(1)	-0.432(3)
20	F-4	NA	11912.1590(4)	-0.158(1)[b] -0.163(1)[c]

Table 3.4.2 (continued)

Compound	Nucleus	n	ν(F) (Hz)	$^4\Delta^{19}F(^{37/35}Cl)$ (ppb)
27	F-2,6	12	7057.269(9)	-0.53(3)
28	F-2,6	NA	7795.546(7)	≤ 0.45

a. Each transition was split into three peaks (see discussion above). Only 16 shifts from the central to the smaller peaks were resolved.

b. The shift from the high frequency peaks, attributed to isotopomers containing two ^{35}Cl isotopes, to the central peaks, attributed to isotopomers containing a ^{35}Cl and a ^{37}Cl isotope.

c. The shift from the central peaks to the low frequency peaks, attributed to isotopomers containing two ^{37}Cl isotopes.

d Spectrum acquired at 210 K.

e. The shift from the highest frequency peaks, attributed to the isotopomer containing three ^{35}Cl atoms, to the next peak, attributed to isotopomers containing two ^{35}Cl atoms and one ^{37}Cl atom.

f. The shift from the second highest frequency peaks in the multiplet to the third peak, attributed to isotopomers containing one ^{35}Cl and two ^{37}Cl atoms.

g. Appeared as broad peaks, perhaps because of the overlap of $^4\Delta^{19}F(^{37/35}Cl)$ from the three chemically equivalent sidegroup chlorine atoms with $^4\Delta^{19}F(^{37/35}Cl)$ from the Cl-2 site.

h. Two isotope shifts were observed, one from Cl-2 and one from Cl-α. These two cannot be positively distinguished (see discussion above).

i. Prepared as a 5 mol% solution in CS_2, containing also 0.25 mol% C_6F_6, 0.25 mol% TMS and 10 mol% C_6D_{12}.

j. Measured as a very dilute impurity in **4**.

Table 3.4.3 Five-bond chlorine isotope shifts on the ^{19}F NMR spectra of some substituted fluorobenzenes

Compound	Nucleus	n	ν(F) (Hz)	$^{5}\Delta^{19}F(^{37/35}Cl)$ (ppb)
11	F-4	9	13343.1963(9)	-0.324
13	F-4	NA	14719.985(3)	-0.54(3)
15	F-4	16	6444.2805(3)	-0.457(4)
16	F-4	11	15386.645(2)	-0.395(7)
18	F-4	NA	1855.744(2)	-0.680(2)
21	F-5	8	14325.456(3)	-0.23(1)
22	F-5	7	14878.9131(3)	-0.39(3)
23	F-4,6	NA	14470.422(3)	≈ -0.4[a]
24	F-5	8	14513.141(3)	-0.28(5)
27	F-3,5	15	742.352(8)	-0.33(3)
28	F-35	NA	1288.417(6)	≤ 0.25
30	F-2	NA	16886.1	≤ 1

a. The observed isotope shift in this region was -1.04 ppb, which is the average value of $^{3}\Delta^{19}F(^{37/35}Cl)$ and $^{5}\Delta^{19}F(^{37/35}Cl)$ (see the discussion in Section 3.1.8). This approximate value is assigned on the assumption that the $^{3}\Delta^{19}F(^{37/35}Cl)$ component of the isotope shift is at most as large as the largest observed $^{3}\Delta^{19}F(^{37/35}Cl)$ reported in Table 3.4.1.

Table 3.4.4 Other chlorine isotope shifts.

Compound	Nucleus	Parameter	Isotope Shift
27	F-4	$^{6}\Delta^{19}F(^{37/35}Cl)$	not observed[a]
28	F-4	$^{6}\Delta^{19}F(^{37/35}Cl)$	-0.81(3)
29	F-α	$^{2}\Delta^{19}F(^{37/35}Cl)$	-5.0(1)[b] -5.1(1)[c]
30	F-4	$^{7}\Delta^{19}F(^{37/35}Cl)$	≤ 0.04
45	F-equatorial	$^{2}\Delta^{19}F(^{37/35}Cl)$	-7.4(2)
46	F-equatorial	$^{2}\Delta^{19}F(^{37/35}Cl)$	-7.2(1)
47	F-equatorial	$^{2}\Delta^{19}F(^{37/35}Cl)$	-6.9(3)

a. Line widths of 3 Hz at the F-4 position precluded the measurement of isotope shifts to this nucleus.

b. Isotope shift as measured from the isotopomer containing ^{12}C-α and ^{12}C-β (see Table 3.1.12 for a diagram of **29**).

c. Isotope shift as measured from the three resolved peaks of the isotopomer containing either ^{13}C-α or ^{13}C-β.

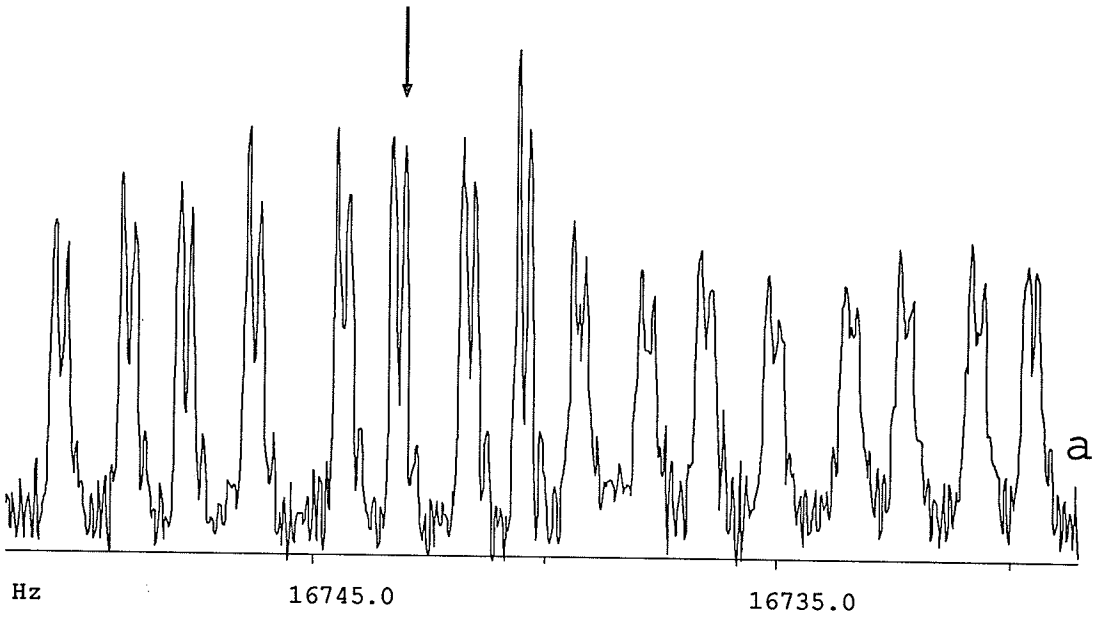
a
Hz
16745.0
16735.0

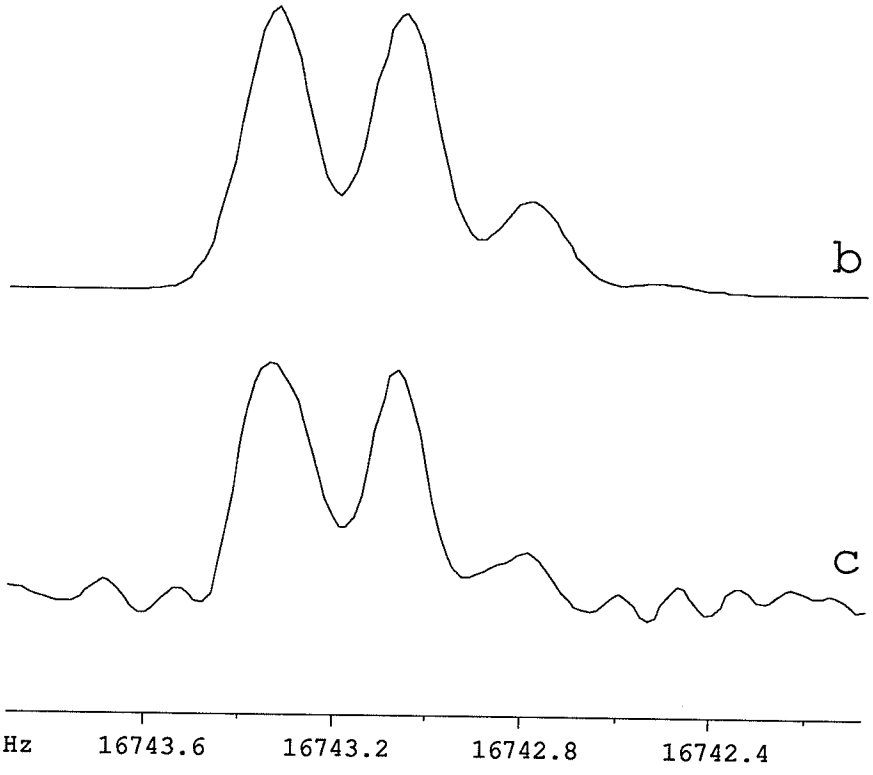
b
c
Hz
16743.6
16743.2
16742.8
16742.4

Figure 3.4.1

The experimental ^{19}F NMR spectrum of the more abundant conformational isomer of 2-chloro-6-fluorobenzal chloride, **4**, acquired at 282.363 MHz, at a probe temperature of 210 K (a). Trace (b) is a simulation of the multiplet indicated with an arrow in (a), assuming isotope shifts of -0.92 ppb from each of the three chlorine atoms. The experimental spectrum of this multiplet is shown in trace (c). The scale is in Hz to high frequency of internal C_6F_6.

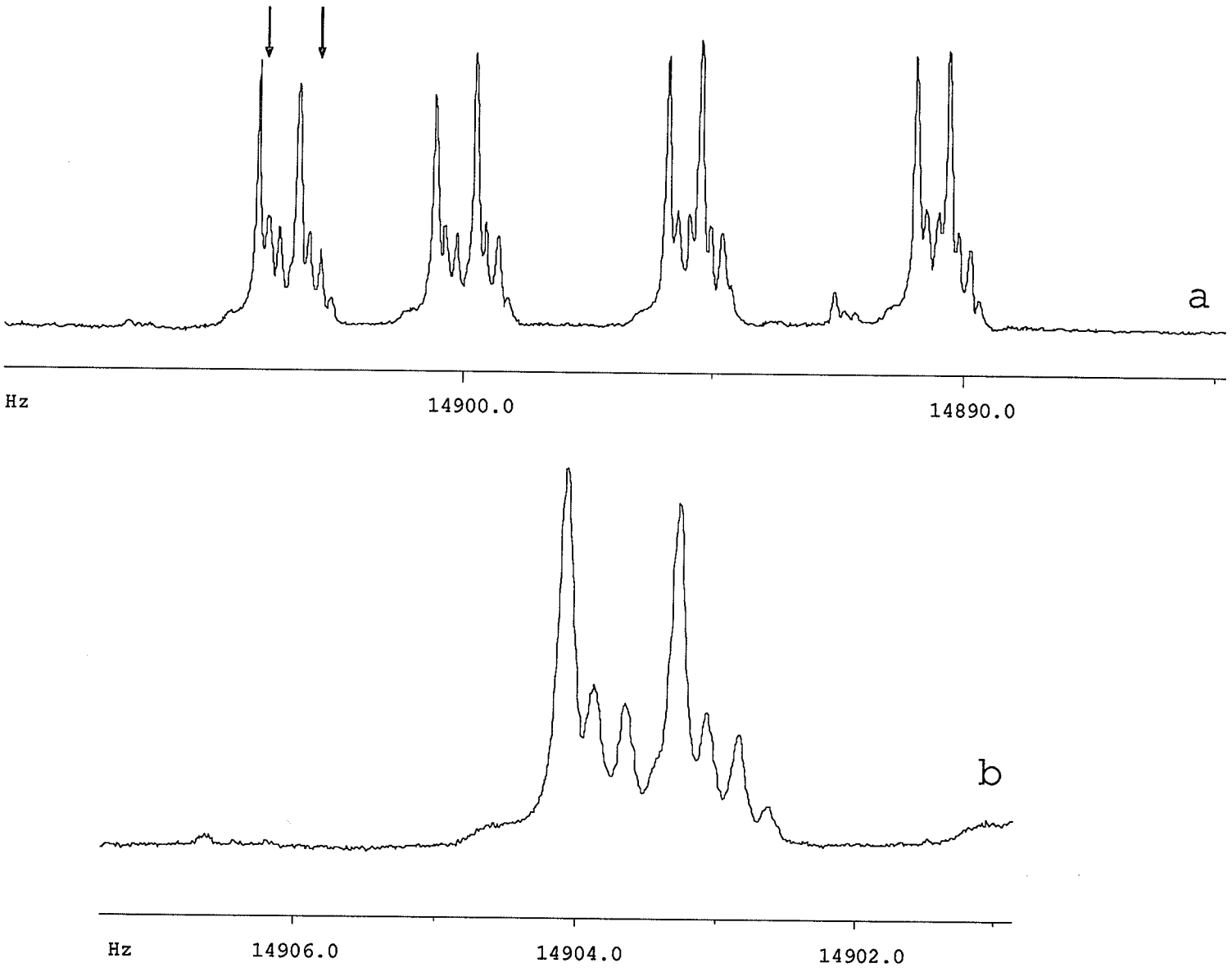
a
Hz
14900.0
14890.0
b
Hz
14906.0
14904.0
14902.0

Figure 3.4.2

The ^{19}F NMR spectrum of 1,2-dichloro-3-fluorobenzene, **9**, which appeared as an impurity in 2-chloro-6-fluorobenzal chloride, **4**, acquired at a probe temperature of 300 K at 282.363 MHz (a). Trace (b) shows an expansion of the multiplets indicated with arrows in (a). The 9:3:3:1 peak intensity ratio of the multiplets is attributed to a larger $^{3}\Delta^{19}F(^{37/35}Cl)$, whose peaks are subdivided again by $^{4}\Delta^{19}F(^{37/35}Cl)$. The scale is in Hz to high frequency of internal C_6F_6.

3.5 Bromine isotope shifts on the ^{19}F NMR spectra of some aromatic compounds.

Spectra of the bromofluorobenzene compounds were analyzed as for the chlorofluorobenzene derivatives described above. The results of these analyses are reported in Tables 3.5.1 - 3.5.3. Unlike chlorine isotope shifts, the almost equal natural abundance of the bromine isotopes resulted in peaks of almost equal intensity, making assignment of a sign less certain. In spectra where most of the low frequency peaks were of lower intensity, a sign has been included, the parentheses indicating that this sign is not absolutely certain, since other factors may account for such small differences in peak intensity. For less well resolved spectra, no consistent difference in intensity was observed. These isotope shifts are indicated with a ± sign. As well, some splitting patterns were ambiguous. These are reported in parentheses since the observed pattern cannot be definitely attributed to $^{n}\Delta^{19}F(^{81/79}Br)$.

Table 3.5.1 Three-bond bromine isotope shifts on the ^{19}F NMR spectra of some substituted fluorobenzenes

Compound	Nucleus	n[a]	ν(F) (Hz)	$^3\Delta^{19}F(^{81/79}Br)$
33	F-2	NA	7525.350(3)	(-)0.283(1)
34	F-3	NA	19158.0127(9)	(-)0.277(1)[b] (-)0.287(1)[c]
37	F-2,6	NA	17063.720(1)	(-)0.256(3)
38	F-4	16	18204.914(6)	±0.20(2)[d]
39	F-2	NA	16910.557(3)	(-)0.26(2)[e] (-)0.30(2)[f]
	F-4,6	NA	10436.071(3)	≤ 0.28[g]
40	F-4	16	12887.07(1)	±0.22(2)
41	F-2,6	17	8404.272(1)	(-)0.20(3)
42	F-2	16	16979.363(2)	(-)0.223(7)
44	F-2	NA	10532.680(2)	(-)0.227(2)
	F-6	NA	15201.873(2)	(-)0.223(2)

a. See footnote (a) of Table 3.4.1.

b. The shift from the high frequency peaks to the third peak of the multiplet. This shift is attributed to isotopomers with a ^{79}Br isotope at the C-1 position undergoing isotopic substitution at the C-2 position.

c. The shift from the second peak of the multiplet to the fourth. Here, the C-1 position contains an ^{81}Br isotope while the bromine at the C-2 position is substituted.

d. Transitions in this region were split into triplets which, within experimental error, had the same splitting. These triplets may result from $^3\Delta^{19}F(^{81/79}Br)$, reported above, having the same magnitude as $^6J_{HF}$.

e. The shift from the high frequency peak, attributed to the isotopomer containing two ^{79}Br atoms, to the central peak, attributed to the isotopomer containing both isotopes of bromine.

f. The shift from the central peak to the low frequency peak, attributed to isotopomers containing two ^{81}Br atoms.

g. An isotope shift at this nucleus would have been the average of $^{3}\Delta^{19}F(^{81/79}Br)$ and $^{5}\Delta^{19}F(^{81/79}Br)$. The number reported is the maximum value of $^{3}\Delta^{19}F(^{81/79}Br)$ that would be observed if the $^{5}\Delta^{19}F(^{81/79}Br)$ component of the isotope shift were negligible. Such an isotope shift would have required an observed chemical shift of 0.14 ppb.

Table 3.5.2 Four-bond bromine isotope shifts on the ^{19}F NMR spectra of some substituted fluorobenzenes.

Compound	Nucleus	n	ν(F) (Hz)	$^4\Delta^{19}F(^{81/79}Br)$
31	F-4	NA		not observed[a]
32	F-3,5	NA	15557.5(1)	≤ 0.07
33	F-3	NA	9032.096(3)	≤ 0.1
	F-5	NA	13849.959(3)	≤ 0.1
34	F-3	NA	19158.0127(9)	(-)0.101(1)[b] (-)0.110(1)[c]
	F-5	NA	15119.0356(9)	≤ 0.1
35	F-3	NA	23508.380(2)	(±0.15(1))[d]
	F-5	NA	15179.246(1)	≤ 0.07
36	F-4	NA	13737.3094(9)	≤ 0.15
	F-6	NA	11457.5244(9)	≤ 0.2
39	F-5	NA	878.718(3)	≤ 0.15
41	F-3,5	NA	571.633(5)	≤ 0.1
43	F-6	4	10024.94(2)	(±0.26(5))[e]
44	F-4	NA	104.304(2)	≤ 0.2

a. Several samples of **31** were prepared, both in acetone-d_6 and CCl_4 (see section 3.4 for a discussion of the sample preparation). Line widths of approximately 1 Hz in all these samples precluded a measurement of $^4\Delta^{19}F(^{81/79}Br)$.

b. The shift from the first to the second peak in the multiplets appearing in the F-3 region. This shift is attributed to isotopomers containing a ^{79}Br at the C-2 position undergoing isotopic substitution at the C-1 position.

c. The shift from the third to the fourth peak in the multiplets. Here, the C-2 position contains an ^{81}Br isotope while the bromine at C-1 is substituted.

d. Unexplained multiplets appear in this region. A regular splitting (see Figure 3.1.7) is probably due to $^{4}\Delta^{19}F(^{81/79}Br)$.

e. The four multiplets in the ^{19}F region were split into apparent triplets. This may be due to $^{4}\Delta^{19}F(^{81/79}Br)$ from the two bromine atoms, although other factors, such as coupling to the amino protons or simply an artifact of the acquisition process may be responsible for the observed shift. A proton decoupled spectrum was attempted, but the resolution was poor.

Table 3.5.3 Five-bond bromine isotope shifts on the ^{19}F NMR spectra of some substituted fluorobenzenes.

Compound	Nucleus	n	ν(F) (Hz)	$^{5}\Delta^{19}F(^{81/79}Br)$ (ppb)
34	F-5	NA	15119.0356(9)	≤ 0.1
37	F-4	NA	15054.054(1)	≤ 0.1
39	F-4,6	NA	10436.071(3)	not observed[a]
41	F-4	NA	2211.645(5)	≤ 0.1
42	F-4	NA	14850.591(1)	≤ 0.07
44	F-4	NA	8525.146(2)	≤ 0.16

a. From the peak widths, an isotope shift of 0.14 ppb or greater would have been observed at this site. This shift, had it been observed, would have been the average of $^{3}\Delta^{19}F(^{81/79}Br)$ and $^{5}\Delta^{19}F(^{81/79}Br)$.

3.6 Deuterium isotope shifts on some fluoroanilines.

Isotope shifts on the ^{19}F NMR spectra of compounds **31** and **48-52**, attributed to deuterium substitution at the amino group, were observed. Exchange was promoted by the addition of D_2O to **31**, and a 3.8 M solution of NaOH dissolved in D_2O to **48-52.** Proton decoupled ^{19}F NMR spectra of **48-52**, as well as a fully coupled spectrum of **31**, were acquired at 282.363 MHz. The results of these analyses are reported in Table 3.6.1.

The sample of **31** prepared in acetone-d_6 apparently was exchanging with the solvent. A large doublet, attributed to $^3J_{CF}$, was observed, as well as a low intensity doublet to high frequency. The high frequency doublet was attributed to the isotopomer containing one deuterium and one proton at the amino position. Following the addition of D_2O, an additional doublet, attributed to isotopomers containing two deuterium atoms at the amino position, appeared to higher frequency. The intensity of these peaks increased, relative to the NH_2 peak, as D_2O was added, verifying the positive sign for this isotope shift (Figure 3.6.1). A similar pattern was observed for the sample prepared in CCl_4, although exchange did not occur with the solvent in this case. The remaining samples were treated in a similar manner, albeit with a $NaOH/D_2O$ solution instead of D_2O; similar effects were observed in the ^{19}F spectra of these compounds, although some of the isotope shifts were to low frequency.

Table 3.6.1 Deuterium isotope shifts (in ppb) on the ^{19}F NMR spectra of some fluoroaniline compounds.

	n[a]	Vol. (μL)[b]	acetone-d_6			CCl_4		
			NDH[c]	ND_2[d]	ν(F)[e]	NDH[c]	ND_2[d]	ν(F)[e]
31[f]	6	0.0	+16.6(2)	+24.3(2)[g]	11167.51(7)			11349.47(4)
		7.5				+16.2(1)	---	
		15.0				+16.1(1)	+23.2(1)	
		20	+17.29(7)	+24.93(7)				
		40	+17.86(7)	+25.55(7)				
		60	+18.22(7)	+26.31(7)				
48	4	0.0	---	---	7630.48(2)			7368.2(1)
		7.5	-5.4(1)	---		-15.8(2)	-7.8(2)	
		15.0	-3.2(1)	-1.8(1)		-16.0(4)	-7.8(4)	
		22.5	---	---		-16.1(3)	-8.1(3)	
		30.0	-1.9(2)	-2.4(2)		---	---	

Table 3.6.1 (cont.)

	n[a]	Vol. (μL)[b]	acetone-d_6			CCl_4		
			NDH[c]	ND_2[d]	ν(F)[e]	NDH[c]	ND_2[d]	ν(F)[e]
49[f]	5	0.0	---	---	13844.84(2)			13873.92(3)
		7.5	+3.8(5)	+4.2(5)		+7.4(2)	+7.7(2)	
		15.0	+3.9(6)	+4.2(6)		+7.4(4)	+7.7(4)	
		22.5	+3.8(4)	+4.3(4)		+7.3(6)	+7.6(6)	
		30.0	---	+4.0(3)				
50	6	0.0	---	---	9572.91(2)			9943.39(8)
		7.5	+12.3(4)	+20.7(4)		+19.3(4)	+26.0(4)	
		15.0	+14.3(3)	+21.8(3)		+19.1(5)	+25.7(5)	
		22.5	+15.0(8)	+22.6(8)		+18.8(6)	+25.5(6)	
		30.0	+15.8(2)	+23.4(2)		+18.0(2)	+25.4(2)	
51	4	0.0	---	---	8592.3(2)			8126.95(1)
		3.0	+3.93(5)	+10.34(5)	8596.81(1)	≤ 5[h]		
		6.0	+3.9(4)	+10.6(4)	8593.84(1)			
		9.0	+3.9(4)	+10.6(4)	8593.84(1)			
		12.0	+4.2(1)	+11.0(1)	8600.62(3)			
		15.0	+4.14(8)	+10.62(8)	8597.75(2)			
		21.0	+4.2(7)	+11.0(7)	8601.2(2)			
52	6	0.0	---	---	8468.61(8)			
		7.5	+12.6(1)	+20.9(1)				
		15.0	+13.3(2)	+21.7(2)				

a. The number of intervening bonds between the observed and substituted nuclei.

b. For **31**, the indicated volume of D_2O was added directly to the sample prepared in either acetone-d_6 or CCl_4. The remaining samples had the indicated volume of a 3.8 M solution of NaOH, dissolved in D_2O, added to the solution.

c. The shift from the peaks attributed to the isotopomer containing two protons to the central peaks, attributed to the isotopomer containing both a deuterium and a proton.

d. The shift from the central peaks to the peaks attributed to isotopomers containing two deuterium atoms.

e. Spectral references were only acquired for the samples for which a chemical shift is reported.

f. The compounds investigated were 2,6-dibromo-3-chloro-4-fluoroaniline, **31**, 2-fluoroaniline, **48**, 3-fluoroaniline, **49**, 4-fluoroaniline, **50**, 2,6-difluoroaniline, **51** and 3-chloro-4-fluoroaniline, **52**.

g. This datum was obtained from a degassed sample, acquired several months after preparation to permit exchange of the amino protons with the acetone-d_6; the remaining data for this sample originates from an open sample, prepared as described in Section 2.1.

h. A poorly resolved multiplet was observed in this region. Isotope shifts totaling 5 ppb or more would have been sufficiently resolved to obtain data.

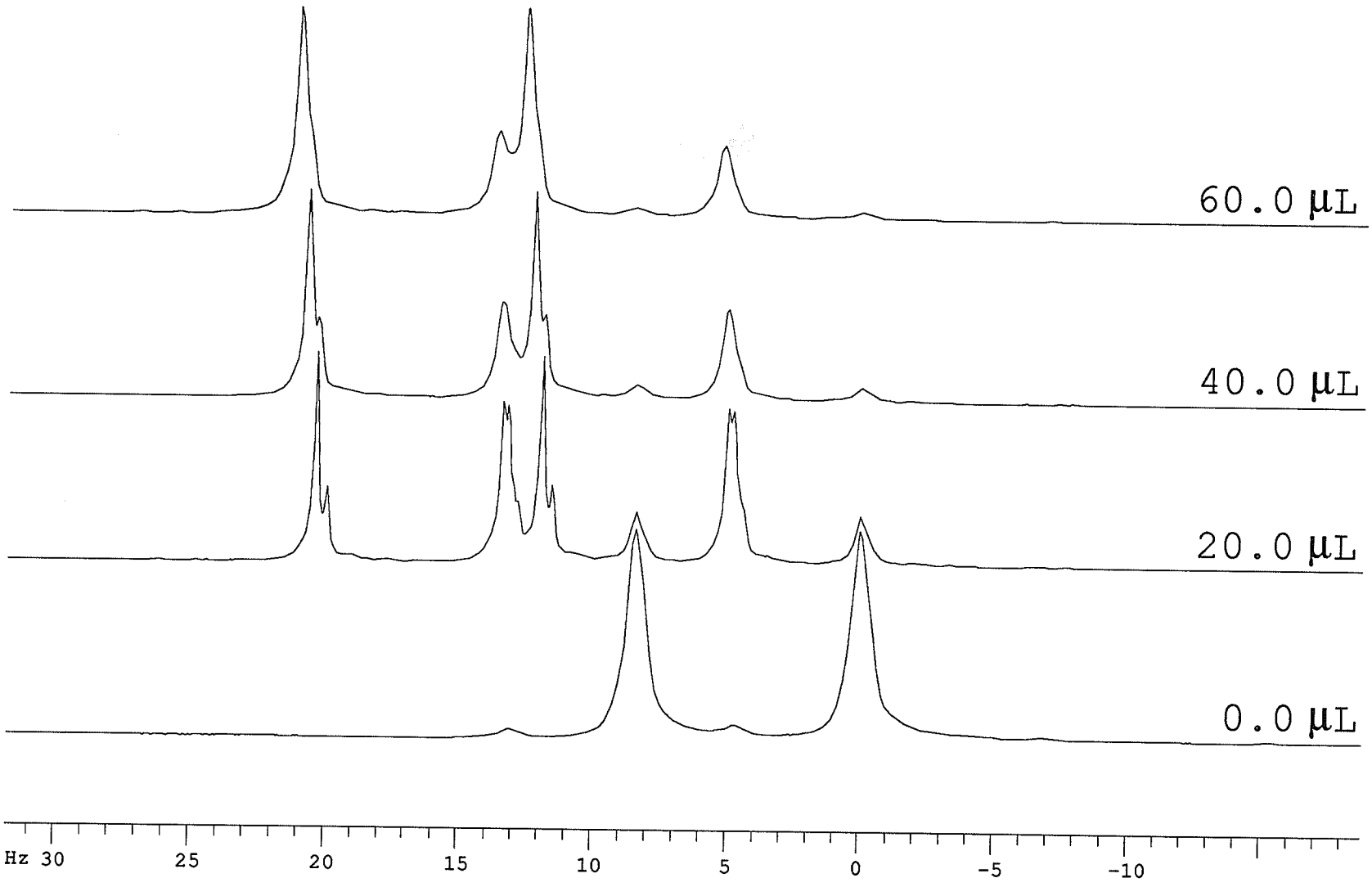
60.0 µL
40.0 µL
20.0 µL
0.0 µL
Hz 30
25
20
15
10
5
0
-5
-10

Figure 3.6.1

The ^{19}F NMR spectrum of 2,6-dibromo-3-chloro-4-fluoroaniline in acetone-d_6, **31**, acquired at 282.363 MHz, illustrating the positive sign of $^{6}\Delta^{19}F(^{2/1}H)$. Deuterium exchange with the solvent, discernible in the lower trace, was promoted by addition of the indicated volume of D_2O directly to the sample tube immediately preceding the acquisition of the spectrum. The scale (in Hz) has been set with the high frequency peak set to zero to simplify comparison of the spectra.

3.7 Other Isotope Shifts.

In the course of this work, other isotope shifts, reported in Table 3.7.1, were observed. The chlorine isotope shifts on the ^{13}C NMR spectra resulted in 3:1 peak intensity ratios as was observed for the ^{19}F spectra (see Figure 3.1.1). $^{1,2}\Delta^{19}F(^{13/12}C)$ were determined by measuring the shift from the large central peak, attributed to the isotopomer containing a ^{12}C atom, to the centre of the doublet resulting from $^{1,2}J_{CF}$.

Besides the expected 3:1 peak intensity ratio resulting from the isotopes of chlorine in compounds **45-47**, a low intensity peak was observed to low frequency (Figure 3.7.1). This was attributed to $^{1}\Delta^{19}F(^{34/32}S)$, which should have a peak intensity ratio of approximately 20:1, corresponding to the natural abundances of ^{32}S and ^{34}S (95.0% and 4.2% respectively). There was no indication of an isotope shift from the ^{33}S isotopomer, probably because of its low natural abundance (0.8%).

Table 3.7.1 Other isotope shifts.

Compound	Nucleus	Parameter	Isotope Shift (ppb)
3	C-2	$^{1}\Delta^{13}C(^{37/35}Cl)$	-3.7(3)
6	C-2	$^{1}\Delta^{13}C(^{37/35}Cl)$	-2.3(3)
29	F-α	$^{1}\Delta^{19}F(^{13/12}C)$	-143(1)
	F-α	$^{2}\Delta^{19}F(^{13/12}C)$	-13.6(4)
45	F-equatorial	$^{1}\Delta^{19}F(^{34/32}S)$	-59.1(7)
46	F-equatorial	$^{1}\Delta^{19}F(^{34/32}S)$	-59.1(7)
47	F-equatorial	$^{1}\Delta^{19}F(^{34/32}S)$	not resolved

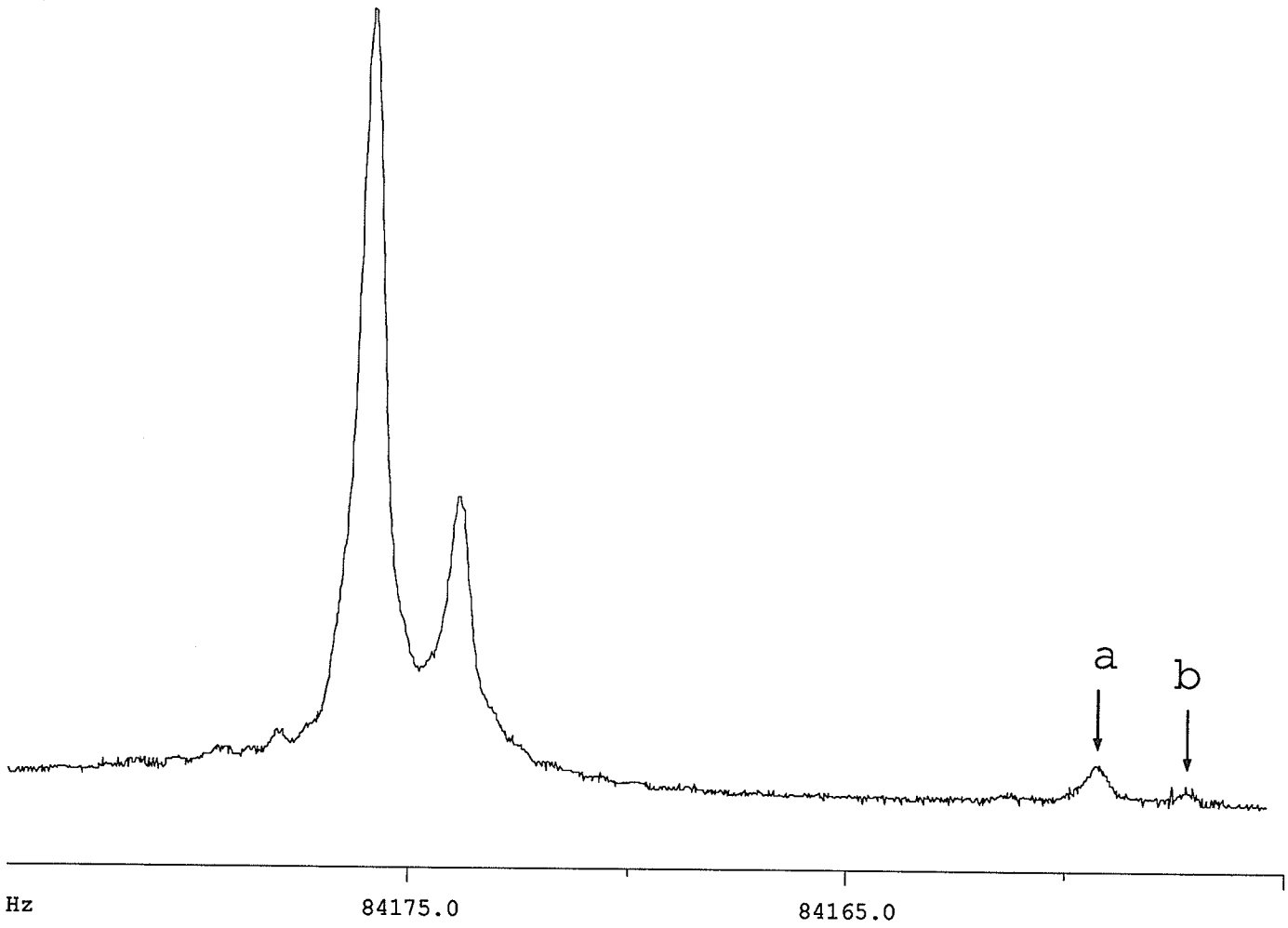
a
b
Hz
84175.0
84165.0

Figure 3.7.1

The proton decoupled ^{19}F NMR spectrum of *p*-nitrophenylsulfur(VI) tetrafluoride monochloride, **46**, acquired at 282.363 MHz. The large peaks to high frequency are attributed to the isotopomer containing a ^{32}S atom, the 3:1 peak intensity ratio resulting from the isotopes of chlorine. The peak labeled (a) is attributed to the isotopomer containing a ^{34}S and a ^{35}Cl atom, while the peak labeled (b) results from the isotopomer containing a ^{34}S and a ^{37}Cl atom. Within experimental error, there is no indication of a sulfur isotope effect on $^{2}\Delta^{19}F(^{37/35}Cl)$. The scale is in Hz to high frequency of internal C_6F_6.

4. Discussion

4. Discussion.

4.1 Chlorine and bromine isotope shifts.

4.1.1 Trends.

The general trends in isotope shifts, discussed below, hold for the observed chlorine and bromine isotope shifts. However, most trends dealing with empirical relationships (*a-e* in Section 1.2) did not hold. These are discussed in later sections.

i. Isotope shifts are usually negative.

All observed chlorine isotope shifts (Tables 3.4.1-3.4.4) are negative. The sign of the bromine isotope shift is less certain because of the almost equal natural abundance of the two bromine isotopes. Nevertheless, on the well-resolved spectra, most low frequency peaks of the resulting doublets are of slightly lower intensity, as expected for a negative isotope shift. In no instance is the opposite observed, although in some cases no consistent difference in peak intensity can be discerned.

ii. The magnitude of the isotope shift decreases as the number of intervening bonds is increased.

There is an approximately three-fold decrease in $^{n}\Delta^{19}F(^{37/35}Cl)$ for each additional intervening bond for n = 2,3,4. However, the average magnitude of $^{4}\Delta^{19}F(^{37/35}Cl)$ (-0.57 ppb) is not significantly larger then that of $^{5}\Delta^{19}F(^{37/35}Cl)$ (-0.40 ppb). $^{4}\Delta^{19}F(^{37/35}Cl)$ is smaller then $^{5}\Delta^{19}F(^{37/35}Cl)$ for pentafluorochlorobenzene, **18**, (-0.432 ppb compared to -0.68 ppb). The smallest $^{4}\Delta^{19}F(^{37/35}Cl)$ is -0.16 ppb for 2,6-dichloro-4-fluorophenol, **20**, less than the -0.23 ppb observed for 2-chloro-5-fluoroanisole, **21**, the smallest measured

$^{5}\Delta^{19}F(^{37/35}Cl)$. The small difference in $^{4}\Delta^{19}F(^{37/35}Cl)$ compared to $^{5}\Delta^{19}F(^{37/35}Cl)$ may be a consequence of the three-fold decrease in isotope shifts with each additional bond, observed for smaller values of n. Since ring systems are considered here, there are two paths between the substituted and observed nuclei. Thus, $^{3}\Delta^{19}F(^{37/35}Cl)$ may be referred to as $^{3}\Delta^{19}F(^{37/35}Cl) + {}^{7}\Delta^{19}F(^{37/35}Cl)$, $^{4}\Delta^{19}F(^{37/35}Cl)$ as $^{4}\Delta^{19}F(^{37/35}Cl) + {}^{6}\Delta^{19}F(^{37/35}Cl)$, and $^{5}\Delta^{19}F(^{37/35}Cl)$ as $2[^{5}\Delta^{19}F(^{37/35}Cl)]$. If $^{7}\Delta^{19}F(^{37/35}Cl)$ is negligible, then, if the threefold decrease in isotope shifts with increasing n holds for larger values of n, $^{6}\Delta^{19}F(^{37/35}Cl) \approx (1/27)[^{3}\Delta^{19}F(^{37/35}Cl)]$ (The six-bond isotope shift of pentafluorophenylsulfonyl chloride, **28**, discussed in section 4.1.2, is much larger, perhaps because of its molecular conformation). With $2[^{5}\Delta^{19}F(^{37/35}Cl)] \approx (2/9)[^{3}\Delta^{19}F(^{37/35}Cl)]$, a ratio of 0.60 for $2[^{5}\Delta^{19}F(^{37/35}Cl)]/[^{4}\Delta^{19}F(^{37/35}Cl)+{}^{6}\Delta^{19}F(^{37/35}Cl)]$ is expected. This compares to a ratio of 0.61 observed for 1-chloro-3-fluorobenzene, **1**, and 1-chloro-4-flurobenzene, **11**, which have no substituents. This ratio, for all observed $^{4,5}\Delta^{19}F(^{37/35}Cl)$, is 0.77. This approach was used by Künzer *et al.* to rationalize unexpectedly large $^{n}\Delta^{13}C(^{2/1}H)$ norbornenyl systems[49] (see **q**, Scheme 1).

Although little data is available, $^{3}\Delta^{19}F(^{81/79}Br)$ also is approximately three times larger than $^{4}\Delta^{19}F(^{81/79}Br)$. $^{5}\Delta^{19}F(^{81/79}Br)$ was not observed, despite line widths at half-height of less than 0.04 Hz in some cases. Since $^{4}\Delta^{19}F(^{81/79}Br)$ is below the detection limit for most molecules investigated, $^{5}\Delta^{19}F(^{81/79}Br)$ would not have been detected unless these values were on average larger than $^{4}\Delta^{19}F(^{81/79}Br)$; this is not the case.

iii. The magnitude of an isotope shift is related to the shift range of the observed nucleus.

This is apparent when considering the chlorine and bromine isotope shifts, which are observed in the ^{19}F and ^{13}C NMR spectra. Yet, despite line widths of as little as 0.03 Hz, which would have allowed the measurement of an $^{n}\Delta^{1}H(^{37/35}Cl)$ of approximately 0.04 ppb, isotope shifts were not observed in the ^{1}H spectra. As an example, while $^{2}\Delta^{19}F(^{37/35}Cl)$ is -5.0 ppb for 2-chloro-2,2-difluoroacetophenone, **29**, there is no indication of $^{2}\Delta^{1}H(^{37/35}Cl)$ at the sidegroup proton of 2-chloro-6-fluorobenzal chloride, **4**, despite line widths which would allow the measurement of an isotope shift of as small as 0.3 ppb.

iv. The magnitude of the isotope shift is related to the fractional change in mass upon isotopic substitution.

Comparison of $^{3,4}\Delta^{19}F(^{37/35}Cl)$ with $^{3,4}\Delta^{19}F(^{81/79}Br)$ reveals that the larger fractional change in mass following isotopic substitution of the chlorine atoms does indeed result in larger isotope shifts. This is particularly evident when comparing $^{3}\Delta^{19}F(^{37/35}Cl)$ to $^{3}\Delta^{19}F(^{81/79}Br)$ for the bromo analogs of some chlorofluorobenzene derivatives, such as 1-chloro-2,4-difluorobenzene, **13**, compared to 1-bromo-2,4-difluorobenzene, **42,** 1-chloro-2,4,6-trifluorobenzene, **16**, compared to 1-bromo-2,4,6-trifluorobenzene, **37** and chloropentafluorobenzene, **18,** compared to bromopentafluorobenzene, **41** (Tables 3.4.1 and 3.5.1), where an approximately sevenfold decrease for $^{3}\Delta^{19}F(^{81/79}Br)$ compared to $^{3}\Delta^{19}F(^{37/35}Cl)$ is seen.

v. Isotope shifts are usually additive.

The chlorine isotope shifts investigated appear to be additive. Both samples of 1,3-dichlorofluorobenzene, **19**, have, within experimental error, equal isotope shifts following the first and second isotopic substitutions. The isotope shifts for 2,6-dichloro-4-fluorophenol, **20**, deviate by slightly more than the uncertainty. This is probably a consequence of the small isotope shift at this site — the peaks are not completely resolved.

The additivity of isotope shifts is less certain for bromine substitution. The isotope shift at F-2 of 1,3-dibromo-2,4,5,6-tetrafluorobenzene, **39**, a consequence of isotopic substitution of chemically equivalent bromine atoms, results in asymmetric multiplets (Figure 3.1.8), suggesting a slight deviation from additivity. Jameson and Osten have argued that non-additivity may be a consequence of either secondary isotope effects on the bond lengths of non-substituted atoms or vibrational effects from non-symmetric isotopomers of otherwise symmetric molecules.[30(b)] $^{3,4}\Delta^{19}F(^{81/79}Br)$, observed for 1,2-dibromo-3,5-difluorobenzene, **34**, also deviate slightly from additivity. Here, the bromine atoms are not in chemically equivalent positions relative to the observed nucleus (F-3). Nevertheless, if there is no isotope effect on the isotope shifts, $^{3}\Delta^{19}F(^{81/79}Br)$ should be equal regardless of which isotope of bromine is at the C-1 position. Likewise, both measurements of $^{4}\Delta^{19}F(^{81/79}Br)$ should be equal. Yet, both isotope shifts are 0.01 ppb greater when an ^{81}Br is at the C-1 or C-2 position, respectively. Since a shift in the position of any one of the four peaks in the multiplets of the F-3 region would affect both $^{3,4}\Delta^{19}F(^{81/79}Br)$, it is not possible to ascribe this non-additivity to a particular isotope shift; it may arise

from both isotope shifts being slightly non-additive. As for **39**, this may be due to a secondary isotope effect on the C—Br bond length at the unsubstituted nucleus.

4.1.2 General observations.

Although not investigated extensively, chlorine isotope shifts appear to be independent of the solvent (all bromine isotope shifts measured were prepared in acetone-d_6). The isotope shifts of **19**, prepared in acetone-d_6 and CS_2, and those of 2,6-dibromo-3-chloro-4-fluoroaniline, **31**, prepared in acetone-d_6 as well as CCl_4, are, within experimental error, equal. The chlorine isotope shifts of **31** remain constant as the concentration of D_2O is increased. Yet, both the largest and smallest $^4\Delta^{19}F(^{37/35}Cl)$ (-1.16 ppb for 2-chloro-6-fluorobenzaldehyde, **8**, and -0.16 ppb for 2,6-dichloro-4-fluorophenol, **20**), are observed for the only two samples prepared in CS_2 for which this value is measured. NMR data for **8** suggests that there is not a large solvent effect on conformer populations for this sample, the aldehydic group being coplanar with the phenyl ring, with the oxygen preferentially located *cis* to the chlorine.[61] Thus, the large value of this isotope shift is not a consequence of solvent-induced conformational changes. However, solvation of the hydroxyl proton of **20** may be a factor in this isotope shift. If so, the small value suggests a conformational dependence of isotope shifts rather than a solvent dependence.

This solvent-independence suggests that these isotope shifts are transmitted through the molecular framework. If there were a significant through-space component involved in the transmission of these isotope shifts, a solvent dependence would be expected, since the

large differences in the dielectric constants of the various solvents might well moderate the transmission of electronic information.

Tables 3.1.1-3.1.18 show that there are no significant isotope effects on coupling constants, the largest difference being the 0.037 Hz deviation in $^{4}J_{35}$ following isotopic substitution of the chlorine atom of **28**, slightly greater than the uncertainty. A few other coupling constants deviate by more than the uncertainty, but these are all less than 0.01 Hz. Hence, these deviations are attributed to experimental error. This agrees with other observations; isotope effects on coupling constants have only been observed following substitution of a proton with deuterium or tritium.[62]

The fluorobenzenes with a chlorine atom at the *ortho, meta* and *para* positions, **11, 1** and **13** respectively, permit a comparison of isotope shifts unperturbed by substituents. The magnitude of the isotope shift decreases as the number of intervening bonds increases, from -1.43 ppb through -0.53 ppb to -0.324 ppb for **13**. As discussed above, the small difference between $^{4}\Delta^{19}F(^{37/35}Cl)$ and $^{5}\Delta^{19}F(^{37/35}Cl)$ is a consequence of the ring system, the isotope shifts in fact decreasing in a fairly linear fashion relative to the number of intervening bonds. This differs from the effects of deuterium substitution observed by Yannoni for the deutero analogs of the above fluorobenzenes.[63] The isotope shifts on the ^{19}F spectra, over 3, 4 and 5 bonds, were -285, -8 and -11 ppb, respectively. The much larger $^{3}\Delta^{19}F(^{2/1}H)$ is attributed to a steric interaction between the deuterium and the fluorine atom. Nevertheless, the monotonic decrease with increasing number of bonds, observed for chlorine and bromine isotope shifts, is not seen here.

A surprising value of -0.81 ppb is observed for $^{6}\Delta^{19}F(^{37/35}Cl)$ of pentafluorophenylsulfonyl chloride, **28**, - larger than all $^{5}\Delta^{19}F(^{37/35}Cl)$ and all but one $^{4}\Delta^{19}F(^{37/35}Cl)$. The conformation of benzenesulfonyl chloride has been determined by Caminati and coworkers using microwave spectroscopy.[64] The equilibrium conformer is the one in which the S—Cl bond is perpendicular to the phenyl plane. With steric repulsion between the chlorine atom and the *ortho* fluorine atoms of **28**, the perpendicular conformer is probably also preferred here. While conclusions cannot be reached from one sample (see section 5.1 for suggested further research), one is reminded of the large coupling at the *para* position from a nucleus at the α position, observed when the bond to the resonant nucleus on the sidegroup is perpendicular to the phenyl plane.[65] For example, a large value of $^{6}J_{HF}$, observed by Schaefer and Parr for benzenesulfonyl fluoride, is attributed to the perpendicular conformation of the S—F bond.[66] Perhaps the σ-π mechanism, a major component of the large coupling constants to the *para* position, also plays a significant role in the transmission of the isotope shift to the *para* fluorine, accounting for the unexpected value of $^{6}\Delta^{19}F(^{37/35}Cl)$.

In this context, it is interesting to note that $^{7}\Delta^{19}F(^{37/35}Cl)$ is not observed for 2-chloro-2',4'-difluoroacetophenone, **30**, despite line widths of 0.03 Hz, which would permit the observation of an isotope shift of as small as 0.04 ppb. Here, the chlorine atom is coplanar with the phenyl ring, the sidegroup protons straddling the *ortho* fluorine atom.

Symmetry appears to be a factor in determining the magnitude of $^{4}\Delta^{19}F(^{37/35}Cl)$. The isotope shift of 1-chloro-3-fluorobenzene, **1**, which has C_s symmetry, is -0.53 ppb, close to

that of 1-chloro-3,4-difluorobenzene, **15**, which has the same symmetry. However 1-chloro-3,5-difluorobenzene, **12**, and 1-chloro-2,3,5,6-tetrafluorobenzene, **17**, both of which have 2-fold symmetry (C_{2v}), have smaller isotope shifts (-0.32 and -0.38 ppb respectively). Likewise, the isotope shift of chloropentafluorobenzene, **18**, also with C_{2v} symmetry, is only -0.432 ppb, although it should be noted that a small value was also observed for 1-chloro-2,5-difluorobenzene, which has C_s symmetry. Osten and coworkers have proposed that smaller isotope shifts may be a consequence of bond angle deformation, the effects of which cancel in highly symmetric molecules. However, this would not be the case for molecules with C_{2v} symmetry. Also, it will be shown in the next section that bond angle deformation is probably not a significant factor in these isotope shifts. The authors also suggest that the effect may be purely electronic, the nuclear shielding term at symmetric sites being less sensitive to dynamic factors.

While symmetry plays a significant role in $^4\Delta^{19}F(^{37/35}Cl)$, it is not a factor in either $^3\Delta^{19}F(^{37/35}Cl)$ or $^5\Delta^{19}F(^{37/35}Cl)$. Tables 3.4.1 and 3.4.3 show that there is no relationship between the magnitude of these isotope shifts and the symmetry of the molecule. Indeed, the largest observed $^{3,5}\Delta^{19}F(^{37/35}Cl)$ are for **18** and 1,3-dichloro-2,4,6-trifluorobenzene, **23**, both molecules with C_{2v} symmetry. Small isotope shifts are also observed for molecules with this symmetry.

4.1.3 Three-bond isotope shifts.

Three-bond isotope shifts are largely invariant to the substitution pattern of the phenyl ring. All measured $^{3}\Delta^{19}F(^{37/35}Cl)$ values fall within a 0.39 ppb range, from -1.25 ppb to -1.64 ppb. This range falls to 0.23 ppb, with an average value of -1.52(7) ppb, if the datum for 3-chloro-2,4-difluoroaniline, **26**, is rejected, although there is no reason to do so. If all three-bond bromine isotope shifts are assumed to have the same sign, then these isotope shifts also fall within a small range, between (-)0.20 ppb and (-)0.30 ppb, with an average value of (-)0.24(3) ppb. Within experimental error, this range is proportional to that observed for $^{3}\Delta^{19}F(^{37/35}Cl)$. Hence, the ensuing discussion of $^{3}\Delta^{19}F(^{37/35}Cl)$ may be applied equally to $^{3}\Delta^{19}F(^{81/79}Br)$.

The invariance of $^{3}\Delta^{19}F(^{37/35}Cl)$ to the substitution pattern on the ring permits some conclusions about chlorine isotope shifts in general. The primary dynamic factor, believed to be the major cause of these isotope shifts, apparently is not significantly affected by the substitution pattern on the ring. This must also be true for $^{4,5}\Delta^{19}F(^{37/35}Cl)$. Similarly, while different groups *ortho* to either the chlorine or fluorine atoms will affect the C—C—F and C—C—Cl bond angles, and thus the Cl-F internuclear separation, $^{3}\Delta^{19}F(^{37/35}Cl)$ is apparently insensitive to these variations in bond angles. Hence, $^{4,5}\Delta^{19}F(^{37/35}Cl)$ are probably also insensitive to variations in bond angles.

The nearly constant values of $^{3}\Delta^{19}F(^{37/35}Cl)$ implies that the electronic path between the chlorine and fluorine atoms is also invariant to the substitution pattern on the ring, probably because the path is dominated by these two electronegative atoms.

Neither $^{3}\Delta^{19}F(^{37/35}Cl)$ nor $^{3}\Delta^{19}F(^{81/79}Br)$ exhibit any dependence on the ^{19}F NMR chemical shift. Examination of the data in Table 3.4.1 shows that $^{3}\Delta^{19}F(^{37/35}Cl)$, which is virtually invariant, is not dependent on the ^{19}F chemical shift, which ranges over almost 9000 Hz. Likewise, all $^{3}\Delta^{19}F(^{81/79}Br)$ are contained within a 0.1 ppb range, while the chemical shifts of the observed nuclei cover an almost 12000 Hz range.

4.1.4 The 1-substituted-2-chloro-6-fluorobenzenes.

$^{4}\Delta^{19}F(^{37/35}Cl)$, observed for the series of 1-substituted-2-chloro-6-fluorobenzenes, covers a wide range, from -0.37 ppb to -1.16 ppb, suggesting a large dependence of this value on the substituent at the *ipso* position. Since $^{1}J_{CF}$ in aromatic systems is affected by the substituents on the phenyl ring,[60] a correlation between $^{1}J_{CF}$ and $^{4}\Delta^{19}F(^{37/35}Cl)$ would provide some insight into the mechanism of this parameter. However, a plot of $^{4}\Delta^{19}F(^{37/35}Cl)$ vs $^{1}J_{CF}$ (Figure 4.1) failed to show a linear correlation.

Since the transmission of coupling information from C-2 to F-6 covers a similar electronic path as does $^{4}\Delta^{19}F(^{37/35}Cl)$ to F-2, a linear correlation would be expected between $^{3}J_{C\text{-}2,F}$ and $^{4}\Delta^{19}F(^{37/35}Cl)$ if the secondary electronic factor, which depends on the transmission path, were the major factor in determining the magnitude of $^{4}\Delta^{19}F(^{37/35}Cl)$. Figure 4.2 shows that such a correlation does not exist.

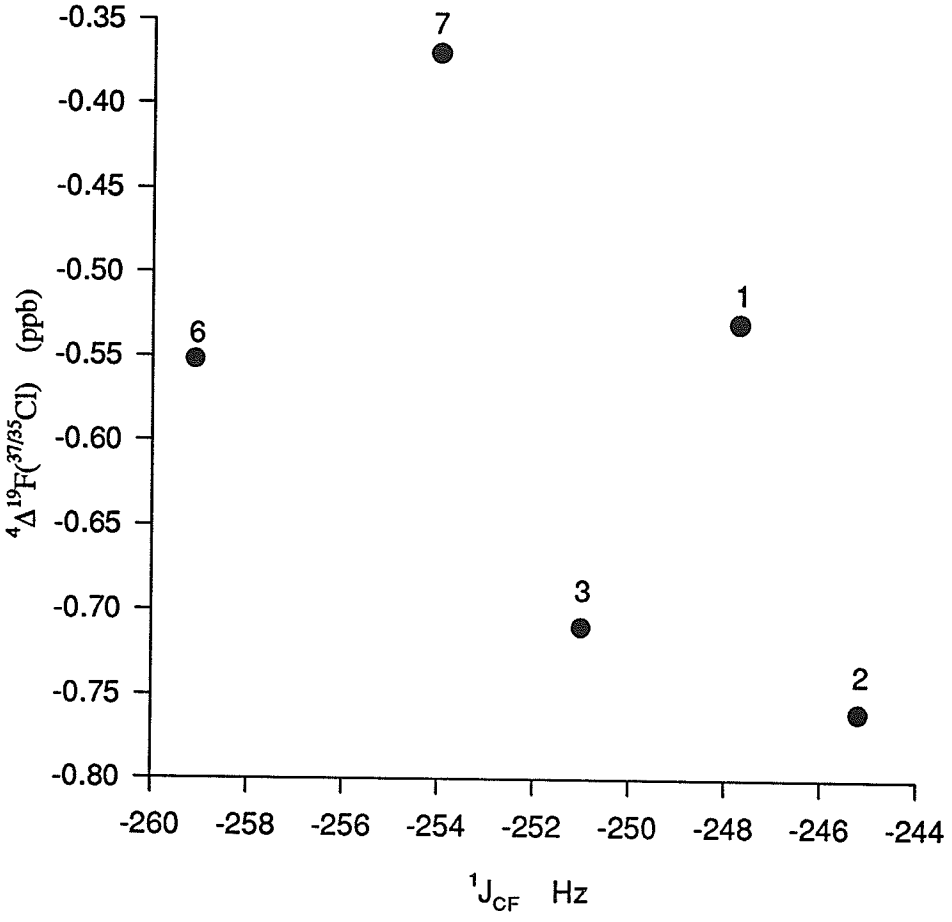

Figure 4.1

A plot of the 4-bond chlorine isotope shifts versus the 1-bond CF coupling constants in 1-chloro-3-fluorobenzene, **1**, 2-chloro-6-fluorotoluene, **2**, 2-chloro-6-fluorobenzyl chloride **3**, 2-chloro-6-fluorobenzonitrile, **6** and 2-chloro-6-fluorobenzyl chloride, **7**.

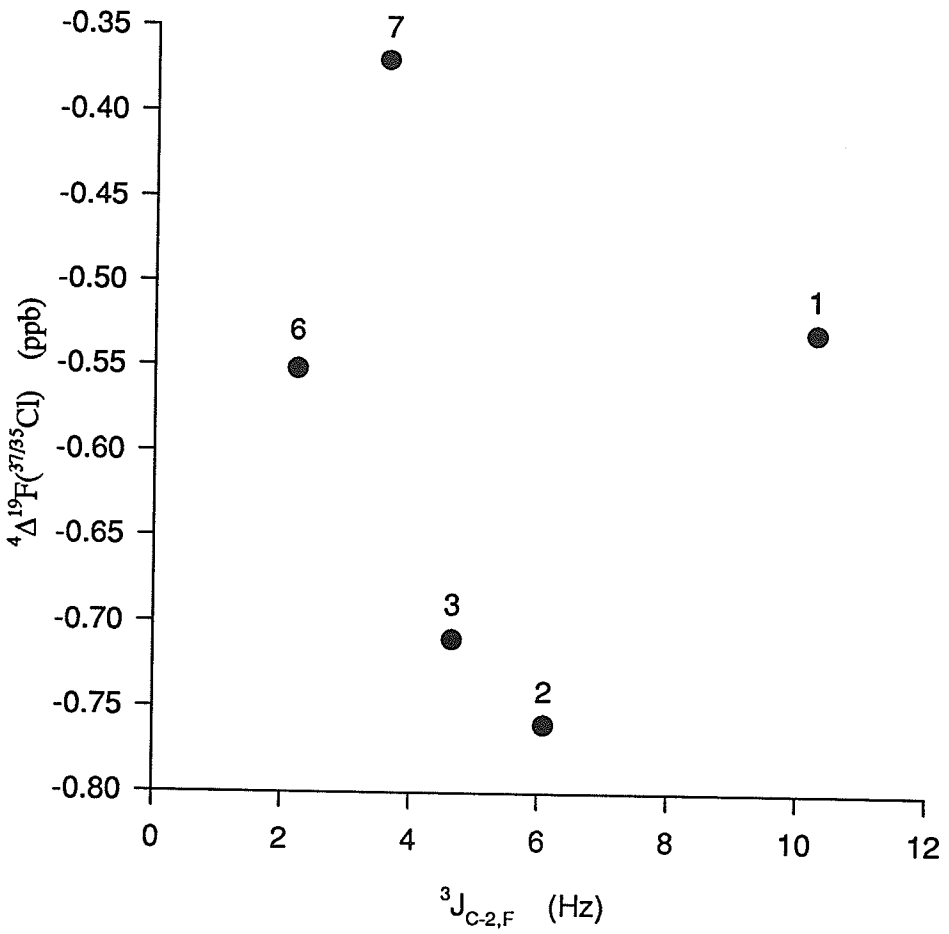

Figure 4.2

The four-bond chlorine isotope shifts are plotted against the three-bond CF coupling to C-2. The compounds are as listed in the figure caption for Figure 4.1.

In Figures 4.3 and 4.4, $^{4}\Delta^{19}F(^{37/35}Cl)$ for the series of 1-substituted-2-chloro-6-fluorobenzenes are plotted against $\nu(^{13}C\text{-}6)$ and $\nu(^{13}C\text{-}2)$ respectively. While some of the data suggest a correlation, the limited data preclude any conclusions, apart from the observation that any correlations which may exist are not all-encompassing, since some of the points are scattered.

Molecular orbital calculations were performed to investigate possible relationships between some molecular properties and $^{4}\Delta^{19}F(^{37/35}Cl)$ (Table 3.3.1). A survey of the data shows that there are no correlations.

Steric crowding may be a factor in these isotope shifts. In their investigation of methylated benzenes, Berger and Diehl found that a steric correction term had to be included in order to predict $^{n}\Delta^{13}C(^{2/1}H)$ based on an incremental system, which is itself based on a correlation with ^{13}C NMR chemical shifts.[46] Likewise, the size of the substituent at the *ipso* position appears to be a factor in $^{4}\Delta^{19}F(^{37/35}Cl)$. The largest isotope shift is for the benzaldehyde derivative, **8**, which is known to be planar, resulting in steric crowding at the fluorine atom.[61] $^{4}\Delta^{19}F(^{37/35}Cl)$ for the benzal chloride derivative, **4**, in which the chlorine atoms of the sidegroup straddle the fluorine atom, also is large (-0.92 ppb). However, a smaller value, -0.71 ppb, is measured for the benzyl chloride derivative, **3**. The C—Cl bond has been found to be perpendicular to the phenyl plane in benzyl chloride.[67] With steric interactions between the sidegroup chlorine and the fluorine and chlorine atoms at the *ortho* position, the C—Cl bond in **3** must also be perpendicular to the phenyl plane, resulting in lower steric interactions between the sidegroup chlorine atom and the fluorine atom, compared to **4**. The toluene and chloro derivatives, **2,** and **9,** respectively, have isotope shifts

similar to those observed for **3**, despite different electronic properties. Both of these have bulky substitutents at the *ipso* position, although **3** is bulkier than **2**, showing that any relationship that may exist between size and $^{4}\Delta^{19}F(^{37/35}Cl)$ is of a general nature. This is also seen from the isotope shift of the benzoyl chloride derivative, **7**, which has the smallest observed isotope shift of the series (-0.37 ppb). While molecular orbital calculations (Section 3.3) show that the C—Cl bond is perpendicular to the phenyl plane, reducing steric interactions between the fluorine and sidegroup chlorine atoms, 1-chloro-3-fluorobenzene, **1**, has a larger isotope shift (-0.53 ppb), despite the much smaller substituent at the *ipso* position.

In the preceding discussion, $^{4}\Delta^{19}F(^{37/35}Cl)$ of **4** was considered. It should be noted that this value was obtained at 210 K, rather than at 300 K as for the remaining data. In their investigation of chlorinated methanes, Sergeyev and coworkers found a temperature dependence of $^{1}\Delta^{13}C(^{2/1}H)$,[44] the absolute magnitude of $^{1}\Delta^{13}C(^{2/1}H)$ increasing by 0.015 ppb/°C. Comparable data on $^{4}\Delta^{19}F(^{37/35}Cl)$ are not available.

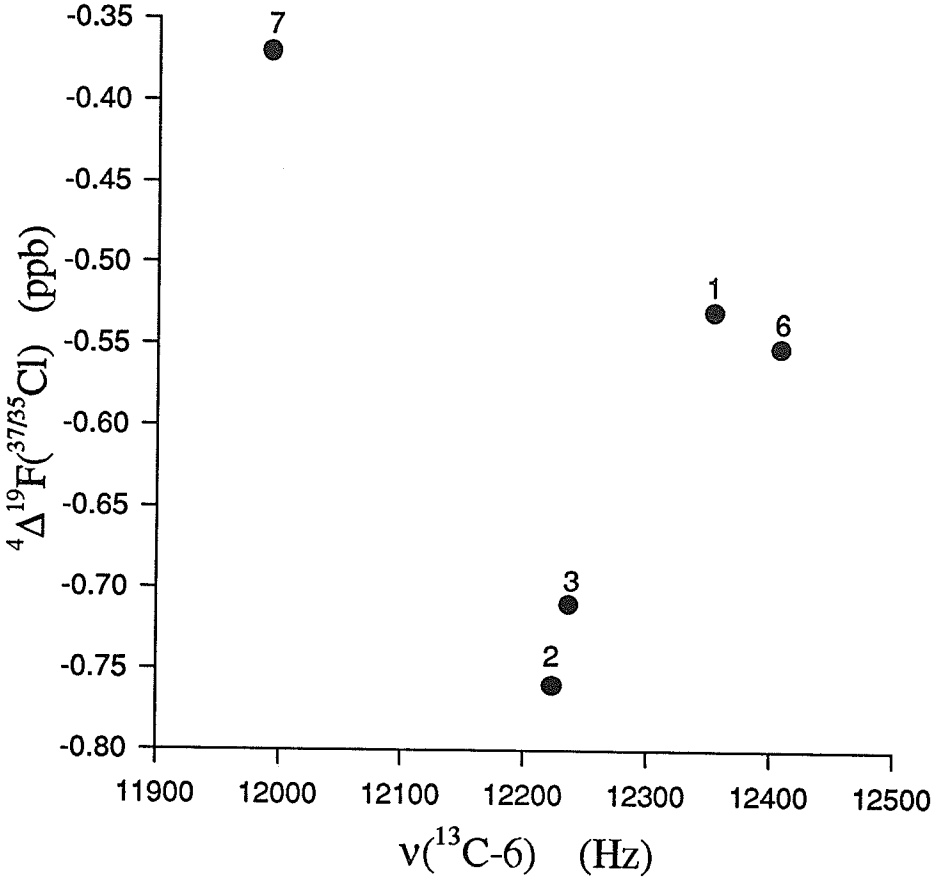

Figure 4.3

The four-bond chlorine isotope shift of some 1-substituted-2-chloro-6-fluorobenzenes are plotted against the ^{13}C NMR chemical shift of the carbon at the fluorine site (labeled $\nu(^{13}C\text{-}6)$. The compounds are as listed in the figure caption for Figure 4.1.

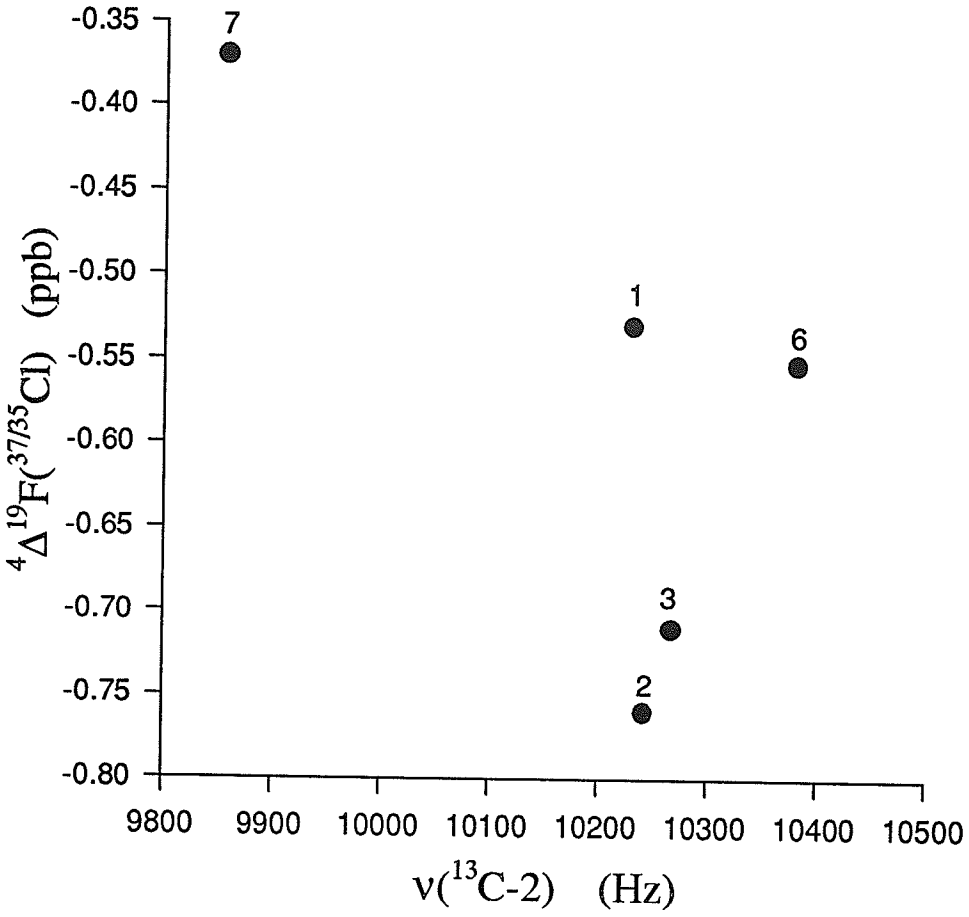

Figure 4.4

The four-bond chlorine isotope shifts of some 1-substituted-2-chloro-6-fluorobenzenes are plotted against the ^{13}C NMR chemical shift of the carbon at the substitution site (labeled $\nu(^{13}C\text{-}2)$. The compounds are as listed in the figure caption for Figure 4.1.

4.1.5 Correlations with chemical shift.

A plot of $^{4}\Delta^{19}F(^{37/35}Cl)$ vs $\nu(^{19}F)$ appears to be random (Figure 4.5). The isotope shift of pentafluorobenzoyl chloride, **27**, falls within the range of other isotope shifts, although $^{4}\Delta^{19}F(^{37/35}Cl)$ originates from a sidegroup in this case. While some points on Figure 4.6, a plot of $^{5}\Delta^{19}F(^{37/35}Cl)$ vs $\nu(^{19}F)$, appear to be linear, a good correlation can only be obtained if **27**, as well as three other points, are ignored. While the deviation of **27** may be a consequence of the isotope shift originating from a sidegroup chlorine atom, there is no reason to reject the remaining three points.

The close relationship between chemical shifts and substituents has permitted the development of substituent-induced chemical shift (SCS) parameters. With these parameters, the chemical shifts of commonly observed nuclei can be predicted, usually giving values in qualitative agreement with experimental values.[68] If the transmission of isotope shifts to remote nuclei involves the same mechanism as the chemical shift, it should be possible to predict the isotope shifts of multiply substituted benzene derivatives from a combination of simpler analogs. For example, from $^{5}\Delta^{19}F(^{37/35}Cl)$ of 1-chloro-4-fluorobenzene, **11**, and 1-chloro-2,4-difluorobenzene, **13**, the effect on $^{5}\Delta^{19}F(^{37/35}Cl)$ of a fluorine substituent *meta* to the observed fluorine ($\Delta^{5}\Delta$) is -0.21(3) ppb. Similarly, from 2-chloro-5-fluoroanisole, **21**, $\Delta^{5}\Delta$ for a methoxy group *meta* to the observed nucleus is 0.09(1) ppb. Hence, from these two values, $^{5}\Delta^{19}F(^{37/35}Cl)$ for 2-chloro-3,5-difluoroanisole is predicted to be -0.44(3) ppb, which, within experimental error, is in agreement with the experimental value (-0.39(3) ppb). However, using $\Delta^{5}\Delta$ for a fluorine *meta* to the observed fluorine, $^{5}\Delta^{19}F(^{37/35}Cl)$ is predicted to be -0.74(4) ppb for 1-chloro-2,4,6-trifluorobenzene, **16**,

greater than the experimental value of -0.395(7) ppb. Likewise, from $\Delta^5\Delta$ = -0.136(5) ppb for a fluorine atom *ortho* to the observed fluorine, $^5\Delta^{19}F(^{37/35}Cl)$ is predicted to be -1.02(5) ppb for chloropentafluorobenzene, **18**, compared to the experimental value of -0.68(2) ppb.

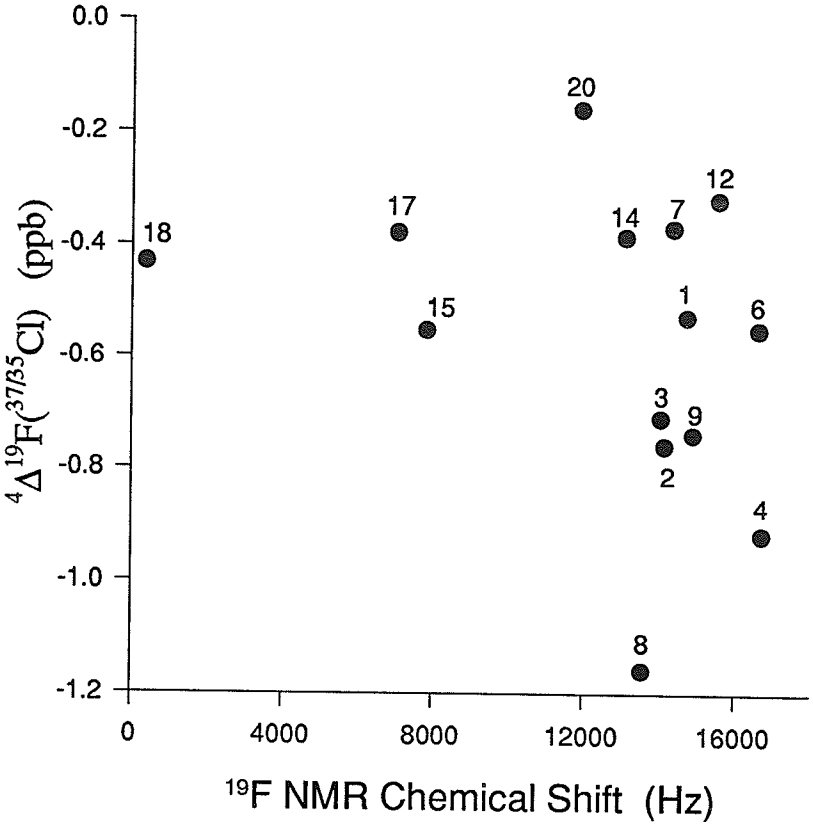

Figure 4.5

$^4\Delta^{19}F(^{37/35}Cl)$ is plotted against the ^{19}F NMR chemical shift of the observed nucleus. The points appear to be completely random. These points are 1-chloro-3-fluorobenzene, **1**, 2-chloro-6-fluorotoluene, **2**, 2-chloro-6-fluorobenzyl chloride, **3**, 2-chloro-6-fluorobenzal chloride, **4**, 2-chloro-6-fluorobenzonitrile, **6**, 2-chloro-6-fluorobenzoyl chloride, **7**, 2-chloro-6-fluorobenzaldehyde, **8**, 1,2-dichloro-3-fluorobenzene, **9**, 1-chloro-3,5-difluoro-benzene, **12**, 1-chloro-2,5-difluorobenzene, **14**, 1-chloro-3,4-difluorobenzene, **15**, 1-chloro-2,3,5,6-tetrafluorobenzene, **17**, and chloropentafluorobenzene, **18**.

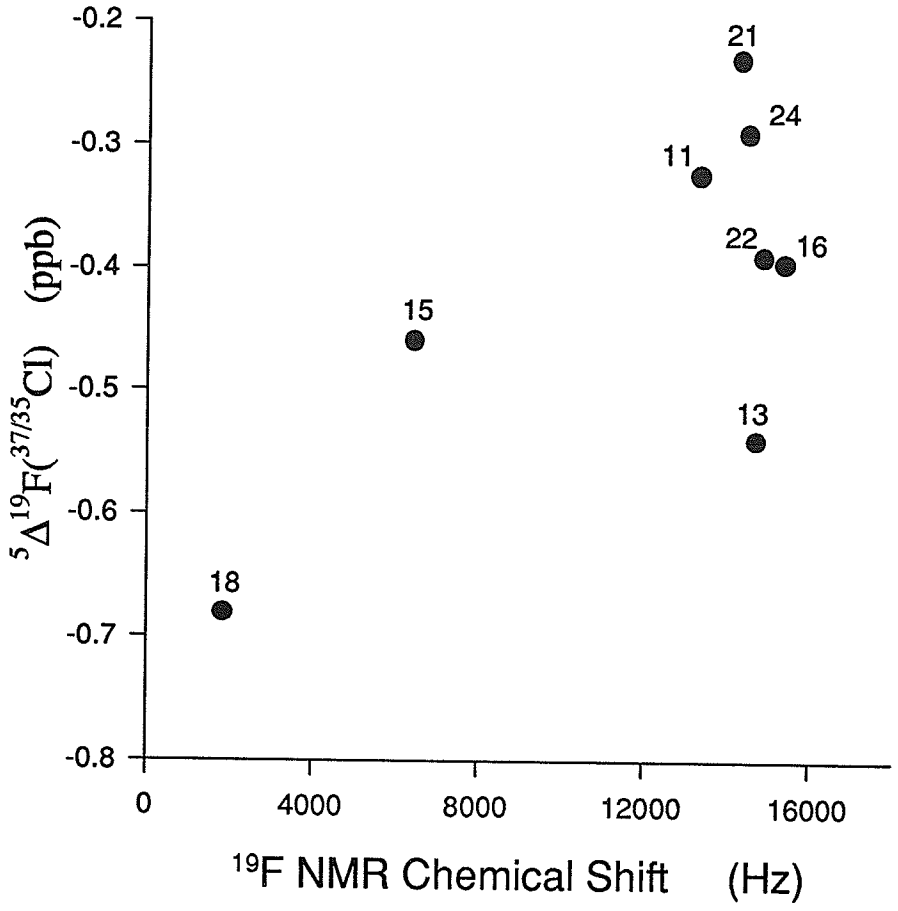

Figure 4.6

$^5\Delta^{19}F(^{37/35}Cl)$ is plotted against the ^{19}F NMR chemical shift of the observed nucleus. The points are 1-chloro-4-fluorobenzene, **11**, 1-chloro-2,4-difluorobenzene, **13**, 1-chloro-3,4-difluorobenzene, **15**, 1-chloro-2,4,6-trifluorobenzene, **16**, chloropentafluorobenzene, **18**, 2-chloro-5-fluoroanisole, **21**, 2-chloro-3,5-difluoroanisole, **22**, and 2-chloro-3,5-difluoro-phenol, **24.** Although a dependence on the ^{19}F NMR chemical shift is suggested for some points, there is no reason to disregard the outliers.

4.1.6 Correlations with bond lengths and atomic charge.

Gombler found a linear dependence of $^{1}\Delta^{19}F(^{34/32}S)$ on the S—F bond length (r_{SF}).[69] From the data provided, equation 4.1 was derived

$$r_{SF}(Å) = 0.00196[^{1}\Delta^{19}F(^{34/32}S)] + 1.68 \quad (r = 0.92). \tag{4.1}$$

From equation (4.1) and the data in Table 3.7.1, the S—F bond length of phenylsulfur(VI) tetrafluoride monochloride, **45**, and its *p*-nitro derivative, **46**, are expected to be 1.56(2) Å. This compares to the calculated (Gaussian 94 at the 6-31G* level) bond length of 1.59 Å for both **45** and **46**.

A correlation between $^{5}\Delta^{19}F(^{37/35}Cl)$ and the calculated Mulliken atomic charge, q, of the observed nucleus is suggested by Figure 4.7. If the datum for 1-chloro-2,4-difluoro-benzene, **13**, is rejected (the isotope shift of pentafluorobenzoyl chloride, **27**, which originates from the sidegroup, is also excluded), a linear correlation is obtained

$$^{5}\Delta^{19}F(^{37/35}Cl) = -9.92q - 4.09 \quad (r = 0.94). \tag{4.2}$$

The atomic charge of an atom is related to the bond length to this atom. This can be seen from the data in Table 3.3.4. A plot of the ^{19}F atomic charge vs calculated C—F bond lengths (not shown) yields a correlation coefficient of 0.96. Hence, a correlation between $^{5}\Delta^{19}F(^{37/35}Cl)$ and the calculated C—F bond lengths is expected. Yet, such a plot (Figure 4.8) shows only a modest correlation (r=0.86), although there is a definite trend, $^{5}\Delta^{19}F(^{37/35}Cl)$ decreasing in magnitude with increasing C—F bond length. Since equilibrium bond lengths are purely electronic phenomena,[21] this correlation confirms that the electronic factor is important in determining $^{5}\Delta^{19}F(^{37/35}Cl)$. The poor correlation coefficient

may be a consequence of other factors, such as secondary dynamic factors. However, the high sensitivity of the ^{19}F shielding derivative to bond extension make it very difficult to calculate the C—F bond length with sufficient accuracy. Jameson and Osten have calculated the shielding derivatives of the fluorine nucleus following bond extension in a series of halomethanes.[70] They calculated shielding derivatives $\left(\partial\sigma^F/\partial\Delta r_{CF}\right)$ ranging from -1180 ppm $Å^{-1}$ to -2400 $Å^{-1}$. If an aromatic C—F bond falls within this range, a deviation of 10^{-7}

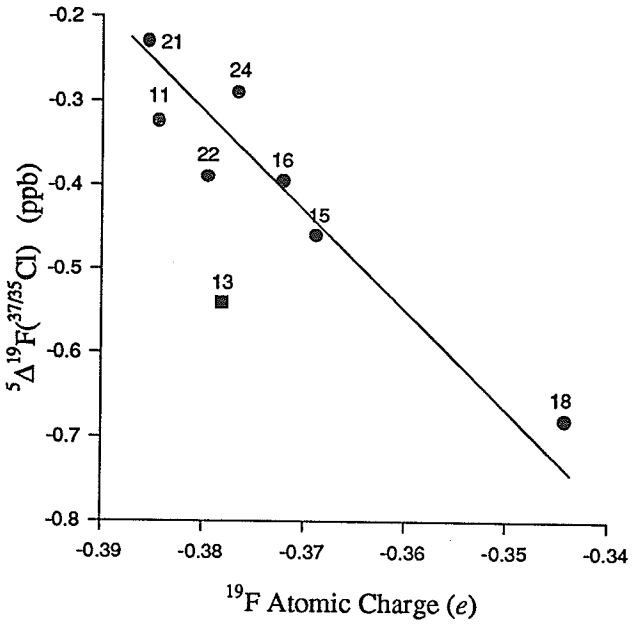

Figure 4.7

$^{5}\Delta^{19}F(^{37/35}Cl)$ for 1-chloro-4-fluorobenzene, **11**, 1-chloro-2,4-difluorobenzene, **13**, 1-chloro-3,4-difluorobenzene, **15**, 1-chloro-2,4,6-trifluorobenzene, **16**, chloropentafluoro-benzene, **18**, 2-chloro-5-fluoroanisole, **21**, 2-chloro-3,5-difluoroanisole, **22** and 2-chloro-3,5-difluorophenol, **24** are plotted against the calculated Mulliken atomic charges at the observed nucleus. The Mulliken charges were determined using Gaussian 94 at the 6-31G* level. The line, the best fit obtained if **13** is rejected, yields the empirical formula $^{5}\Delta^{19}F(^{37/35}Cl) = -9.92q - 4.09$, with a correlation coefficient of 0.94. Here q is the Mulliken atomic charge, in atomic units, at the observed ^{19}F nucleus.

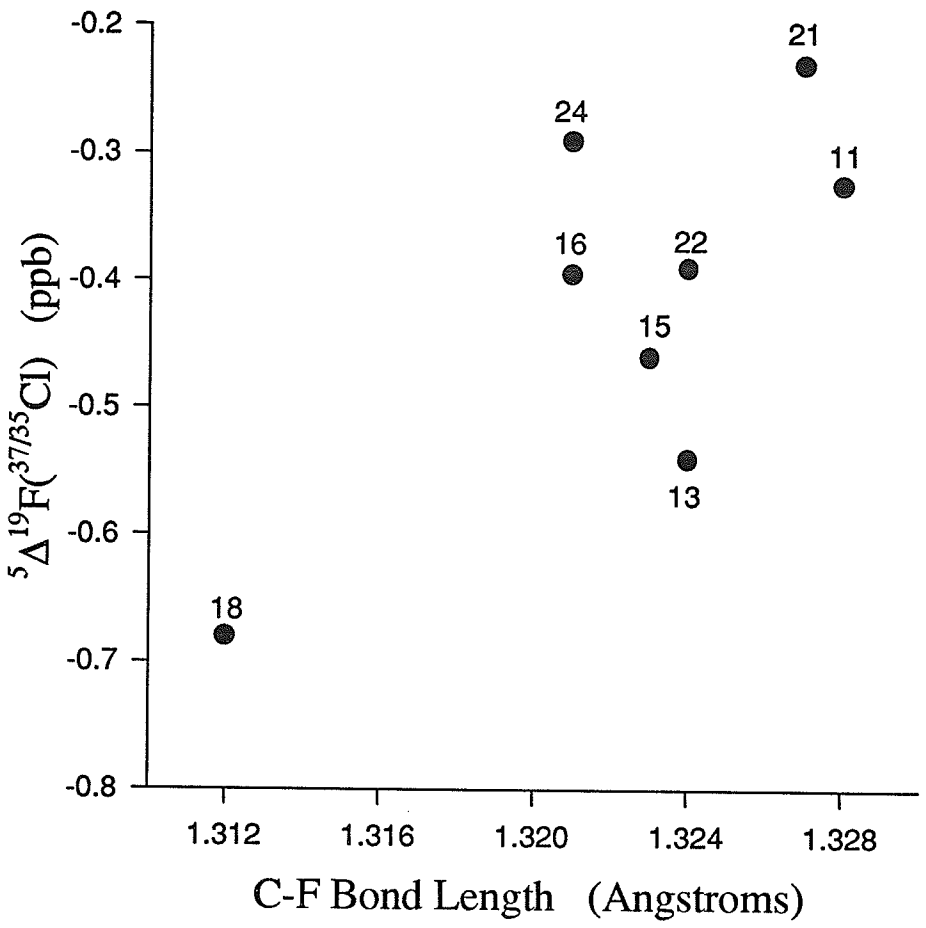

Figure 4.8

$^5\Delta^{19}F(^{37/35}Cl)$ is plotted against the calculated C—F bond length as determined by Gaussian 94 at the 6-31G* level. The molecules are as listed in the figure caption for Figure 4.7.

4.1.7 Parameter correlations - conclusions.

Thus far, long-range isotope shifts have only been investigated systematically for deuterium substitution of protons, observed on various nuclei. As discussed in the introduction, these isotope shifts have been correlated with other parameters, such as chemical shifts and coupling constants. The authors have argued that these correlations show that the transmission of isotope shifts must be governed by the same mechanism as the parameters to which they are correlated. However, Jameson and Osten have shown that such correlations are only possible if the secondary shielding term in equation (1.4), arising from the primary dynamic factor, is the only significant term contributing to the isotope shift.[20]

The absence of any linear relationships between chlorine and bromine isotope shifts on the one hand, and chemical shifts or coupling constants on the other, implies that the secondary shielding derivative is not the only significant contributor to these isotope shifts. This is reinforced by the failure of an additivity scheme analogous to the SCS parameters. Since the shielding of the fluorine nucleus is very susceptible to changes in C—F bond lengths, a very small isotope effect on this bond length would manifest itself as a significant primary shielding term (the second term in equation (1.4)).

The primary dynamic factor originates from the lower zero-point energy of the heavier isotopomer. Hence, the shielding of the observed nucleus may be affected by vibrational coupling. In general, a normal vibrational mode of a molecule entails displacement of all the atoms in the molecule. However, if the vibrational mode involves the stretching or bending of a terminal bond in which the terminal atom is much smaller than the atom to

which it is bonded, the vibrational mode will be essentially localized at that site. Thus, when considering a terminal C—H bond, the much greater mass of the carbon atom, relative to the proton, means that it does not undergo a significant displacement when the bond is stretched or bent. Although deuterium has twice the mass of hydrogen, there is still a large mass difference between it and carbon, ensuring that vibrational modes involving a terminal C—D bond are also localized.[71] Hence, deuterium isotope effects on the vibrational modes will be localized. Yet, Aydin *et al.* argue that vibrational coupling may be the cause of unexpectedly large $^{3,4}\Delta^{13}C(^{2/1}H)$ for antiperiplanar conformations of several molecules.[72] The coupling is believed to occur here (the authors do not offer any corroborating evidence for it) because the deuterium and the observed ^{13}C are both at symmetric positions.

To investigate possible vibrational coupling, normal mode analyses were performed on some representative molecules, 1-chloro-4-fluorobenzene, **11**, 1-chloro-3,4-difluorobenzene, **13** and chloropentafluorobenzene, **18**, using Gaussian 92 at the HF/6-31G* level.[73] These vibrational modes were visualized using Ani-Mol.[74] Several bending and stretching modes of the C—F bonds also involve some displacement of the chlorine atom. For example, a normal mode of **18** at 1225.47 cm^{-1} involves significant stretching of both the chlorine and *para* fluorine atoms. Since HF/6-31G* calculations overestimate vibrational frequencies by 9 - 11%,[75] a band at approximately 1100 cm^{-1} is expected, which falls in the 1000 - 1200 cm^{-1} range observed experimentally for aromatic C—F stretching.[76] However, at the experimental temperature (300 K), there would not be a significant population undergoing this vibrational mode (< 1%, as calculated assuming a Boltzman distribution).

Lower vibrational frequencies, such as the 188.97 cm^{-1} band calculated for **18**, also show vibrational coupling between the chlorine atom and one or more of the fluorine atoms. This mode involves out-of-plane bending of the *para* fluorine and the chlorine atoms and also falls within the expected range of C—F bending modes, once the calculated frequency has been corrected, as discussed above. Other vibrational modes show coupling between the chlorine atom and fluorine atoms at other positions on the ring.

The only successful parameter correlations, between the five-bond isotope shifts and either the calculated Mulliken atomic charge or the calculated C—F bond lengths, suggests that the observed isotope shift is dependent on the electronic state of the observed nucleus. However, since this is primarily a localized phenomenon, these correlations do not significantly elucidate the mechanism of isotope shifts.

4.1.7 Summary

Chlorine and bromine isotope shifts follow the general trends (*i* - *v* in section 1.2) observed for most isotope shifts. These shifts are invariant to the solvent and have no effect on coupling constants.

The virtually constant values of $^{3}\Delta^{19}F(^{37/35}Cl)$ allows some conclusions about chlorine isotope shifts in general. The primary dynamic factor apparently is unaffected by the substitution pattern on the ring regardless of which isotope shift is considered. While the substituents will affect the bond angles, these variations do not affect $^{3}\Delta^{19}F(^{37/35}Cl)$, and probably not $^{4,5}\Delta^{19}F(^{37/35}Cl)$.

The large range of observed $^{4,5}\Delta^{19}F(^{37/35}Cl)$ appears to be a consequence of numerous factors. The size of the intervening group is a factor in the magnitude of $^{4}\Delta^{19}F(^{37/35}Cl)$ in the 1-substituted-2-chloro-6-fluorobenzenes, larger isotope shifts being observed when bulkier groups are at the *ipso* position. $^{4}\Delta^{19}F(^{37/35}Cl)$ also appears to be smaller for molecules of C_{2v} symmetry compared to molecules of C_s symmetry; $^{3,5}\Delta^{19}F(^{37/35}Cl)$ were unaffected by symmetry.

These isotope shifts do not correlate with either coupling constants or chemical shifts, implying that the primary shielding term in equation (1.4), or some higher order terms, are a significant component of these isotope shifts. Normal mode analyses on some representative molecules suggest the observed fluorine atom and the substituted chlorine atom are subject to significant vibrational coupling, perhaps accounting for the failure of most parameter correlations. Whether this or other factors are responsible for the failure of the parameter correlations, this failure implies that long-range chlorine isotope shifts cannot be explained solely in terms of changes to the secondary shielding derivative, as has been done for long-range deuterium isotope shifts.

4.2 Deuterium isotope shifts on the ^{19}F NMR spectra of some fluoroanilines.

Deuterium isotope shifts were observed in all but one of the molecules investigated. Hence, the exchange of amino protons with D_2O must be slow. The data (Table 3.6.1) reveal many anomalous details, unexpected in view of the general trends in isotope shifts (*i* to *v* in section 1.2). Most of the isotope shifts are positive, non-additive, and their magnitudes appear unrelated to the number of intervening bonds between the observed and substituted nuclei. Unlike $^{n}\Delta^{19}F(^{37/35}Cl)$ and $^{n}\Delta^{19}F(^{81/79}Br)$, these isotope shifts are very sensitive to the solvent, significant effects sometimes being observed following the addition of a few μL of D_2O to the sample tube.

Both negative and positive isotope shifts occur, suggesting that at least two mechanisms are involved.[39,77,78] The negative component must arise from the anharmonic nature of the potential energy surface.[20] Conjugation of the lone-pair electrons of the amino nitrogen with the π electrons of the phenyl ring results in a pyramidal structure about the nitrogen atom, with the electron pair lying in a plane perpendicular to the phenyl ring.[79] This increases the electron density in the phenyl ring, increasing the chemical shielding of the ^{19}F nuclei, particular in the *ortho* or *para* positions.[80] If deuteration of the amino group reduces the conjugation of this group, positive isotope shifts will occur.

4.2.1 Five and six bond isotope shifts.

The amino group shields a *para* fluorine nucleus by 14.6 ppm relative to the ^{19}F NMR chemical shift of fluorobenzene.[81] Monodeuteration of the amino group in the acetone-d_6 sample of 4-fluoroaniline, **51**, reduces this shielding by approximately 12 ppb, a change of

less than 0.1%, suggesting a slight perturbation of the conjugation. The negative, vibrational component of these isotope shifts is dominated by the conjugational perturbation. Substitution of the remaining proton with a deuteron results in a significantly larger shift.

Contradictory solvent effects are noted here. Addition of D_2O to the acetone-d_6 sample, which increases the polarity of the solvent, deshields the ^{19}F nucleus. Yet, this nucleus is further deshielded in the non-polar CCl_4, and is shielded when D_2O is added to this solvent.

The isotope shifts of 3-chloro-4-fluoroaniline, **52**, are nearly equal to those of **50**. Hence the chlorine atom, *meta* to the amino group, has no significant effect on these isotope shifts. The isotope shifts of 2,6-dibromo-3-chloro-4-fluoroaniline, **31**, are larger for the acetone-d_6 sample, compared to **50**, but smaller when the corresponding CCl_4 samples are compared. The different values must be a consequence of the *ortho* bromine atoms, which perturb the isotope shift, either by their inductive effect, which, from the work on chlorine and bromine isotope shifts, is known to affect the vibrational component of the isotope shifts, or as a consequence of intramolecular hydrogen bonding.

Positive isotope shifts are also noted for $^5\Delta^{19}F(^{2/1}H)$ of 3-fluoroaniline, **49**, although the effect is much smaller. Perturbation of conjugation will not have such a dramatic effect here, since an amino group *meta* to a fluorine atom increases the shielding of the fluorine atom by only 0.2 ppm, relative to the ^{19}F chemical shift of fluorobenzene.[81] The positive component of this isotope shift is further moderated by the larger vibrational component expected for $^5\Delta^{19}F(^{2/1}H)$, compared to $^6\Delta^{19}F(^{2/1}H)$. As for $^6\Delta^{19}F(^{2/1}H)$, the isotope shifts of the CCl_4 sample are significantly larger, although the addition of D_2O to the sample does

not affect the isotope shift in this case. Within experimental error, these isotope shifts are additive.

4.2.2 Four-bond isotope shifts.

Positive isotope shifts are observed for $^{4}\Delta^{19}F(^{2/1}H)$ of 2,6-difluoroaniline, **51**, although these values are much smaller than those for $^{6}\Delta^{19}F(^{2/1}H)$. Since conjugation of an amino group has a large effect on the chemical shift of an *ortho* fluorine atom (23.1 ppm),[81] perturbation of conjugation will result in a large positive component to the isotope shift, negated to a large extent by the negative vibrational component.

Isotope shifts on the CCl_4 sample of **51**, if present, are not resolved, and hence must be smaller than those of the acetone-d_6 sample. Thus, unlike $^{5,6}\Delta^{19}F(^{2/1}H)$, the CCl_4 sample has a greater negative, or a smaller positive component, than its corresponding acetone-d_6 sample. As for most other samples investigated, these isotope shifts exhibit a high degree of non-additivity.

Contrary to other $^{n}\Delta^{19}F(^{2/1}H)$, negative values occur for both samples of 2-fluoroaniline, **48**. Hence, the vibrational component of the isotope shift dominates the positive conjugative component. This may be a consequence of the stronger negative isotope shifts observed for intramolecular hydrogen bonded species.[82,83] The stronger hydrogen bonding possible in the absence of solvation effects rationalizes the larger negative isotope shifts observed for the CCl_4 sample. Since deuteration will weaken the intramolecular hydrogen bond,[84] the conformation of the amino group may be affected here, the N—H bond being closer, on average, to the *ortho* fluorine than the N—D bond. Although intramolecu-

lar hydrogen bonding is weaker in the acetone-d_6 sample, the conformation may nevertheless be affected by the stronger intermolecular hydrogen bond to the solvent, which is strengthened by deuteration.[85] This favours a conformation similar to that discussed for the CCl_4 sample, since the N—D bond is more easily solvated if it is *trans* to the fluorine atom.

4.2.3 Conclusions.

There has been no previous investigation of deuterium isotope shifts on the ^{19}F NMR spectra of fluoroanilines. In his investigation of $^{n}\Delta^{13}C(^{2/1}H)$ of anilines, Reuben only observed isotope shifts over two and three bonds.[83] Hence, conclusions are difficult to reach based on a survey of the few representative molecules investigated here (see Further research, Section 5.3).

Competing factors contribute to the observed isotope shifts. The positive component of these shifts, attributed to perturbation of conjugation, dominates in all but one case, showing that this component is less susceptible to the number of intervening bonds than is the negative component. These positive effects suggest that deuterated amino groups are poorer electron releasing groups than are their non-deuterated analogs.

A striking feature of these isotope shifts is their non-additivity, which cannot be explained in terms of intrinsic isotope effects.[39(b)] The effects of intramolecular and intermolecular hydrogen bonding, as well as different strengths of the corresponding deuterium bond, may contribute to the non-additivity. However, similar effects are observed for both solvents, although intermolecular hydrogen bonding should not be an important factor in

the CCl_4 samples. It is interesting to note that the only isotope shift not displaying significant non-additivity is that for *meta*-fluoroaniline, the site least susceptible to perturbation of conjugation. Also, the second deuteration always results in a more positive isotope shift, an effect which is also attributed to perturbation of conjugation. In the only known study of isotope shifts following deuteration of the amino group of aniline derivatives, Reuben found that $^{2,3}\Delta^{13}C(^{2/1}H)$ is negative and additive.[83] However, non-additive effects, with both positive and negative isotope shifts, are reported by Hansen and coworkers for $^{3}\Delta^{19}F(^{2/1}H)$ of some acyl derivatives.[86] The authors attribute the non-additivity to a combination of intrinsic effects, altered rotamer populations following deuteration and vibrational coupling.

In summary, the anomalous isotope shifts observed for these fluoroanilines are attributed to competing effects. More data on the isotope shifts in general are needed to investigate whether any trends, which may help to elucidate these effects, will emerge. Accurate data on the solvent effect on the amino group of these fluoroanilines would also be useful, since the observed isotope shift may be sensitive to the conformation of this group.

5. Suggestions for Further Research

5. Suggestions for further research.

5.1 Chlorine and bromine isotope shifts on the ^{19}F NMR spectra of some fluorobenzenes.

This work represents the first study of long-range chlorine and bromine isotope shifts on the ^{19}F NMR spectra of fluorobenzenes. As such, an overview of various molecules was undertaken. In order to better understand the mechanism of these isotope shifts, a more systematic study, analogous to that on the 1-substituted-2-chloro-6-fluorobenzenes should be done, with substituents elsewhere on the ring. Steric factors apparently contributed to the observed $^{4}\Delta^{19}F(^{37/35}Cl)$ of this series. It would be useful to investigate systematically the effect of substituents in the absence of steric effects. For example, a series of 1-chloro-3-fluoro-5-substituted molecules might be investigated. In addition, the remaining mono-chlorofluorobenzenes should be synthesized and studied.

Vibrational coupling has been cited as the probable cause of the unsuccessful parameter correlations. This should be further investigated. *Ab initio* frequency calculations should be done on more molecules experiencing $^{4,5}\Delta^{19}F(^{37/35}Cl)$. These calculated vibrational frequencies should be verified on at least some of the molecules by the acquisition of vibrational spectra.

Apart from one low temperature experiment, the experimental conditions were held virtually constant. Temperature has been found to be a factor in $^{1}\Delta^{13}C(^{2/1}H)$.[44] It might be instructive to investigate the temperature effect on these samples. Other experimental conditions might also be investigated, such as solute concentration and solvent effects.

Only one example of $^{6}\Delta^{19}F(^{37/35}Cl)$ was observed, for pentafluorophenylsulfonyl chloride, **28**. Further fluorophenylsulfonyl chlorides might be investigated. In particular, it

would be instructive to determine if the large isotope shift observed for **28** is a consequence of the conformation of the S—Cl bond, perpendicular to the phenyl plane. If not, molecules susceptible to $^{6}\Delta^{19}F(^{37/35}Cl)$, but with the X—Cl bond in the phenyl plane, such as 2,4-difluorobenzyl chloride, should be studied. Finally, it would be interesting to determine the range of these isotope shifts. This can be accomplished through the preparation of suitable fused-ring compounds, such as 2-chloro-4-fluoronaphthalene.

5.2 2-chloro-6-fluorobenzal chloride, 4.

The low temperature study of **4** yielded some interesting results. Unfortunately, at 210 K, only the peaks of the more abundant conformational isomer, whose sidegroup chlorine atoms straddle the fluorine atom, were sufficiently resolved to measure $^{4}\Delta^{19}F(^{37/35}Cl)$. Lower temperature experiments should be performed to resolve the peaks of the remaining conformer, in which the sidegroup chlorine atoms straddle the *ortho* chlorine atom. This would provide data on $^{4}\Delta^{19}F(^{37/35}Cl)$ for the abundant conformer at different temperatures, permitting a temperature study of this isotope shift, as well as allowing a study of conformational effects on $^{4}\Delta^{19}F(^{37/35}Cl)$. Other investigators have found that $^{n}\Delta(trans) > {}^{n}\Delta(cis)$.[35, 86,87] It would be useful to determine if this holds true for $^{4}\Delta^{19}F(^{37/35}Cl)$.

Although temperature effects on the ^{1}H region of this spectrum were discerned at 210 K, the spectrum was not fully resolved. If possible (acetone freezes at 179 K), the temperature should be lowered sufficiently to resolve this region, permitting a determination of stereospecific molecular properties, such as the signs of $^{4}J_{H\text{-}\alpha,F}$, for both conformers of **4**.

5.3 Deuterium isotope shifts on the ^{19}F NMR spectra of fluoroanilines.

The survey of deuterium isotope shifts on the ^{19}F nuclei of fluoroanilines is only the beginning of a study of this matter. A thorough study entails the acquisition, or synthesis, of several fluoroanilines. With more data, trends may emerge, perhaps elucidating the apparently anomalous data observed in this work. Empirical relationships, successfully used to study deuterium isotope shifts (Section 1.4) may be useful here. Some of the substituted fluoroanilines, particularly 2,6-difluoroaniline, **51**, gave markedly different results from the mono-fluoroaniline analogs. Hence, a study of substituent effects on these isotope shifts might be informative.

The large solvent effects noted for these molecules should be further studied. Molecules might be studied in solvents with a large range of dielectric constants to determine if any relationships exist. The effect of varying the solute concentration should also be investigated.

Particularly surprising were the non-additive isotope shifts. Reuben found the isotope shifts of $^{2,3}\Delta^{13}C(^{2/1}H)$ in anilines to be additive, although effects over 4 and 5 bonds were not investigated.[83] Since non-additive effects were observed on the ^{19}F NMR spectra of some fluoroacyl compounds,[86] the possibility that the fluorine atom plays a role in this non-additivity should be investigated. If possible, $^{n}\Delta^{13}C(^{2/1}H)$ should be determined for the same fluoroanilines for which $^{n}\Delta^{19}F(^{2/1}H)$ was determined. This would show if the non-additivity is peculiar to fluoroanilines, or indeed if the observed fluorine atom is itself a factor.

The conformation of the amino group probably plays a significant role in the magnitude and signs of the observed isotope shifts. A greater understanding of these isotope shifts would follow from accurate information on the conformation of this group, particularly the interaction of the solvent with the N—H(D) bonds. This might be accomplished through high resolution NMR.[79] If experimental information is not available, high level molecular orbital calculations might be undertaken, including the calculation of solvent effects.

It would also be useful to study the effects of substitution on the amino group. For example, the steric effect of a methyl, or larger, group would affect its conformation. It would be instructive to determine if the isotope shifts are altered, although only monodeuteration would be possible in this case.

6. Appendix

6. Appendix

6.1 Analysis of an ABX system.

In the X region of an ABX system, A and B representing tightly coupled nuclei, the spectrum will contain two intense transitions (Figure 6.1) which carry half the total intensity of the region.[88,89,90,91,92] These transitions, centred on ν_X, will be separated by the sum of the coupling from X to A and B ($J_{AX} + J_{BX}$). Four other transitions, also centred on ν_X, may occur. The intensities of these transitions may be deduced from equations (6.1) to (6.5), where $C > 0$ and $0 \leq \Theta \leq 180°$.

$$2C_{\pm 1/2}\cos\left(2\Theta_{\pm 1/2}\right) = \left[\left(\nu_A - \nu_B\right) \pm \frac{1}{2}\left(J_{AX} - J_{BX}\right)\right] \tag{6.1}$$

$$2C_{\pm 1/2}\sin\left(2\Theta_{\pm 1/2}\right) = J_{AB} \tag{6.2}$$

$$2C_{\pm 1/2} = \left\{\left[\left(\nu_A - \nu_B\right) \pm \frac{1}{2}\left(J_{AX} - J_{BX}\right)\right]^2 + J_{AB}^2\right\}^{1/2} \tag{6.3}$$

$$P(f_1) = P(f_6) = \sin^2\left[\Theta_{1/2} - \Theta_{-1/2}\right] \tag{6.4}$$

$$P(f_3) = P(f_4) = \cos^2\left[\Theta_{1/2} - \Theta_{-1/2}\right] \tag{6.5}$$

In these equations, (ν_A - ν_B) is the positive difference in the resonance frequencies of A and B, and P is the probability of transition. Peaks f_1 and f_6, the combination lines, will be seen if the probability of transition is sufficiently large to distinguish these peaks from the noise; this will depend on the relative magnitudes of J_{AB} and C.

The X spectrum will yield ν_X, ($J_{AX} + J_{BX}$), as well as two values C. However, if one or both of A and B undergo an isotope shift, due to the presence of, for example, chlorine isotopes, then 4 values C become available. If the coupling constants do not experience an

isotope effect (all known isotope effects on coupling constants arise from $^{1}H/^{2}H$ or $^{1}H/^{3}H$ substitution),[62] these four values may be used to solve equation (6.3), permitting the determination of $(J_{AX} - J_{BX})$, J_{AB} and the two values $(\nu_A - \nu_B)$, from which the isotope shift may be determined. Since $(J_{AX} + J_{BX})$ is already known, the individual couplings J_{AX} and J_{BX} may also be calculated.

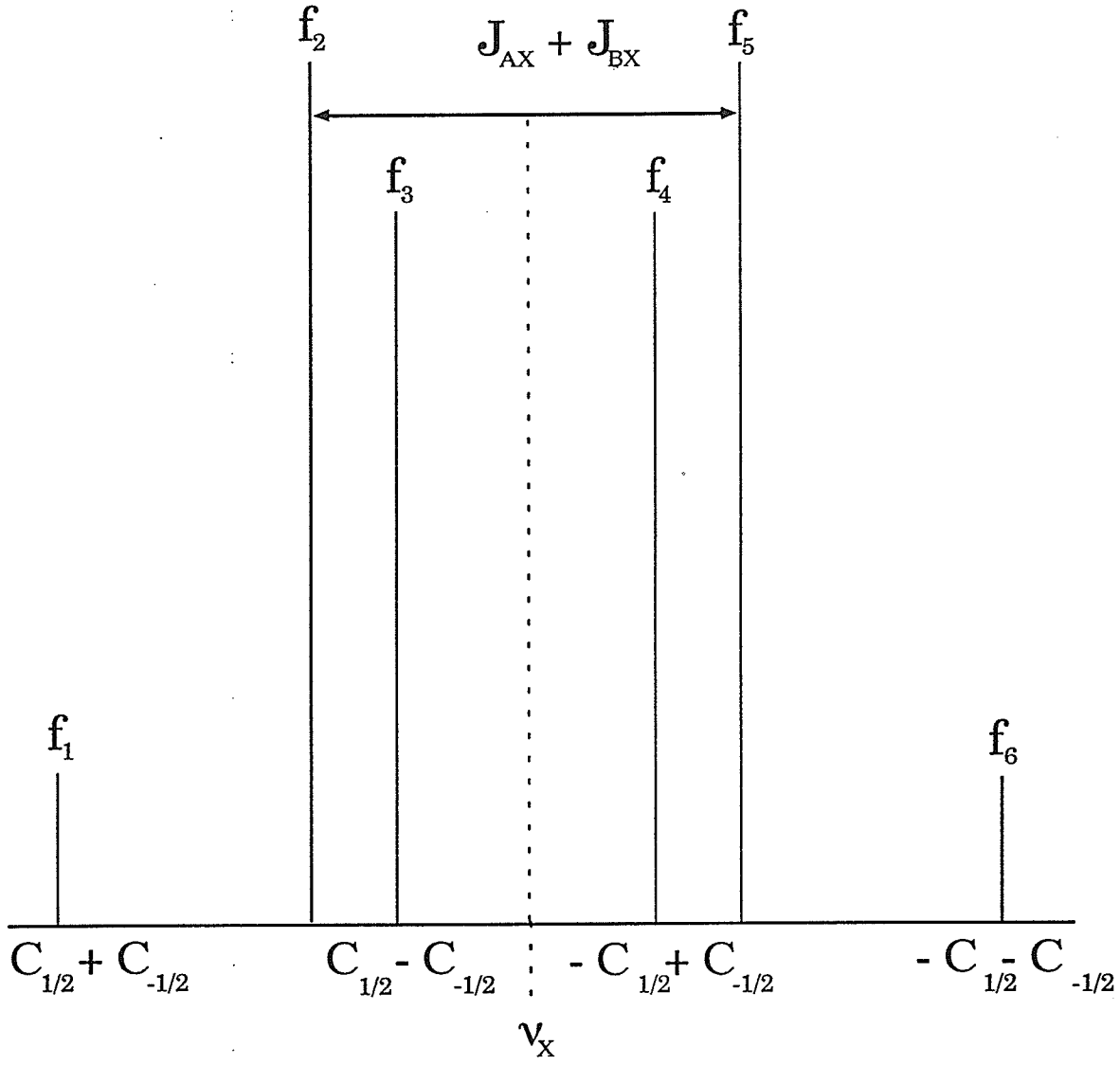

Figure 6.1

The X region of an ABX system, showing the two intense lines, f_2 and f_5, as well as the combination lines, f_1 and f_6. The intensity of $f_1 + f_3$ is equal to that of f_2. Similarly, since the multiplet is symmetrical about ν_X, the chemical shift of X, the intensity of $f_4 + f_6 = f_5$.

6.2 The ABMRX··· spectrum.

By extension of equations (6.1) to (6.5), one obtains, for example, equation (6.6) where m, r, x··· can each be ± 1/2.

$$2C_{mrx\cdots} = \left\{\left[(\nu_A - \nu_B) + m(J_{AM} - J_{BM}) + r(J_{AR} - J_{BR}) + x(J_{AX} - J_{BX}) + \cdots\right]^2 + J_{AB}^2\right\}^{1/2} \tag{6.6}$$

If, as for the ABX system described above, the X region displays combination lines, then the spectrum of X will be a superposition of the patterns shown in Figure 1, the centres of each being displaced from ν_X by $mJ_{MX} + rJ_{RX} + \cdots$. The number of positive constants $C_{mrx\cdots}$ is 2^n, where n is the number of M, R, X ··· nuclei. Since the spectral quantities in equation (6.6) increase in number only as (n+2), spectra with $n \geq 2$ will have sufficient variables to solve the equation. Similar generalizations would be possible for systems of the type $ABM_nR_oX_p\cdots$, or $AB_2M_nR_oX_p\cdots$.[93]

If an isotope shift on one or both of A or B exists, the number of C parameters becomes 2^{n+1} while the number of quantities within equation (6.6) increases to (n + 3), permitting the determination of the isotope shift. One method of accomplishing this would be to repeat the above procedure on the ^{37}Cl peaks of the X region.

6.3 Analysis of an ABMX system.

If the X region of an ABMX region contains combination lines, four values C are obtained, corresponding to the four possible combinations of m and x (referred to as ++, +-, -+ and -- below). Thus, solution of equation (6.6), which contains four spectral quantities in this case, is possible. Hence, if we let

$$\beta = C_{++}^2 - C_{--}^2 + C_{+-}^2 - C_{-+}^2 \tag{6.7}$$

and

$$\chi = C_{++}^2 - C_{+-}^2 + C_{-+}^2 - C_{--}^2, \tag{6.8}$$

it can be shown that

$$\nu_A - \nu_B = \left[\frac{\beta\chi}{4(C_{++}^2 - C_{-+}^2) - 2\chi}\right]^{1/2} \tag{6.9}$$

$$J_{AM} - J_{BM} = \frac{\beta}{(\nu_A - \nu_B)} \tag{6.10}$$

$$J_{AX} - J_{BX} = \frac{\chi}{(\nu_A - \nu_B)} \tag{6.11}$$

and

$$J_{AB} = \left\{4C_{++}^2 - \left[(\nu_A - \nu_B) + \frac{1}{2}(J_{AM} - J_{BM}) + \frac{1}{2}(J_{AX} - J_{BX})\right]^2\right\}^{1/2}. \tag{6.12}$$

Using equations (6.6) to (6.12), the spectral parameters for 2-chloro-3,5-difluorophenol, **24,** for which the protons (A and B) were tightly coupled and F-3 (X) showed combination lines, were calculated. Combination lines were not seen in the F-5 (M) region. A comparison of the calculated and experimental parameters is shown in Table 6.1 - the

complete spectral parameters are reported in Table 3.1.10. The calculated values come close to, but do not agree exactly with, the experimental values. This is attributed to second order effects arising from the proximity of the chemical shifts of the two ^{19}F nuclei. This system was effectively an ABXY system - the hydroxyl proton was broadened and did not couple with the remaining nuclei - but the calculations show that close agreement is possible even for systems in which the first order approximation for the M and X nuclei does not hold absolutely.

Table 6.1 The calculated and experimental ^{1}H and ^{19}F NMR spectral parameters for 2-chloro-3,5-difluorophenol, **24**.

Parameter	Experimental	Calculated
υ_A-υ_B	4.21(1)	4.26
J_{AM}-J_{BM}	-1.13(3)	-1.07
J_{AX}-J_{BX}	11.73(3)	11.40
J_{AB}	2.85(3)	2.85

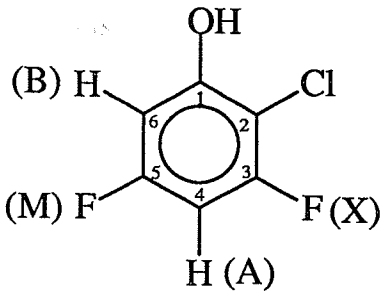

24

6.4 Analysis of an ABMRX system.

In a manner analogous to the analysis of the ABMX system (section 6.3), equation (6.6) may be used to analyze an ABMRX system, yielding an equation with five unknown variables. If combination lines are present in one or more of M, R or X, then four subspectra of the type shown in Figure 6.1 will provide eight values of C_{mrx}, permitting the solution of the equation (6.6). Thus, letting

$$\beta = C^2_{+++} - C^2_{-++} + C^2_{+--} - C^2_{---} \tag{6.13}$$

$$\chi = C^2_{+++} - C^2_{+-+} + C^2_{-+-} - C^2_{---} \tag{6.14}$$

and

$$\Delta = C^2_{+++} - C^2_{++-} + C^2_{--+} - C^2_{---}, \tag{6.15}$$

it can be shown that

$$\nu_A - \nu_B = \left[\frac{\Delta(\beta + \chi)}{4\left(C^2_{+++} - C^2_{++-}\right) - 2\Delta} \right]^{1/2} \tag{6.16}$$

$$J_{AM} - J_{BM} = \frac{\beta}{(\nu_A - \nu_B)} \tag{6.17}$$

$$J_{AR} - J_{BR} = \frac{\chi}{(\nu_A - \nu_B)} \tag{6.18}$$

$$J_{AX} - J_{BX} = \frac{\Delta}{(\nu_A - \nu_B)} \tag{6.19}$$

and

$$J_{AB} = \left\{ 4C_{+++}^{2} - \left[(\nu_A - \nu_B) + \frac{1}{2}(J_{AM} - J_{BM}) + \frac{1}{2}(J_{AR} - J_{BR}) + \frac{1}{2}(J_{AX} - J_{BX}) \right]^2 \right\}^{1/2}. \quad (6.20)$$

If one or both of A and B undergo an isotope shift, it will be reflected in the X region as a result of the two values (ν_A - ν_B). However, if both nuclei are subject to isotope shifts, only the difference in isotope shifts is obtained, although a good estimate of the two isotope shifts become possible if one of these is essentially invariant, as has been noted in this work for $^{3}\Delta^{19}F(^{37/35}Cl)$.

Using equations (6.13) - (6.20), the ^{19}F NMR parameters of 1-chloro-2,4-difluorobenzene, **13**, for which the two fluorine nuclei are tightly coupled, were calculated. These calculated values are compared to experimental values in Table 6.2. The H-5 (X) region of the ^{1}H NMR spectrum is shown in Figure 6.2. The results of the complete analysis are tabulated in Table 3.1.8.

Table 2 The calculated and experimental ^{1}H and ^{19}F NMR spectral parameters for 1-chloro-2,4-difluorobenzene, **13**.

Parameter	Experimental	Calculated
ν_A - ν_B	7.356(5)	7.351
J_{AM}-J_{BM}	-2.762(3)	-2.761
J_{AR}-J_{BR}	-0.816(3)	-0.814
J_{AX}-J_{BX}	9.639(5)	9.654
J_{AB}	6.830(5)	6.832

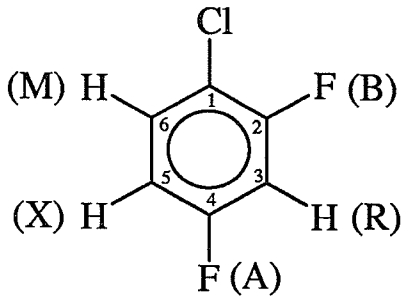

13

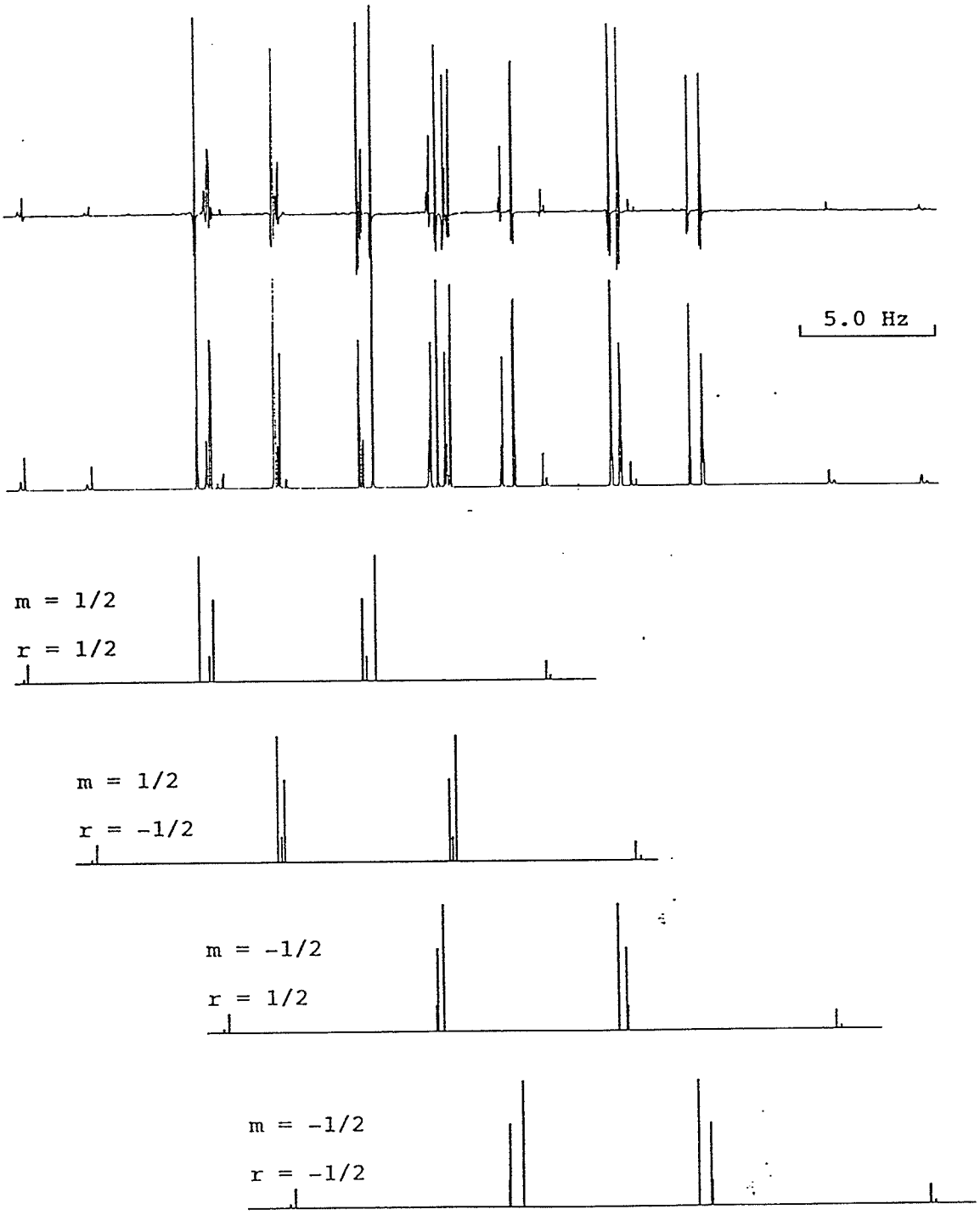
5.0 Hz
m = 1/2
r = 1/2
m = 1/2
r = -1/2
m = -1/2
r = 1/2
m = -1/2
r = -1/2

Figure 6.2

The ^{1}H NMR spectrum at 300 K and 300.135 MHz of the H-5 (X) region of 1-chloro-2,4-difluorobenzene, **13**, as a 5 mol% solution in acetone-d_6, is shown on top. Below it is shown the calculated spectrum using the spectral parameters in Table 3.1.8. The subspectra corresponding to various spin states of H-3 (R) and H-6 (M) are indicated by stick spectra. Each of these consists of a set of intense peaks, attributed to the ^{35}Cl isotopomer, and an additional four peaks from the ^{37}Cl isotopomer - the intense peaks corresponding to $J_{AX} + J_{BX}$ coincide since there is no isotope effect on the coupling constants.

7. References

1 W. Gombler, *J. Am. Chem. Soc.* **104**, 6616 (1982).

2 H. Wennerström, W. Egan and S. Forsén, *Chem. Phys. Lett.* **38**, 96 (1976).

3 N. F. Ramsey, *Phys. Rev.* **87**, 1075 (1952).

4 T. F. Winett, *Phys. Rev.* **91**, 476 (1953).

5 G. V. D. Tiers, *J. Am. Chem. Soc.* **79**, 5585 (1957).

6 G. V. D. Tiers, *J. Chem. Phys.* **29**, 963 (1958).

7 P. R. Carey, H. W. Kroto and M. A. Turpin, *J. Chem. Soc. Chem. Commun.* 188 (1969).

8 G. M. Bernard and R. W. Schurko, *Magn. Reson. Chem.* **33**, 879 (1995).

9 M. Tordeux, I. Balme, C. Wakselman, *New J. Chem.* **19**, 287 (1995).

10 For a list of observed isotope shifts to 1982, see P. E. Hansen in *Annual Reports on NMR Spectroscopy*, G. A. Webb (ed.) Vol 15, p. 105. Academic Press, London (1983).

11 C. J. Jameson, D. Rehden and M. Hock, *J. Am. Chem. Soc.* **109**, 2589 (1987).

12 E. Kupce, E. Liepens, I. Zicmane and E. Lukevics, *J. Chem. Soc. Chem. Commun.* 818 (1989).

13 G. J. Schrobilgen, *J. Chem. Soc. Chem. Commun.* 863 (1988).

14 J. P. Jokissari, L. P. Ingman, G. J. Schrobilgen and J. C. P. Sanders, *Magn. Reson. Chem.* **32**, 242 (1994).

15 For a review of the deuterium isotope shifts on ^{19}F and ^{13}C NMR, see S. Berger in *NMR- Basic Principles and Progress*, P. Diehl, E. Fluck, H. Günther, R. Kosfeld and J. Selig (eds.) Vol. 22, p. 1, Springer-Verlag, Berlin (1990).

16 S. Berger and H. Künzer, *Ang. Chem. Int. Ed.* **22**, 321 (1983).

17 V. A. Chertkov and N. M. Sergeyev, *J. Magn. Reson.* **52**, 400 (1983).

18 T. Schaefer, J. Peeling and G. H. Penner, *Can. J. Chem.* **64**, 2161 (1986).

19 H. Batiz-Hernandez and R. A. Bernheim in *Progress in NMR Spectroscopy,* J. W. Emsley, J. Feeney and L. H. Sutcliffe (eds.) Vol 3, p. 63. Pergamon Press, Oxford (1967).

20 For a theoretical discussion of isotope shifts, see C. J. Jameson and H. J. Osten in *Annual Reports on NMR Spectroscopy,* G. A. Webb (ed.), Vol. 17, p. 1. Academic Press, London (1986).

21 C. J. Jameson in *Isotopes in the Physical and Biomedical Sciences*, E. Buncel and J. R. Jones (eds.), Vol. 2, p. 1. Elsevier, N. Y. (1991).

22 J. S. Winn, Physical Chemistry, Harper Collins College Publishers, N.Y. (1995).

23 R. A. Hegstrom, *Phys. Rev.(A)* **19**, 17 (1979).

24 D. B. Chesnut, *Chem. Phys.* **110**, 415 (1986).

25 Y. Nakashima and K. Takahashi, *Bull. Chem. Soc. Jpn.* **64**, 3166 (1991).

26 R. Ditchfield, *Chem. Phys.* **63**, 185 (1981).

27 W. T. Raynes, M. Grayson, N. M. Sergeyev and N. D. Sergeyeva, *Chem. Phys. Lett.* **226**, 433 (1994).

28 F. A. L. Anet and M. Kopelevich, *J. Am. Chem. Soc.* **109**, 5870 (1987).

29 T. Schaefer and R. Sebastian, *J. Am. Chem. Soc.* **109**, 6508 (1987).

30 (a) H. J. Osten and C. J. Jameson, *J. Chem. Phys.* **81**, 4288 (1984); (b) C. J. Jameson and H. J. Osten, *J. Chem. Phys.* **81**, 4292 (1984).

31 R. E. Wasylishen and J. O. Friedrich, *J. Chem. Phys.* **80,** 585 (1984).

32 N. M. Sergeyev, N. D. Sergeyeva and W. T. Raynes, *Chem. Phys. Lett.* **221**, 385 (1994).

33 R. K. Harris, Nuclear Magnetic Resonance Spectroscopy, Longman Scientific and Technical, Essex (1986).

34 S. G. Frankiss, *J. Phys. Chem.* **67**, 752 (1963).

35 H. J. Osten, C. J. Jameson and N. C. Craig, *J. Chem. Phys.* **83**, 5434 (1985).

36 Z. Majerski, M. Žuanić and B. Metelko, *J. Am. Chem. Soc.* **107,** 1721 (1985), and references cited within.

37 T. Schaefer, J. Peeling, and T. A. Wildman, *Can. J. Chem.* **61**, 2177 (1983).

38 K. Mlinarić-Majerski, V. Vinković, Z. Meić, P. G. Gassman and L. J. Chyall, *J. Molec. Struct.*, **267**, 389 (1992).

39 J. R. Wesener and H. Günther, *Tetrahedron Lett.* **23**, 2845 (1982).

40 K. L. Brown, X. Zou and B. M. Webb, *Inorg. Chem.* **33**, 4189 (1994) and references cited within.

41 D. Vikić-Topić, M. Hodošćek, A. Graovac, E. D. Becker, G. Lodder and H. Zuilhof, in *Nuclear Magnetic Shieldings and Structure*, J. A. Tossell (ed.), NATO ASI Series C, Vol. 386, p. 574. Kluwer Academic Publishers, Dordrecht, 1993.

42 Z. Mieć, P. Novak, D. Vikić-Topić and V. Smrečki, *Magn. Reson. Chem.* **34**, 36 (1996) and references cited within.

43 P. Atkins, Physical Chemistry *5th Ed.* W. H. Freeman and Company, N. Y. (1994).

44 N. M. Sergeyev, P. Sandor, N. D. Sergeyeva and W. T. Raynes, *J. Magn. Res. (A)* **115**, 174 (1995).

45 P. E. Hansen, *Magn. Reson. Chem.* **31**, 23 (1993).

46 S. Berger and B. W. K. Diehl, *Magn. Reson. Chem.* **24**, 1073 (1986).

47 H. H. Balzer and S. Berger, *Magn. Reson. Chem.* **28**, 437 (1990).

48 J. R. Wesener, D. Moskau and H. Günther, *J. Am. Chem. Soc.* **107**, 7307 (1985).

49 H. Künzer, C. E. Cottrell and L. A. Paquette, *J. Am. Chem. Soc.* **108**, 8089 (1986).

50 C. A. Coulson, B. O'Leary and R. B. Mallon, Hückel Theory for Organic Chemists, Academic Press, London (1978).

51 D. J. Sardella and A. E. El-Din, *Magn. Reson. Chem.* **27**, 253 (1989).

52 P. Vujanić, E. Gacs-Baitz , Z. Meić, T. Šuste and V. Smrečki, *Magn. Reson. Chem.* **33**, 426 (1995) and references cited within.

53 V. Smrečki, N. Müller, D. Vikić-Topić, P. Vujanić and Z. Meić, *J. Molec. Struct.* **348**, 69 (1995).

54 L. Kozerski, *J. Molec. Struct.* **321**, 89 (1994) and references cited within.

55 L. Ernst, private communication.

56 X. Ou, G. M. Bernard, and A. F. Janzen, in preparation, to be submitted to *Can. J. Chem.*

57 J. S. Martin, A. R. Quirt and K. E. Worvill, *The NMR Program Library,* Daresbury Laboratory, Daresbury (1971).

58 Gaussian 94, revision B.2, M.J Frisch,, G. W. Trucks, H. B. Schlegel, P. M. W. Gill, B. G. Johnson, M. A. Robb, J. R. Cheeseman, T. Keith, G. A. Petersson, J. A. Montgomery, K. Raghavachari, M. A. Al-Laham, V. G. Zakrzewski, J. V. Ortiz, J. B. Forseman, C. Y. Peng, P. Y. Ayala, W. Chen, M. W. Wong, J. L. Andres, E. S. Replogle, R. Gomberts, R. L. Martin, D. J. Fox, J. S. Binkley, D. J. Defrees, J. Baker, J. P. Stewart, M. Head-Gorman, C. Gonzalez and J. A. Pople, Gaussian Inc., Pittsburgh PA, 1995.

59 W. B. Moniz, E. Lustig and E. A. Hansen, *J. Chem. Phys.* **51**, 4666 (1969).

60 For a complete tabulation of fluorine coupling constants to 1977, see J. W. Emsley, L. Phillips and V. Wray, Fluorine Coupling Constants, Ed. Pergamon Press Ltd., Toronto (1977).

61 a) CS_2 sample: unpublished data from this laboratory. b) acetone-d_6 sample: R. E. Wasylishen and T. Schaefer, *Can. J. Chem.* **49**, 3216 (1971).

62 N. M. Sergeyev in *NMR Basic Principles and Progress*, **22**, 33 (1990).

63 C. S. Yannoni, *J. Am. Chem. Soc.* **91**, 4581 (1969).

64 W. Caminati, A. Maris, A. Millemaggi and P. G. Favero, *Chem. Phys. Lett.* **243**, 302 (1995).

65 W. J. E. Parr and T. Schaefer, *Acc. Chem. Res.* **13**, 400 (1980).

66 T. Schaefer and W. J. E. Parr, *Can. J. Chem.* **56**, 1717 (1978).

67 T. Schaefer, L. J. Krucynski and W. J. E. Parr, *Can. J. Chem.* **54**, 3210 (1976).

68 a) For a discussion of SCS, including several tables, see H. Günther, NMR Spectroscopy 2nd Ed., John Wiley and Sons, Toronto (1994). b) For a review of ^{13}C SCS parameters, see D. F. Ewing, *Org. Magn. Reson.* **12**, 511 (1979). c)For a review of ^{19}F SCS parameters to 1968, see M. I. Bruce, *J. Chem. Soc. A* 1459

(1968). d) For more recent SCS parameters for ^{19}F NMR, see S. Ando and T. Matsuura, *Magn. Reson Chem.* **33**, 639 (1995).

69 W. Gombler, *Z. Naturforsch. B*, **40**, 782 (1985).

70 C. J. Jameson and H. J. Osten, *Mol. Phys.* **55**, 383 (1985).

71 J. M. Hollas, Modern Spectroscopy, 2nd Ed. John Wiley and Sons, Chichester (1992).

72 R. Aydin, J. R. Wessener and H. Günther, *J. Org. Chem.* **49**, 3845 (1984).

73 Gaussian 92, Revision C, M. J. Frisch, G. W. Trucks, M. Head-Gordon, P. M. W. Gill, M. W. Wong, J. B. Foresman, B. G. Johnson, H. B. Schlegel, M. A. Robb, E. S. Replogle, R. Gomberts, J. L. Andres, K. Raghavachari, J. S. Binkley, J. J. P. Stewart and J. A. Pople, Gaussian Inc., Pittsburgh, Pa. (1992).

74 Ani-Mol, version 0.02, R. Cleve and K. M. Gough, Brock University (1994).

75 W. J. Hehre, L. Radom, P. v.R. Schleyler and J. A. Pople, Ab Initio Molecular Orbital Theory, John Wiley and Sons, New York (1986).

76 H. A. Szymanski and R. E. Erickson, Infrared Band Handbook Vol. 1, 2nd Edition, IFI/Plenum, New York (1970).

77 C. H. Arrowsmith and A. J. Kresge, *J. Am. Chem. Soc.* **108**, 7918 (1986).

78 L. Ernst, H. Hopf, D. Wullbrandt, *J. Am. Chem. Soc.* **105**, 4469 (1983).

79 T. Schaefer and G. H. Penner, *Can. J. Chem.* **63**, 2253 (1985), and references cited within.

80 J. W. Emsley, J. Feeney and L. H. Sutcliffe, High Resolution Nuclear Magnetic Resonance Spectroscopy, Vol. 2, Pergamon Press, Oxford (1966).

81 H. S. Gutowsky, D. W. McCall, B. R. McGarvey and L. H. Meyer, *J. Am. Chem. Soc.* **74**, 4809 (1952).

82 For a review of intramolecular hydrogen bonding, see T. Dziembowska, *Polish J. Chem.* **68**, 1455 (1994).

83 J. Reuben, *J. Am. Chem. Soc.* **109**, 316 (1987).

84 P. E. Hansen, *Acta Chem. Scand. Ser. B*, **42**, 423 (1988).

85 S. Scheimer and M. Čuma, *J. Am. Chem. Soc.* **118**, 1511 (1996).

86 P. E. Hansen, F. M. Nicolaisen and K. Schaumburg, *J. Am. Chem. Soc.* **108**, 625 (1986).

87 a) J. B. Lambert, L. G. Greifenstein, *J. Am Chem. Soc.* **95**, 6150 (1973). b) H. Jensen, K. Schaumburg, *Mol. Phys.* **22**, 1041 (1971).

88 G. A. Williams and H. S. Gutowski, *J. Chem. Phys.* **25**, 1288 (1956).

89 J. A. Pople, W. G. Schneider and H. J. Bernstein, High Resolution Nuclear Magnetic Resonance McGraw-Hill, New York (1959) Chapter 6.

90 P. L. Corio, Structure of High-Resolution NMR Spectra Academic Press, New York (1966) Chapter 7.

91 R. J. Abraham, Analysis of High-Resolution NMR Spectra Elsevier, Amsterdam (1971) Chapetr 6.

92 J. A. Pople and T. Schaefer, *Mol. Phys.* **3**, 547 (1960).

93 P. Diehl and J. A Pople, *Mol Phys.* **3**, 557 (1960).